UNIVERSITY OF OKLAHOMA

GRADUATE COLLEGE

MOLECULAR ENGINEERING STRATEGIES FOR THE PRODUCTION OF FUELS FROM CONVENTIONAL AND RENEWABLE RESOURCES

A DISSERTATION

SUBMITTED TO THE GRADUATE FACULTY

in partial fulfillment of the requirements for the

Degree of

DOCTOR OF PHILOSOPHY

By

STEVEN CROSSLEY
Norman, Oklahoma
2009

Downloaded from SHAREOK. Persistent Handle URL: https://hdl.handle.net/11244/319331

MOLECULAR ENGINEERING STRATEGIES FOR THE PRODUCTION OF FUELS FROM CONVENTIONAL AND RENEWABLE RESOURCES

A DISSERTATION APPROVED FOR THE
SCHOOL OF CHEMICAL, BIOLOGICAL & MATERIALS ENGINEERING

BY

Dr. Daniel E. Resasco, Chair

Dr. Richard G. Mallinson

Dr. Lance L. Lobban

Dr. Walter E. Alvarez

Dr. Robert P. Houser

© Copyright by STEVEN CROSSLEY 2009
All Rights Reserved.

ACKNOWLEDGEMENTS

I would like to acknowledge my wife and best friend, Lindsay for always encouraging me to pursue my dreams. Without her constant loving support, I don't know where I would be right now. I can't imagine going through this journey without her by my side.

I would also like to thank my parents for always encouraging me to pursue the things I am most passionate about. They have always made me believe that I could do whatever I set out to accomplish, and without their support I would definitely not be here today.

I feel extremely privileged to work at OU in this group at this time. I cannot imagine a better scenario. I have been able to work with so many amazing people during my time here and I am very grateful. The wonderful discussions and insights brought about by all of the brilliant professors in our group meetings have helped me tremendously in my development. I would especially like to thank Dr. Richard Mallinson, Dr. Lance Lobban, Dr. Tawan Sooknoi, Dr. Roberto Galiasso, Dr. Friederike Jentoft, and Dr. Rolf Jentoft. Each brings a unique area of expertise ranging from fundamental surface chemistry to industry. The end result is a very powerful and exciting group which I am very happy to have been a part of.

Dr. Walter Alvarez has helped me tremendously. He helped convince me to pursue a PhD, and this is a decision which I could not be happier with. I enjoy very

much the wisdom that he has given me as well as the tremendous opportunities. I am looking forward very much to working with him in the near future.

I would like to thank all of my fellow students and post-docs which I have met and worked with during my time at OU. Most of all I would like to thank Giulio Lolli, who acted as a second mentor to me during my early years at OU. I would also like to thank Roberto Santana, for first diving into the area of structure property prediction of fuel properties which has turned out to be essential for our research. There are many other bright students and post-docs who I am extremely happy to have known over the years, many whom I have been privileged to work with. They are Phuong, Andrea, Jeab, Meaow, Pac, Martina, Stefano, Federico, Jorge, Trung (Hoang), Trung (Pham), Tanate, Air, Quincy, Huy, Lyon, Amalia, Jimmy, Santiago, Ricardo, Tan, Veronica, Leandro, Pilar, Dachuan, Anh, Dipanjan, Deborah, Mai, Jose, Jeff, Kyu, Nok, Jerry, Sergio, Min, Xinli, Anirudh, Robbie, Ariela, Kyle, Matt, Kassie, Armando, David, Brian, Rajesh, Selda, Roman, Mohamed, and Satesh.

I would also like to thank the people who help keep everything moving. Alan, Terry, Donna, and Vernita. Thank you very much for all of the help you have given me.

Finally I would like to thank Dr. Resasco. I can't even begin to explain how amazing he is, and how grateful I am that he was my advisor. He taught me to love research. I have never before met a person with the combination of knowledge, creativity, enthusiasm, and kindness that he possesses. I thank him for the countless

hours he has spent helping me with my research, and for showing me how research should be conducted.

TABLE OF CONTENTS

1. Overview of Molecular Engineering Strategies as Applied to Fuel Upgrading 1

1.1. Introduction 1
1.2. Methodology 3
1.2.1.Relationship1: Molecular Structure-Properties 4
1.2.2.Relationship2: Catalyst-Reactivity-Strucuture 6
1.3. Utilization of molecular engineering strategies towards upgrading of fuels 7

2. Prediction of Fuel Properties for Conventional Fuels 10

2.1. Importance of fuel property predictions 10
2.2. QSPR methods for property predictions 11
2.3. Correlation methods 14
2.3.1. Genetic Algorithms 14
2.3.1.1.General overview of genetic algorithms as applied to descriptor selection 14
2.3.1.2. Fitness function and initial sample selection 16
2.3.2. All Possible Subsets regression 17
2.3.3. Regression of Principal Components 18
2.3.4. Artificial Neural Networks (ANN) 19
2.4. Model validation 20
2.5. Prediction of important fuel properties of conventional fuels 22
2.5.1. Prediction of Cetane Number 22
2.5.2. Prediction of Octane Number 28
2.5.3. Prediction of Threshold Sooting Index 34
2.6.Correlation between Particulate Matter (PM) emissions and fuel properties 36

3. Development of a Novel Micropyrolysis Index (MPI) to Estimate Sooting Tendency of Fuels 42

3.1.Overview of applicability towards molecular engineering strategy 42
3.2.Introduction 42
3.3.Experimental 46
3.3.1.Carbon deposition 46
3.3.2.Temperature Programmed Oxidation (TPO) 48
3.3.3.Definition of MPI 49
3.3.4.Effect of injection speed, temperature, and pressure 50
3.3.5.Repeatability 51
3.4.Results and discussion 52

3.4.1. Effects of molecular structure on MPI 52
3.4.2. Comparison with TSI 54
3.4.3. MPI of oxygenates 58
3.4.4. MPI of aromatics 58
3.4.5. Development of QSPR models to estimate MPI 62
3.4.6. Results from predicted MPI values 65
3.4.7. Comparison between predicted MPI values and Cetane Number 68
3.4.8. MPI measurements of real fuel mixtures 72
3.5.Conclusions 73
3.6. Acknowledgment 73

4. Development of Strategies for Upgrading of Conventional Fuels 77

4.1. Introduction 77
4.2.Influence of nitrogen containing compounds and number of aromatic rings on the inhibition of hydrogenation activity over sulfided NiMo/Al_2O_3 79
4.2.1. Introduction 79
4.2.2. Experimental 81
4.2.2.1. Reactor tests 81
4.2.2.2. Kinetics 83
4.2.2.3. Theoretical calclulations 83
4.2.3. Results and discussion 84
4.2.3.1. Competative adsorption among aromatic rings 84
4.2.3.2.Competitive adsorption among nitrogen containing compounds 86
4.2.4. Conclusions 90
4.2.5. Applications to molecular engineering strategy 90
4.3. Aromatics removal in gasoline while minimizing ON losses 91
4.3.1. Introduction 91
4.3.2. Overview of potential catalytic strategies for ON improvement 92
4.3.3. Implementation of catalytic strategies for improvement of ON 97
4.3.4. Conclusions 100
4.4.Insight gained towards improvement of CN of diesel fuels 100
4.5 Conclusions 101

5. Primary Product Selectivity Prediction over Ir/Al_2O_3 as a Novel Approach towards Fundamental and Practical Problems in Fuel Upgrading. 104

5.1. Introduction 104
5.2 Effect of selective ring opening on fuel properties 106
5.3 Experimental 108
5.3.1. Catalyst preparation 108
5.3.2. Catalyst characterization 108

5.3.3. Catalytic activity measurement and data analysis 109
5.4.Results 110
5.4.1.Selection of molecules and ratios 110
5.4.2.Development of QSPR models to estimate product selectivity 113
5.4.3.Results from predicted values 116
5.4.3.1.Predicted trends in ratios 116
5.4.3.2.Incorporation of predicted product selectivities and fuel properties 122
5.5.Conclusions 125

6. Transition of the Molecular Engineering Approach towards the Upgrading of Biofuels 127

6.1.Viability of Molecular Engineering approach as applied towards biofuel refining 127
6.2. Potential applications in the upgrading of biofuels 130
6.3. Estimation of biofuels properties 131
6.4. Conclusions 136

7. Influence of Temperature and Oxygen Content on Pyrolytic Sooting Tendency as Determined by the Micropyrolysis Index 138

7.1.Introduction 138
7.2.Experimental 139
7.2.1.Variations from original MPI method 139
7.3.Results and discussion 140
7.3.1.Influence of temperature on the nature of soot from toluene 140
7.3.2.Influence of oxygen incorporation on MPI 148
7.3.2.1.Methyl esters 148
7.3.2.2.Aromatic oxygenates 152
7.4.Application to Molecular Engineering strategy 156

8. Development of Strategies for Upgrading of Renewable Fuels 158

8.1. Introduction 158
8.2.Upgrading of triglycerides and methyl esters to fuels and specialty chemicals 159
8.2.1.Introduction 159
8.2.2.Influence of deoxygenation of on fuel properties 161
8.2.3.Estimation of olefin content and alpha olefin selectivity 163
8.2.4.Proof-of-concept reactive distillation semi batch reactor for maximizing alpha olefin yields 166
8.3.Influence of equilibrium and metal particle size on the hydrogenation/hydrogenolysis of diethylketone 171
8.3.1.Introduction 171
8.3.2.Experimental 173

8.3.2.1.Catalyst preparation 173
8.3.2.2.Catalyst characterization 173
8.3.2.3.Catalytic activity measurements 174
8.3.3.Results and discussion 175
8.3.3.1.Product equilibrium as a function of temperature 175
8.3.3.2.Reaction results as a function of temperature 177
8.3.3.3.Influence of metal particle size on product selectivity 182
8.3.3.4.Influence of ketone hydrogenation on resulting fuel properties 186
8.3.4.Conclusions 188
8.4.Condensation of light compounds present in bio-oil 189
8.4.1. Introduction 189
8.4.2.Condensation of light aldehydes and acids 191
8.4.3.Etherification of aldehydes and alcohols via metal catalysts 196
8.4.4.Overview of strategy for condensation of light bio-oil compounds 199
8.5.Conclusions 201

9. Novel Emulsion Catalysts for Upgrading of Bio-Oil 204

9.1. Introduction 204
9.2.Experimental 209
9.2.1.Catalyst preparation 209
9.2.2.Reaction procedure 209
9.3.Results and discussion 210
9.4.Conclusions and potential applications 212

10. Outlook and Path Forward 214

LIST OF TABLES

Table2.1 (a) Predicted fuel property values for paraffins and cycloparaffins. (b) Predicted fuel property values for aromatics and olefins. 27

Table2.2 Parameter values for equation (1). 31

Table3.1 MPI values of several hydrocarbons (n-alkanes, isoalkanes, and cycloalkanes) in the C_6-C_{11} range. 53

Table3.2 Equation used and molecular information encoded in the descriptors used to predict MPI of unmeasured molecules. 63

Table3.3 Experimental TSI values and predicted MPI values for several pure hydrocarbons. 67

Table3.4 MPI and compositional analysis of several real fuel mixtures. 72

Table4.1 Feeds utilized in this study. 82

Table4.2 Adsorption constants of various nitrogen containing compounds. 88

Table5.1 Model compounds utilized in the present study. 111

Table5.2 Definition of ratios used to predict product selectivity. 112

Table5.3 Predicted values for CN, MPI, and specific gravity of several substituted cyclohexanes, as well as the linear average of their predicted primary products. 124

Table7.1 Maximum peak heights of TPO profiles as a function of temperature for toluene, benzaldehyde, and benzyl alcohol. 156

Table8.1 Resulting product distributions from the conversion of methyl-laurate at 320°C and 80psig. 169

Table8.2 Resulting product distributions from the conversion of trilaurin at 320°C and 80psig. 170

Table8.3 Influence of metal particle size and support on catalytic activity and selectivity at 200°C. TOF were measured at 12% conversion of DEK, assuming 1 adsorbed CO molecule per active site as measured by CO chemisorption. 183

Table8.4. Reaction results from the etherification of 2-methylpentanal over Pd/SiO_2 catalysts in a flow reactor maintained at 125°C in H_2. 198

LIST OF FIGURES

Figure1.1 Schematic overview of molecular engineering strategy. 3

Figure2.1 a) Calculated *versus* observed CNs. The error is well dispersed, and does not deviate much from the ideal slope of 1. **b)** Comparison between the Root Mean Squared errors of the calculated values and the number of descriptors included in the CN model. 25

Figure2.2 Deviations from non-linear mixing of pure component ON's of a binary mixture. 29

Figure2.3 Predicted *versus* observed RON and MON octane values for olefins and aromatics (a,b), and n, iso, and cycloparaffins (c,d). 33

Figure2.4 Predicted *versus* experimental values for TSI. 35

Figure2.5 Comparison of soot yield for various hexanes. 37

Figure2.6 Molecular composition of matrix fuels. 39

Figure2.7 Engine-out exhaust PM results from tests of several fuels at fixed speed/load conditions of an advanced, high-speed, direct injection diesel engine. 39

Figure3.1 Schematic description of the apparatus used to obtain MPI values by pyrolysis of a 20μL liquid sample across an α-Al_2O_3 placed in a ¼ in. o.d. quartz tube, held at 850 °C. A He flow rate of 25mL/min was maintained through the system, and a backpressure regulator was used in order to maintain a pressure of 10 psig. 47

Figure3.2 Comparison of MPI values obtained in this work with TSI values from the literature. 57

Figure3.3 Effect of aromatic content in mixtures. Aromatics tetralin, toluene, and benzene were blended with methylcyclohexane in various volume percentages. The resulting effect on MPI is shown. 59

Figure3.4 Comparison between MPI values obtained in this work and TSI values from the literature. 61

Figure3.5 Parity plot of predicted vs. experimental values of MPI through the use of QSPR. 64

Figure3.6 MPI predicted values as a function of number of carbon atoms for various classes of non-aromatic hydrocarbons. 66

Figure3.7 Predicted MPI values vs. experimental TSI values obtained from the literature. 68

Figure3.8 (a) Comparison between predicted MPI and experimental CN values obtained from literature for n-alkanes and isoalkanes. (b) Comparison between the (moles of carbon deposited)/(moles of carbon injected) and CN. Arrows indicate the direction of increasing number of carbons/molecule. 69

Figure3.9 (a) Comparison between predicted MPI and experimental CN values obtained from the literature for n-alkanes and cycloalkanes. (b) Comparison between the (moles of carbon deposited)/(moles of carbon injected) and CN. Arrows indicate the direction of increasing number of carbons/molecule. 71

Figure4.1 Overview of catalytic steps involved in the upgrading of diesel and gasoline fuels. 78

Figure4.2 Conversion of tetralin over $NiMo/Al_2O_3$ at 100psig, 345°C. Model feeds 1,4, and 5 (see table 4.1). 84

Figure4.3 Adsorption constants K (obtained from the kinetic fittings) as a function of the number of aromatic rings. 85

Figure4.4 Influence on nitrogen containing compounds on conversion of (a) phenanthrene and (b) tetralin. 87

Figure4.5 Correlation between the adsorption constant of the organonitrogen compounds and the negative Mulliken charges on the nitrogen atoms as calculated with DFT. 89

Figure4.6 RON values of mono-ring aromatic hydrocarbons before and after hydrogenation. 92

Figure4.7 Influence of position of selective ring opening on research octane number for selective ring opening of methylcyclohexane. 93

Figure4.8 RON values for potential ring contraction products resulting from methylcyclohexane. 94

Figure4.9 RON resulting from the selective ring opening of 1,2-dimethylcyclopentane. 95

Figure4.10 Ratio of cleavage at substituted positions on the ring to unsubstituted positions on the ring as a function of conversion over Ir based catalysts in a flow reactor at 593 K and 3540 kPa. The hydrogen/hydrocarbon ratio was maintained at 30. The ratio on the y-axis represents cleavage at positions $(a+b)/c$. Open diamonds represent a support of SiO_2, closed triangles represent Al_2O_3, and open squares represent TiO_2. 96

Figure4.11 Schematic reaction system configurations. 98

Figure4.12 (A) RON and (B) MON of the product mixture resulting from conversion of methylcyclohexane following the reactor bed configurations outlined in figure 4.11. Total pressure = 2MPa; H_2/feed molar ratio=40. 99

Figure5.1 Metal Catalyzed ring opening preceded by acid catalyzed ring contraction. 107

Figure5.2 Parity plots for predicted ratios shown in table 5.2. Numerical values which were predicted are *(a)* Ratio1/statistical ratio, *(b)* Ratio2, *(c)* Ratio3, and *(d)* Ratio4/statistical ratio. 114

Figure5.3 Effect of branch length and position on Ratio 1. 116

Figure5.4 Ratio 2 as a function of increasing number of carbon atoms, and distribution of carbons on the branches. 118

Figure5.5 Ratio 3 as a function of length of alkyl branch for monosubstituted cyclohexanes. 119

Figure5.6 Ratio of cleavage on the branch to cleavage on the ring divided by the statistical ratio of each type of bond available to open for monosubstituted alkylcyclohexanes. 120

Figure5.7 Ratio1 and Ratio 3 plotted against increasing length of linear R group for 1-R-2-methylcyclohexane. 121

Figure5.8 Measured product selectivities and the resulting CN at 4% conversion of 1-propyl-2-methylcyclohexane over Ir/Al_2O_3 at 603K and 500psig of H_2. The linear average CN was obtained by multiplying the product selectivities by each compound's predicted CN, as predicted according to chapter 2. 122

Figure5.9 Predicted CN values and predicted primary product distribution to estimate the CN of primary products. 123

Figure6.1 Conceptual schematic of molecular engineering strategy as applied to biofuels. 127

Figure6.2 Change in a) Research Octane Number (RON); b) water solubility; c) vapor pressure of products exiting a flow reactor across Cu or Pd catalysts as a function of feed conversion. 133

Figure6.3 Predicted vs. Observed values for the calculation of RON of oxygenated hydrocarbons. 134

Figure7.1 Toluene TPO profiles as a function of temperature. 141

Figure7.2 SEM images of MPI soot deposited on Al_2O_3 from 20μL of toluene at 900 and 1000°C. 142

Figure7.3 Same spot TEM images obtained for soot deposition from toluene at 1000°C, followed by a partial oxidation to 550°C via TPO. 143

Figure7.4 Same spot TEM images obtained for soot deposition from toluene at 1000°C, followed by a partial oxidation to 550°C via TPO. 145

Figure7.5 Same spot TEM images obtained for soot deposition at 1000°C, followed by a partial oxidation to 550°C via TPO. 146

Figure7.6 TPO profiles observed for identically prepared samples of n-octane pyrolyzed at 900°C with various heating ramps. Thin blue lines represent the TPO signal, while thick red lines represent the temperature ramp as a function of time. 147

Figure7.7 Influence of oxygen on the amount of carbon deposited at 850°C for various alkanes and their corresponding methyl esters. 149

Figure7.8 Mol C deposited as a function of temperature for n-dodecane and methyl-dodecanoate. 150

Figure7.9 TPO profiles for dodecane and methyl-dodecanoate deposited at 850, 950, and 1000°C. 151

Figure7.10 Measured smoke point heights for toluene, benzaldehyde, and benzyl alcohol. 154

Figure7.11 Mol C deposited as a function of temperature for toluene, benzaldehyde, and benzyl alcohol**.** 155

Figure8.1 Cetane numbers obtained from the literature of methyl esters and n-paraffins as a function of the length of the continuous carbon chain. 163

Figure8.2 H-NMR spectra of n-heptane, 1-heptene and its olefinic isomers. 165

Figure8.3 Schematic of novel reactor for α-olefin conversion from methyl esters and triglycerides. 167

Figure8.4 Equilibrium conversion of diethylketone to 3-pentanol as a function of temperature. 176

Figure8.5 Concentrations leaving the reactor as a function of W/F at 200^{o}C. Solid circles represent the feed (diethylketone), hollow squares represent 3-pentanol, and solid triangles represent pentane and pentene. 177

Figure8.6 Ratio of 3-pentanol/diethylketone as a function of W/F at 200^{o}C. Symbols represent experimental ratios while the line represents the equilibrium ratio. 178

Figure8.7 Concentrations leaving the reactor as a function of W/F at 225^{o}C. Solid circles represent the feed (diethylketone), hollow squares represent 3-pentanol, and solid triangles represent pentane and pentene. 179

Figure8.8 Ratio of 3-pentanol/diethylketone as a function of W/F at 225^{o}C. Symbols represent experimental ratios while the line represents the equilibrium ratio. 180

Figure8.9 Concentrations leaving the reactor as a function of W/F at 250^{o}C. Solid circles represent the feed (diethylketone), hollow squares represent 3-pentanol, and solid triangles represent pentane and pentene. 181

Figure8.10 Ratio of pentanol/diethylketone as a function of W/F at 250^{o}C. Symbols represent experimental ratios while the line represents the equilibrium ratio. 182

Figure8.11 Comparisons of research octane number, water solubility, density, and vapor pressure of products exiting the reactor as a function of conversion for 200, 225, and 250°C. 187

Figure8.12 Schematic base catalyzed of aldol condensation mechanism for propanal. 193

Figure8.13 Schematic of potential route for producing valuable diesel range products from low value bio oil streams. 200

Figure9.1 Conceptual illustration emphasizing the need for selective strategies for upgrading of bio oil. 205

Figure9.2 Preferential orientation of black sand at the oil/water interface upon addition to an oil/water mixture. The top phase is 1-heptene, while the bottom is water. 206

Figure9.3 Schematic of water in oil vs. oil in water emulsions as prepared via nano-hybrids. Blue spheres represent silica particles while black lines represent carbon nanotubes. 207

Figure9.4 Influence of varying decalin/water ratio on emulsion volume. Emulsions are indicated by the black, non-transparent layer. 208

Figure9.5 Conversion of model compounds in the emulsion vs. oil or water phase alone. 211

ABSTRACT

The combination of Quantitative Structure Property Relationships (QSPR) with experimental studies using model compounds provides great promise for fuel upgrading. Through this approach, QSPR software is utilized to predict fuel properties of interest for model compounds as well as for any potential reaction products. Catalytic studies are performed in combination with QSPR, attempting to maximize selectivity to products with the optimal fuel properties of interest. QSPR provides the direction to which specific chemical bonds should be broken or formed to optimize fuel properties, while model compound studies relate the properties of the catalyst and reaction conditions to the selectivity towards specific products. The end result is a guided approach to catalyst design which maximizes knowledge gained, with a constant link to practical application through fuel property prediction. This methodology has a dual benefit. While practical advancement for fuel improvement is gained, fundamental knowledge is developed about relationships between specific molecules and catalysts.

In this contribution, examples will be given for the development of important fuel properties, their prediction with QSPR, and further optimization through model compound studies. A further extension of QSPR will then be made in order to predict not only fuel properties, but primary product selectivities as well. Transitioning of these strategies to oxygenated hydrocarbons more representative of renewable fuel sources

(e.g. biomass) will also be discussed. This methodology allows the development of not only novel catalytic strategies utilizing conventional reactors, but also a new catalytic system with enormous potential through the use of nano-hybrids at the oil-water interface.

CHAPTER 1

1. Overview of Molecular Engineering Strategies as Applied to Fuel Upgrading

1.1 Introduction

Molecular engineering is a term not commonly associated with fuel upgrading. Fuels have become such a fungible quantity over the years that it is a common perception that fuel upgrading technology is well established. In reality, however, increasingly stringent environmental regulations and the transition towards renewable fuel resources have led refiners to embrace the concepts of molecular management and molecular engineering. Through these techniques, advancements are made in leaps and bounds towards establishing improved catalytic strategies for fuel upgrading. In addition to practical applications, valuable fundamental knowledge is obtained which then can be applied towards future strategies.

The concept of *molecular management* has been implemented in refining operations for some time. In simple terms, molecular management implies having the right molecule in the right place, at the right time and at the right price.[1] By applying these concepts, refiners have developed separation and conversion processes that allow them to more accurately select the mix of crudes with properties that maximize the performance of products with higher demand at a given time (gasoline, kerosene, or diesel). The closely related concept of *molecular engineering* as applied to fuels implies a higher level of molecular manipulation, indicating a purposeful design of

molecules with precise structures and well-defined properties. To achieve this high level of chemical specificity, the continuous improvement of catalytic materials is essential.[2]

A number of properties determine the quality of a given fuel. We can mention octane number, cetane number, sooting tendency, water solubility, freezing point, viscosity, flash point, cloud point, autoignition temperature, flammability limits, sulfur content, aromatic content, density, boiling temperature, vapor pressure, heat of vaporization, heating value, thermal and chemical stability, and storability. Many of these properties can be modified by catalytic upgrading. In designing a catalytic upgrading strategy, a refiner must know how each of these properties is affected by the structure of the molecule and how a given catalytic conversion of that structure in turn affects the properties.

For example, catalytic cracking on an acidic zeolite, converting long alkanes into shorter and branched hydrocarbons would increase octane number and vapor pressure, while decreasing viscosity and density. Of course, fuels have a large number of components and for many fuel properties the overall value for the mixture depends non-linearly on the individual properties of the components.[3] However, it is certainly of great value to understand how the structure of a given molecule in the mixture affects each of the properties of interest. This knowledge can serve as a guide to determine what reaction paths would be the best candidates to optimize a specific fuel property of a complex mixture.

There are many examples in the literature in which the molecular engineering approach has been applied for the upgrading of fossil fuels. By contrast, the same rational approach has been used more sporadically in the upgrading of biofuels. This provides enormous opportunity for the development of novel strategies in this area. Although the catalytic strategies which result from the implementation of this molecular engineering approach may be vastly different, the methodology which was utilized is constant. This methodology, and the wide range of problems it can be utilized to solve, will be the focus of this contribution.

1.2 Methodology

The notion of molecular engineering as applied to catalytic upgrading of fuels is illustrated in the conceptual triangle depicted in Figure 1.1.

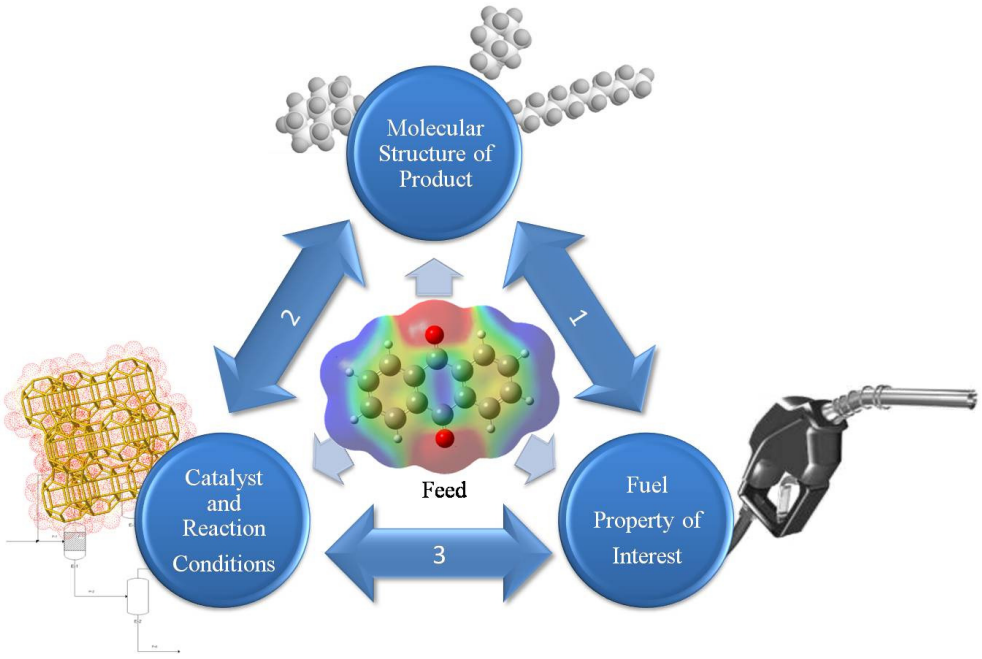


Figure 1.1 Schematic overview of molecular engineering strategy

In order to optimize a fuel property of interest it is first necessary to develop a database of properties for the possible molecular components, which can either be obtained experimentally or predicted with reliable methods based on the molecular structure (*relationship 1*). Then, one needs to obtain fundamental understanding on how different potential catalysts and processes modify the structure of a given reactant to obtain the resulting products (*relationship 2*).

This understanding provides direction towards which specific chemical bonds will be broken or formed under specific conditions. We can identify the "1+2" path as the molecular engineering approach, while the direct path "3" would be an empirical approach. The rational approach takes into account that by knowing the relationship between molecular structure and the desirable fuel properties one has the ability to modify different aspects of the catalyst and the reaction conditions to optimize specific structures, resulting in the optimum properties.

1.2.1 Relationship 1: Molecular Structure-Properties:

While it is advantageous to have reliable experimental data for each of the fuel properties of interest, in many cases the only information known about a given compound is its molecular structure. Therefore, correlations between fuel properties and molecular structure need to be used.

The most commonly used correlations are the so-called Quantitative Structure Property Relationships (QSPR), first used more than 40 years ago in agrochemistry,[4] but they have expanded onto many fields. QSPRs are models that correlate molecular

descriptors, i.e., numerical values calculated from the molecular structure, to specific properties of the corresponding compounds. Molecular descriptors involve geometric, steric and electronic aspects of the molecule and can range from very simple physical parameters such as the number of carbon atoms or branches in a molecule, to more complex parameters such as dipole moment or surface area. Commercial QSPR softwares calculate hundreds of molecular descriptors. Specific, computationally expensive descriptors are sometimes needed and they can be calculated through higher order calculations such as density functional theory.[5] Ideally a researcher could use chemical intuition to select which descriptors are more relevant for a particular property. However, in many cases the relationships between molecular descriptors and properties of interest are too complex, so genetic algorithms and neural networks may be utilized to reduce the number of possible descriptors from several hundreds to a much smaller number that correlate best with the desired property.

After the descriptors have been selected, different models can be created through the use of linear regressions, nonlinear regressions, principal component analysis, genetic algorithms, and artificial neural networks. Care must be taken to ensure that the models capture desired trends without over-fitting the data. For this reason, cross-validation of the model is an important step. Application of QSPR to fuel properties has resulted in models that can estimate Cetane Number,[6,7] Octane Number (research octane number, RON, and motor octane number, MON),[8] and sooting tendencies[9] of any fuel component, only on the basis of the molecular structure.

1.2.2 Relationship 2: Catalyst-Reactivity-Structure:

The understanding of these relationships at the molecular level has been the goal of many modern research studies in catalytic fuel upgrading. Elegant examples abound in the catalysis literature.[10] These relationships can be investigated following different approaches: in one of them, the effect of varying the reactant molecular structure is studied while keeping the type of catalyst unchanged. In another approach, the variable is the structure/composition of the material that catalyzes a fixed probe molecule. An interesting example of this type of study has been the selective ring opening of naphthenic molecules on noble metal catalysts.[11,12] Only one endocyclic C–C bond per naphthene ring must be opened to preserve the reactant molecular weight while producing isoalkanes of high octane number. Over conventional hydrocracking catalysts, the yield of alkanes with the same number of C atoms as the cyclic reactant naphthenes is typically very low due to secondary cracking. Since 5-member rings open much more readily than 6-member rings, an acidic catalyst that catalyzes the ring-contraction reaction converting alkylcyclohexanes into alkylcyclopentanes coupled with a high-activity hydrogenolysis metal catalyst, such as Ir, was proposed.[11] This bifunctional catalyst is many times more selective for ring opening than conventional hydrocracking catalysts. Likewise, alkane cracking reactions on FCC catalysts have been intensively investigated for many years; very good correlations between reactivity and chain length, as well as number and type of substituents have been found for different catalyst compositions and reaction conditions.[13]

The investigation of novel catalyst formulations has evolved from simple parallel screening of different catalysts to modern high-throughput techniques combined

with theoretical calculations (DFT) that guide the selection of formulations, as opposed to empirical testing, and minimize the number of experiments. At the same time modern characterization techniques help to better understand the nature of the active site.[14]

1.3 Utilization of molecular engineering strategies towards upgrading of fuels

The application of this molecular engineering strategy towards fuel upgrading has a vast range of possibilities. This will be expressed with the extensive array of projects with which the strategy has been applied. Behind each project is a fundamental focus on understanding the nature of reactions in order to provide some indication of the surface intermediates involved (relationship 2). The overall strategies are always driven by a practical optimization in fuel properties (relationship 1). Knowledge gained from these studies has both a primary and secondary impact. The primary effect is to directly apply it in order to tailor a catalyst or series of catalysts to optimize the specific feedstock. The secondary effect is the insight gained which can then be applied towards upgrading of various other feedstocks in the future.

Prediction of fuel properties is not a new technique, nor is fundamental heterogeneous catalysis. What is truly novel about this approach is the link between the two, where fundamental studies are conducted with a constant emphasis on fuel property optimization. This provides a crucial link between fundamental research and practical applicability. Through this approach, strategies are developed which not only

work, but valuable knowledge has been gained such that it is known *why* these strategies work as well.

References

1 M.M.S. Aye, M. Zhang *Chem Eng Sci.* **2005**,60,6702.

2 J. R. Katzer *Energy and Transportation: Challenges for the Chemical Sciences in the 21st Century*, The National Academy Press. **2003**.

3 N.V. Pasadakis, V.Gaganis, C. Foteinopoulos *Fuel Proc Tech.* **2006**,87,505.

4 C. Hansch, T. Fujita *J Am Chem Soc.* **1964**,86,1616.

5 T. Puzyn, N. Suzuki, M. Haranczyk, J. Rak *J Chem Inf Model.* **2008**,48,1174.

6 R.C. Santana, P.T. Do, W.E. Alvarez, J.D. Taylor, E.L. Sughrue, D.E. Resasco *Fuel.* **2006**,85,643.

7 J. Taylor, R. McCormick, W. Clark Relationship between molecular structure and compression ignition fuels, both conventional and HCCI. August **2004** NREL Report on the MP-540-36726, Non-Petroleum-Based Fuels

8 P. Do, S. Crossley, M. Santikunaporn, D.E. Resasco *Catalysis: Specialist Periodical Reports*. The Royal Society of Chemistry, London **2007**,20,33.

9 S.P. Crossley, W.E. Alvarez, D.E. Resasco *Energy Fuels.* **2008**,22**,**2455.

10 F.G. Gault *Adv Catal.* **1981**,30,1.

11 G.B. McVicker, M. Daage, M.S. Touvelle, C.W. Hudson, D.P Klein, W.C. Baird Jr., B.R. Cook, J.G. Chen, S. Hantzer, D.E.W. Vaughan, E.S. Ellis, O.C. Feeley *J Catal.* **2002**,210,137.

12 P.T. Do, W.E. Alvarez, D.E. Resasco *J Catal.* **2006**,238,477.

13 Y.V. Kissin *J Catal.* **1990**,126,600.

14 J.C. Dellamorte, M.A. Barteau, J. Lauterbach *Surf Sci.* (in press)

CHAPTER 2

2. Prediction of Fuel Properties for Conventional Fuels

2.1. Importance of fuel property predictions

In order for the molecular engineering approach to be practical, each model compound study must have some connection with fuel properties. This provides guidance for the molecular engineering strategy, with the goal of understanding fundamental reactions while perpetually linking them to the fuel properties which result. The end result is a guided development of optimized catalytic strategies built on a strong fundamental foundation. The optimal approach would be to utilize experimentally measured properties for each model compound produced. The problem with this is even simple model compound reactions can produce a plethora of products. Many compounds which are produced have properties which have not been measured experimentally. Several factors, including cost, separation techniques, volume, and time required make the experimental measurement of each compound produced impractical for most cases. For this reason, some method must be developed in order to estimate the properties of fuels which have not been previously measured.

While links between bulk fuel properties and spectroscopic techniques such as NMR, IR, or GC have been made previously, these traditionally hold only for a specific species of fuels or fuel mixtures. The structure-property relationship which is

ultimately extracted may be very simple, such as correlating aromatic content with octane number, etc. While these techniques are often very practical on a real fuels basis, they rarely are able to distinguish the minute differences between similar molecules which can account for changes in fuel properties. Model compound studies are often conducted in extremely small volumes, and the only thing known about the products is their molecular structure. This places a tremendous value on the ability to predict the properties of molecules based only on their molecular structure. This is conducted through the use of Quantitative Structure Property Relationships, which will be explained shortly, and are widely utilized to provide direction for fuel upgrading.

2.2. QSPR methods for property predictions

As said by George Box, a statistician from the University of Wisconsin, "All models are wrong, some are useful." This statement is especially true for fuel property prediction. One of the most promising techniques for the prediction of fuel properties is based on an assumption which is many times wrong, but very useful. This is the assumption that molecules with similar structures have similar activities and properties.

The fallacy of this technique is known as the SAR paradox, which points out that molecules with very similar structures can have radically different activities based on other aspects. Examples of this effect abound in the literature. A simple example in catalysis is the difference in isomerization reactivity in HZSM-5 for ortho, meta, and para-xylene. These are all molecules with very similar structures, but widely different reactivities. This hurdle can be overcome, however, through the use of *Quantitative Structure Property Relationships* or QSPR's. These are simply models which relate

various aspects of molecular structure to fuel properties of interest. Different weights are placed on various molecular features, such that models are created which are able to relate the underlying molecular features which are responsible for variations in a specific property. For the previous example, the xylene comparison is actually due to the kinetic diameter of the molecules with respect to the zeolite pores, which changes dramatically with the branch positions. This can be estimated by taking into account the proximity of the methyl branches, the ovality of the molecule, and the overall surface area. While this is not a direct measurement of the kinetic diameter, they are related. A model can then be created which emphasizes particular aspects of the structure which are directly responsible for fuel properties. A similar example is the reactivity of α vs. β-tetralone. β-tetralone is a much more reactive compound due to the lack of conjugation with the aromatic ring. In order to estimate this, molecular facets such as the charge on the oxygen atom, or the dipole moment can be utilized to predict this behavior. While this is not the true explanation for why the molecules behave differently, these molecular features can be utilized to capture the trends of interest. For this reason, we are creating models which are not completely accurate from a fundamental sense, but extremely useful.

QSPR's are created by correlating molecular descriptors, which are numerical values calculated from the molecular structure, to properties of molecules. This is accomplished by creating a database with known fuel properties of interest, along with known molecular structures. A model is then created which outputs the desired fuel property as a function of a set of molecular descriptors. The end result is a model with

the ability to estimate fuel properties of molecules based only on their molecular structure.

Molecular descriptors can range from very simple descriptors such as the number of carbon atoms, or branches in a molecule, to more complex descriptors such as dipole moment or surface area. Our group typically uses descriptors calculated via the software MDL® QSAR (version 2.2.0.0.446 (SP1) from MDL Information Systems, Inc.), which has the ability to calculate over 400 descriptors based only on molecular structure. If more complex descriptors are needed, more computationally expensive descriptors may be calculated through the use of density functional theory, etc. In order to determine which molecular descriptors should be utilized in a model, genetic algorithms are utilized. This reduces the number of descriptors from ~400 to a much smaller number which correlate best with the desired fuel property. Many types of models can then be created through the use of linear regression, nonlinear regression, regression of principle components, all possible subsets regression, and artificial neural networks. Each of these models has inherent strengths and weaknesses, and each could be the optimum solution depending on the situation. Because of this, QSPR's are created on a case-by-case basis. A brief outline of the various correlation techniques, along with their applicability to fuel property prediction is discussed in the next section.

2.3- Correlation methods

2.3.1- Genetic algorithms

2.3.1.1 General overview of genetic algorithms as applied to descriptor selection

Genetic algorithms as applied to fuel property prediction are statistical algorithms which function as a random search tool for descriptor selection. The functionality of these is the same as other random search tools, such as various other Monte Carlo techniques, to minimize the computational time required to find an optimum solution. The idea of genetic algorithms is based on the theory of evolution such that over time the animal with the optimal chromosomes will be determined out of random mating. For this reason, statistical terms are replaced with biological terms, but the underlying statistical procedure is very similar to other random search methods. In spite of the random foundation of this technique, genetic algorithms have several tunable parameters which are tailored for the specific problem of interest. The end result is a technique which allows one to find the descriptors which best relate to a given fuel property with minimal computational time.

An overview of the genetic algorithm strategy as applied to QSPR or QSAR will now be attempted with a continual relation to what the model is actually doing to select the best descriptors. As a starting point, the problem is broken up into "animals" which

is synonymous to models which relate molecular descriptors to the desired fuel property. Each animal has a set of "chromosomes" or molecular descriptors associated with it. If a set of descriptors is included in the model or not is indicated by a code consisting of 0's for not included and 1's for included. The order of the numbers remains the same to serve as placeholders, so a model which started with 100 descriptors with an optimized solution of 3 would consist of a code of 97 0's and three 1's. A value is placed on each "animal" or model by comparing how well it is able to correlate the molecular descriptors to the fuel properties in the database, as well as how many degrees of freedom were utilized. This is a tunable parameter such that the number of descriptors selected as an output of the genetic algorithm can be altered by placing a heavier or lighter weight on the number of descriptors utilized. This is very important to have a tunable parameter for this section, as too few descriptors will not capture the trends in the data, while too many will lead to a model which over fits. This provides the direction for which the genetic algorithm operates.

A set of animals is first chosen as the initial population. A larger initial population will increase computational time, but also have a lower chance at arriving at a solution which is a local minimum. The way the model incorporates random search is to rank the models in order of the desired scoring (fitness) and call this set of animals a "generation". The animals of each generation are allowed to "mate" that is randomly exchange descriptors and generate offspring. This allows for the best descriptors to be selected over time. After each generation, some of the weakest members are replaced by some of the best. In order to avoid arriving at a local minima, or "focusing," the term "mutation" is introduced where randomly selected descriptors are changed from

zero to one and vice versa. This increases time to find the solution, but it helps to push the solution out of valleys of local minima and find the optimum solution in the end. Initial sample size, probability of mating, probability of mutation, and rate of population updating are tailored inputs to the model. There is a tradeoff among all of these values between arriving at the global minimum and minimizing computational time.

2.3.1.2 Fitness function and initial sample selection

Thus far, we have discussed the algorithm very generally, though we have not mentioned how the initial populations are obtained, the specifics of the fitness function, or how mating and mutation are handled.

The fitness function utilized is Friedman's Lack-of-fit scoring. This is defined as:

$$Lack\ of\ Fit = \frac{\frac{RSS_p}{N}}{\left(1 - \frac{d * (p+1)}{N}\right)^2}$$

Where

p=number of independent variables (descriptors) in the model

N= number of samples (experimental measurements) in the data set

RSS_p= residual sum of squares based on the regression model using p independent variables

d= smoothing factor (tunable parameter)

The smoothing factor is the tunable parameter in this model, as larger values of d shift the minimum lack of fit towards smaller values of p (less descriptors). As this

function is minimized over time, value is placed on minimizing the error in the data set while also minimizing the number of descriptors required.

Initial sample selection can be conducted through a variety of measurements, but the most common technique utilized for the following procedures is tournament selection. Through this process, each member of the initial population must first win a tournament among itself and a set number of animals, each with randomly selected descriptors. If, for example, the initial population size is 32, and the tournament size is 4, each of the original 32 animals (or models) must first win a tournament (have the best fitness) among itself and three other animals with randomly generated descriptors. This provides a much improved starting point for the genetic algorithm descriptor selection process, further minimizing computational time.

2.3.2 All Possible Subsets Regression

All possible subsets regression is utilized when one wants to compare every possible combination of a given set of descriptors. This ensures that the optimum solution is reached, but the computational time is very expensive. The total number of subsets required is 2^p where p indicates the number of descriptors. For this reason, this method is very useful for finding the optimal solution out of a relatively small set of input descriptors. It is extremely useful, for example, if one wishes to find the optimum five descriptors out of an initial set of 10. When starting with a large set of descriptors, such as 100, this method is not practical. In order to utilize this method, some pre-selection of descriptors is required in order to bring the allotted number to a value

which is reasonable to work with. The ideal method of pre selection is through intuition, but when structure property relationships are complex, statistical techniques may also be utilized. A very useful strategy involves utilizing a genetic algorithm with a low scaling factor. This gives a set of descriptors that is too large to create a model with, but much smaller than the original number. All possible subsets regression is then conducted in order to determine the optimal descriptors out of this set.

2.3.3 Regression of Principal Components

Relationships between a molecular structure and fuel properties are often very complicated. Because of this, multiple descriptors are sometimes needed in order to capture all of the molecular features responsible for variations in a specific fuel property. This may lead to a high degree of correlation, or multicollinearity, between various descriptors for the specific data set. For these cases, principal components are particularly useful.

The idea behind principal component regression is to replace many highly correlated descriptors with few non-correlated descriptors, or principal components. Principal components are found by computing the eigenvectors and eigenvalues of the correlation matrix, and multiplying the matrix of observed values of independent variables by these eigenvectors. Principal components are naturally orthogonal, so complications due to multicollinearity are avoided. Each principal component contains some aspect of each descriptor, and the greatest amount of variance in the data is captured by the principal component with the highest eigenvalue. Because most of the variance in the data is captured by the principal components with the highest

eigenvalues, models are created by utilizing the descriptors with the highest eigenvalues. Ideally with this approach, by fitting a model with only the principal components that capture the most variance, one is capturing the true trends in the data as opposed to the noise. Observations of the contrary have been observed, however, as important trends are sometimes captured by the components with small eigenvalues as well.[1] This is still the exception to the rule, and regression of principal components can serve as an excellent tool for extracting the fundamental links to fuel properties out of highly correlated descriptors.

2.3.4 Artificial Neural Networks (ANN)

Artificial Neural Networks, or ANN's, serve as excellent tools for predicting fuel properties with a relatively large database. The primary advantage of this technique over other regression techniques is the ability to capture nonlinear trends between descriptors and fuel properties with greater efficiency. Through the utilization of ANN's, a greater number of descriptors may be utilized without over fitting the data when compared with other non-linear techniques. The main disadvantage is that it is nearly impossible to extract the fundamental relationships between the original molecular descriptors and the fuel properties. For this reason, ANN's are viewed as a "black box" technique, where data is put in, with a result in the other end. There is unfortunately no easy way to make sense of the true relationships which are being formed. ANN's are excellent tools for providing prediction models, but their black box reputation makes them somewhat less desirable for studying fundamental relationships.

ANN's were designed after the way the human brain works. Input data is fed to several neurons, or nodes, which contain functions. These then relay the data to other neurons in hidden layers, thus creating a series of functions. The most common form of ANN is the multilayer perceptron, or MLP. ANN's fit the data through "learning" or adjusting weights on the functions until the desired output is approached. As the learning process progresses, care must be taken in order to not over-fit the data. For this reason, one must stop the learning process as soon as the desired fitness is reached. One alternative method is to continuously cross-validate the model with an external set of data. This provides the best approach, as the error is minimized while avoiding over-fitting of the data. Genetic algorithms are often incorporated into ANN's in order to find the optimum number of hidden layers or descriptors to input. This provides an extremely useful fitting procedure for many types of problems.

2.4 Model validation

Creating models that fit experimental data is quite simple, with the main challenge in ensuring that the models are reliable. Care must be taken to ensure that the models capture desired trends without over-fitting the data. For this reason, cross-validation of every model is perhaps the most crucial step. This can be accomplished in three ways: cross-validation with an external data set, cross-validation via the leave-one-out method, and visual observation of trends.

The optimal route for model verification is through cross validation with an external data set which was not utilized in the creation of the model. After a model is

created, the molecules in an external data set are predicted and compared with the actual experimental values. If the error in prediction is significantly higher (order of magnitude) than the error in the training set, then the model is over predicting, and fitting the noise in the data. This is the optimal strategy for cross validation as it is a direct measurement of the ability of the model to predict properties of molecules. Care must be taken to ensure that the external data set is representative of the sample, and not a specific niche. As an example, an external dataset for prediction of CN of hydrocarbons should have some representative compounds from each of the species involved, such as paraffins, olefins, naphthenics, and aromatics. If the model was derived around each of these groups, but the external data set only includes paraffins, this is not a reliable test of the model. The only time in which this method should not be utilized is when the amount of data is extremely limited, such that one cannot afford to sacrifice any data points for the external data set. This is the only instance when other techniques, such as the leave-one-out method, should be utilized.

The leave-one-out method for prediction of fuel properties is a useful technique for estimating if a model is over-fitting the data when an external data set cannot be utilized. The concept of this model is very simple, that is a model is created by regressing every data point except for one. This one data point temporarily serves as the external data set, and its value is subsequently predicted by the model. The process is then repeated for each point in the data set, and the error is summed. If this error is significantly higher than the error for the model itself, then the model is over-fitting the data.

The final technique should be utilized every time a QSPR model is built, in collaboration with the above methods of validation. This is the comparison of observed trends to ensure that the model captures the trends in the data. This could be any simple case where one would expect a smooth trend. As an example, one could plot the variation in cetane number as a function of increasing carbon number for n-paraffins. If the model fits this trend in a jagged or sinusoidal fashion, then this is an indication that it is over-fitting the data. Model verification is extremely important for fuel property prediction. This is arguably the most critical step in the process, as without it no model would be trustworthy.

2.5 Prediction of important fuel properties of conventional fuels

2.5.1. Prediction of cetane number

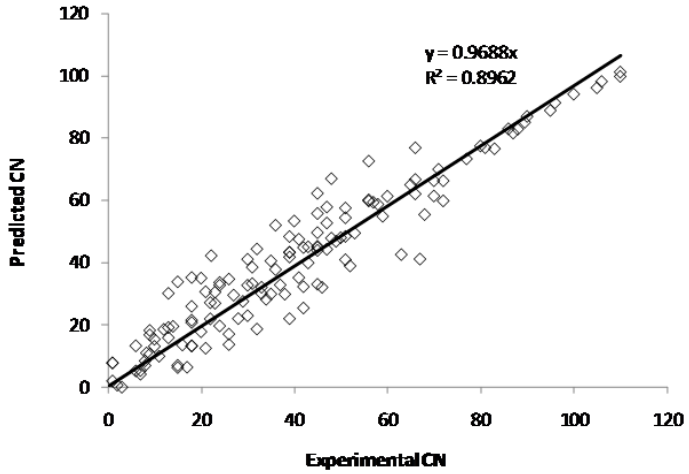
In the case of diesel fuel, an important property that defines the fuel quality is the cetane number (CN). This is a measure of the ability of a fuel to combust upon compression of the engine cylinder at high temperature and pressure. Fuels with low-CN have poor ignition quality (i.e. knocking, noise, PM emissions) and make starting the engine difficult on cold days. [2,3] It is well known that CN is lowest for PAHs and highest for n-paraffins.[4,5] In normal paraffins, CN increases with the number of carbon atoms in the molecule. For naphthenic compounds and isoparaffins the CN falls between those of aromatics and n-paraffins. In isoparaffins, the CN decreases as the degree of branching increases.[6]

Predictions of CN for bulk fuels have been made by several authors using a variety of different types of inputs including ^{13}C NMR, IR spectra, refractive index, parameter lumps, GC analysis, and multiple other types of properties.[7,8] In 1995, Ladommatos et al[8] introduced twenty-two equations to predict the CN of diesel fuel from various experimental properties. The predictive capability of some equations was high (standard error of CN < 2). He also reported that it is unlikely that the standard error can be reduced significantly below 1.5, because the measured cetane numbers are themselves subject to experimental error. However, more than ten years later, Ghosh et al.[9] reported an improvement in CN prediction with standard error of only 1.25. A simple composition-based model is used to correlate CN of diesel fuels with a total of 129 various hydrocarbon lumps determined by a group of supercritical fluid chromatography, gas chromatography, and mass spectroscopic methods.

These models allow us to estimate the CN of diesel fuel mixtures. However, to evaluate the impact of specific reactions on specific molecules, the cetane values of individual compounds are needed. For this purpose, molecular descriptors were used in order to predict the CNs of individual hydrocarbons. The quality of the model is represented by Figures 2.1 a and b. Figure 2.1a shows a plot of the CN values calculated from the model versus the actual measured CN inputs. This plot is important to ensure that the errors in prediction do not deviate significantly to one side or the other in a systematic way. As the number of molecular descriptors used in the model increases, the error between the calculated and measured values in the model continuously decreases. To prevent an over-fitting of the data a maximum number of descriptors is recommended. One can clearly see in Figure 2.1b that, as the number of

descriptors increases, the root mean squared (RMS) error in the model continuously decreases, while the error in an external set of data reaches a minimum and then increases again as over-fitting starts to occur. The external data set is composed of nine data points that represent the entire range of data. The reason for the smaller degree of error in the external dataset than in the model is that the external dataset consisted only of Ignition Quality Tester (IQT™) derived CNs from one particular machine. The database used to feed the model[10] was composed of both, engine test CNs and IQT measurements from various sources. The large variety of sources causes a relatively high error in the database itself, so if possible a single database source should be used.

a)



b)

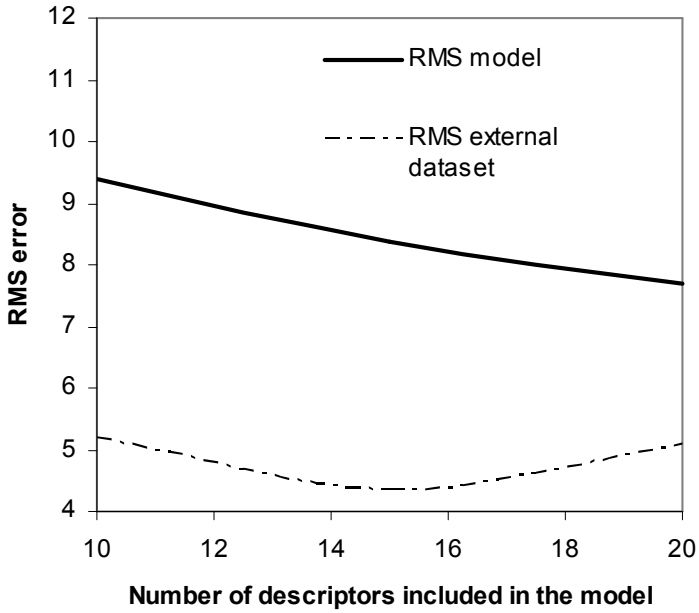


Figure 2. 1 a) Calculated *versus* observed CNs. The error is well dispersed, and does not deviate much from the ideal slope of 1. **b)** Comparison between the Root Mean Squared errors of the calculated values and the number of descriptors included in the CN model.

Compared with the artificial neural network (ANN) approach used in previous work to predict CN[11] the linear regression model by QSAR has a lower cross validation

error, meaning it has a lower degree of over-fitting. Furthermore, models created through this technique are not subject to the "black box" viewpoint, that is the relationship between molecular descriptors and predicted properties can be extracted. The linear regression model also has the added benefit of robustness, such that anyone who has the ability to calculate the QSAR descriptors can easily predict the CN of any individual compound. The predicted CN values, some of which are tabulated in Table 1, will be employed below to evaluate the different catalytic strategies to optimize the fuel.

(a)

Paraffins	TSI	RON	MON	CN	Cycloparaffins	TSI	RON	MON	CN
n-Heptane	2	0	4	52	1,1,2-Trimethylcyclohexane	13	96	91	29
n-Hexane	1	29	33	45	1,1,2-Trimethylcyclopropane	9	105	88	13
2,2,3,3-Tetramethylhexane	15	116	95	26	1,1,*cis*-2, *trans*-4-Tetramethylcyclopentane	12	100	95	21
2,2,3,3-Tetramethylpentane	8	117	92	21	1,3-Dimethylcyclohexane	7	65	64	31
2,2,3-Trimethylbutane	8	113	103	9	1,*cis*-2,*trans*-3-Trimethylcyclohexane	8	84	83	30
2,2,3-Trimethylpentane	9	106	100	14	1,*cis*-2-Dimethylcyclohexane	8	77	76	30
2,2,4-Trimethylpentane	5	96	97	21	1,*cis*-2-Dimethylcyclopropane	4	109	89	17
2,2-Dimethylbutane	8	89	96	23	1,*cis*-3,*trans*-5-Trimethylcyclohexane	6	70	66	23
2,2-Dimethylheptane	9	52	54	49	1,*cis*-3-Dimethylcyclohexane	7	65	64	31
2,2-Dimethylhexane	8	74	80	40	1,*cis*-3-Dimethylcyclopentane	6	76	73	27
2,2-Dimethyloctane	9	49	46	55	1,*cis*-4-Dimethylcyclohexane	7	71	66	23
2,2-Dimethylpentane	7	89	89	30	1,*trans*-2,*trans*-4-Trimethylcyclohexane	7	77	74	28
2,3,3-Trimethylpentane	9	111	102	17	1,*trans*-2-Dimethylcyclohexane	8	77	75	29
2,3-Dimethylpentane	3	88	83	20	1,*trans*-2-Dimethylcyclopropane	4	107	86	14
2,4-Dimethylhexane	2	62	67	29	1,*trans*-3-Dimethylcyclohexane	7	72	66	24
2,4-Dimethylpentane	1	88	83	28	1,*trans*-4-Dimethylcyclohexane	7	63	64	32
2-Methyl-3-ethylpentane	4	81	79	12	1-Methyl-1-ethylcyclohexane	14	67	76	39
2-Methylheptane	3	19	29	46	1-Methyl-*cis*-2-*n*-propylcyclohexane	7	25	37	38
2-Methylpentane	2	75	77	29	1-Methyl-*trans*-2-*n*-propylcyclohexane	7	26	36	36
3,3-Diethylpentane	12	83	97	17	3-Cyclohexylhexane	7	16	43	38
3,4-Dimethylhexane	4	71	73	20	Cyclopentane	5	98	79	26
3-Methylheptane	4	27	35	37	Cyclopentylcyclopentane	15	14	12	52
3-Methylhexane	3	57	59	27	Cyclopropane	5	149	125	5
3-Methylpentane	3	80	78	23	isopropylcyclohexane	9	64	60	35
4,5-Diethyloctane	7	0	25	18	Methylcyclohexane	7	70	70	30
Isononane	4	7	11	39	Methylcyclopentane	7	80	74	24
Isopentane	2	96	93	21	*tert*-Butylcyclohexane	14	96	85	31

(b)

Aromatics	TSI	RON	MON	CN	Olefins	TSI	RON	MON	CN
1,2,3-Trimethylbenzene	57	108	98	8	1-Pentene	6	89	76	14
1,2,4-Trimethylbenzene	54	110	102	5	2,2-Dimethyl-*trans*-3-hexene	12	109	93	12
1,2-Diethyl-3-methylbenzene	59	106	97	6	2,3,3-Trimethyl-1-butene	29	108	91	7
1,2-Dimethylbenzene	54	109	99	11	2,3,3-Trimethyl-1-pentene	31	105	90	16
1,3-Diethylbenzene	55	113	99	4	2,3-Dimethyl-1-butene	17	102	85	13
1,3-Dimethylbenzene	49	115	106	2	2,3-Dimethyl-1-pentene	17	98	83	18
1,4-Diethylbenzene	58	109	94	0	2,3-Dimethyl-2-hexene	16	93	80	24
1.2.3.5-Tetramethylbenzene	56	109	102	6	2,5-Dimethyl-2,4-hexadiene	11	92	76	21
1-Methyl-2-allylbenzene	68	92	81	9	2,5-Dimethyl-2-hexene	6	95	81	27
1-Methyl-3-ethylbenzene	54	113	102	5	2-Methyl-1-hexene	8	86	76	39
1-Methyl-3-*n*-propylbenzene	48	110	96	12	2-Methyl-*trans*-3-heptene	7	90	79	26
1-Methyl-4-ethylbenzene	55	114	102	2	2-Methyl-*trans*-3-hexene	6	99	86	16
Allylbenzene	63	106	93	3	3,4-Dimethyl-*cis*-2-pentene	12	101	85	0
Ethylbenzene	53	112	99	7	3-Methyl-*trans*-2-hexene	5	90	77	10
Isopropyl benzene (CUMENE)	59	112	102	6	3-Methyl-*trans*-2-pentene	6	97	82	6
Mesitylene	48	119	111	−7	4-Methyl-1-hexene	9	86	74	19
ortho-Xylene	54	109	99	10	4-Methyl-1-pentene	9	93	76	20
sec-Pentylbenzene	57	97	89	16	4-Methyl-*trans*-2-hexene	7	94	84	7
Styrene	67	107	94	0	4-Methyl-*trans*-2-pentene	5	98	85	10
tert-Butylbenzene	68	112	107	2	5-Methyl-*trans*-2-hexene	4	90	78	18
Toluene	49	111	101	4	*trans*-3-Hexene	4	92	82	11

Table 2.1 (a) Predicted fuel property values for paraffins and cycloparaffins. (b) Predicted fuel property values for aromatics and olefins.

2.5.2. Prediction of Octane Number

Octane number (ON) is a key parameter in determining the quality of gasoline. High ON means high resistance of the fuel against knocking. In a combustion engine, a compressed mixture of fuel and air is introduced. Due to the thermal stability of each molecule and the ensuing radicals, some molecules tend to burn sooner than others, which causes knocking.[12] There are two types of octane number tests: research octane number (RON) and motor octane number (MON). RON typically provides an indication of how the fuel will perform under mild driving conditions, while MON represents more severe conditions. (RON+MON)/2 is the current ON that is reported at the pump. These values are based on a scale on which isooctane is 100 (minimal knock) and heptane is 0 (bad knock). In general, aromatics (i.e. benzene, toluene, etc.) and isoparaffins have high ONs.[13] For isoparaffins, branching is desirable, because it increases ONs, which is in contrast to CN. Therefore, n-paraffins are undesirable in gasoline, while they are desirable in diesel. To achieve the goal of making gasoline more environmentally friendly, while keeping its ON high, aromatics need to be converted to isoparaffins in order to minimize losses in ON.

Similar to the case of CN predictions, the majority of the work reported in the literature has focused on the prediction of ON of gasoline mixtures.[14,15] For example, in the 1970s, Anderson, et al.[16] constructed a method to estimate the RON of different gasolines by using the results from gas chromatography. This model had a standard error of 2.8 points, probably due to the assumption of linearity in octane blending. Deviations due to nonlinear interactions among different hydrocarbons group (i.e. paraffins, olefins, aromatics, etc.) can be significant.[17] In order to estimate the ON of a

mixture of hydrocarbons, interactions between the molecules involved must be considered. It has been reported that hydrocarbons belonging to the same molecular class blend linearly; i.e., paraffins blend linearly with other paraffins, olefins blend linearly with other olefins, and so on. However, a blend of paraffins and olefins may exhibit significant deviations from linearity. A diagram that helps to illustrate this concept is shown in Figure 2.2.[12] Curve a displays a positive interaction or equivalently a positive deviation from linearity, curve c displays a negative interaction, and curve b displays no interaction.

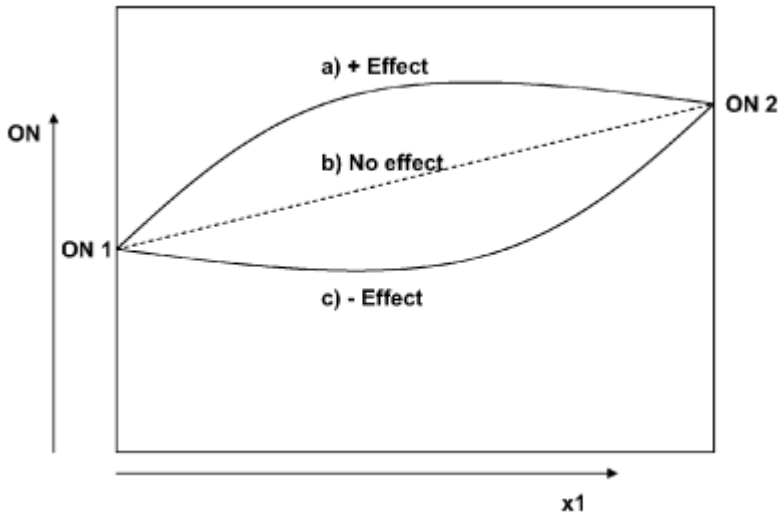


Figure 2. 2 Deviations from non-linear mixing of pure component ON's of a binary mixture. Adapted from ref.12.

For a mixture containing more than two compounds, this system becomes even more complicated. Very recently, Ghosh et al.[9,12] have created an improved model from experimental RON and MON data of 1471 gasoline fuels. GC analysis was conducted in order to determine the compositions of each fuel; then, molecular lumps were

generated and correlated to the RON and MON of the mixtures. Blending parameters were correlated to RON and MON by creating a constrained least-squared minimization problem and utilizing a Levenberg-Marquadt algorithm. Interaction parameters were obtained between large groups of molecules (i.e. between paraffins and olefins, etc.) in order to minimize the number of calculations. This molecular lumping technique proved to be quite accurate, with a standard error of ~1 for prediction of both RON and MON of fuel mixtures. The equation developed can be readily applied as follows:

$$ON = \frac{\sum_{PONA} v_i \beta_i ON_i + \left(\frac{k_{PN}^{(a)} v_n + k_{PO}^{(a)} v_O}{1 + k_{PN}^{(b)} + k_{PO}^{(b)} v_O} \right) \sum_{P} v_i \beta_i ON_i}{\sum_{PONA} v_i \beta_i + \left(\frac{k_{PN}^{(a)} v_n + k_{PO}^{(a)} v_O}{1 + k_{PN}^{(b)} + k_{PO}^{(b)} v_O} \right) \left(\sum_{P} v_i \beta_i - \sum_{P} v_i \right)} \qquad (1)$$

In this equation, all molecules are divided into four groups: paraffins (P), olefins (O), naphthenics (N), and aromatics (A). The v_i values represent the volume fractions of each component used, while the β_i values are the blending values, which were calculated for each of the molecular lumps shown in Table 2. Pure component octane numbers used are designated as ON_i , but one should note that in the development of the model, 57 molecular lumps were made based on GC analysis, and pure component ONs were assigned to each lump, and not necessarily each pure component. The k_i values are calculated interaction parameters between paraffins, olefins, and naphthenics, and are also shown in Table 2.2. Based on this equation, and knowing the composition and pure octane numbers of a fuel mixture, an estimation of the blending ON may then be made.

Molecular class	Molecular lumps	β(RON)	β(MON)
n-Paraffins	nC_4–nC_{12}	2.0559	0.3092
Iso-paraffins	C_4–C_{12} mono-, di-, and trimethyl-iso-paraffins	2.0204	0.4278
Naphthenes	C_5–C_9 naphthenes	1.6870	0.2821
Aromatics	Benzene-C_{12} aromatics	3.3984	0.4773
Olefins/cycloolefins	C_4–C_{12} linear, branched, and cyclic olefins	8.9390	10.0000
Oxygenates	MTBE, EtOH, TAME	3.9743	2.0727
Interaction parameters	$k_{PN}^{(a)}$, $k_{PN}^{(b)}$, $k_{PO}^{(a)}$, $k_{PO}^{(b)}$	0.2,2.4,0.4,3.6	0.2,2.4,0.4,3.6

Table 2. 2 Parameter values for equation (1) adapted from ref.12.

In addition to the ON of gasoline mixtures, ONs of individual compounds are needed when the effect of specific catalytic strategies is to be assessed. Figure 2.3a shows the predicted versus the observed RON values for olefins and aromatics, which utilized 22 descriptors and had a RMS error of 4.8 points with a cross validation error of 8.5. MON predictions for olefins and aromatics (2.3b) utilized 21 descriptors and showed a RMS error of 5.8 points, with a cross validation error of 8.1. Separate models were constructed for the group of n-paraffins, isoparaffins, and cycloparaffins in order to get a better fit of data for the extreme low and high ON molecules. The RON predictions for n-paraffins, isoparaffins, and naphthenes (2.3c) utilized 16 descriptors with an RMS error of 8.7 and cross validation error of 4.1. MON for this set (2.3d) utilized 16 descriptors as well with a RMS error of 6.8 and cross validation error of 6.3. For each of these models, the error in the cross validation step was minimized, as a further increase in descriptors for both cases resulted in better RMS errors but worse cross validation results. For every case, a genetic algorithm was utilized in order to select the initial best descriptors, followed by all possible subsets to obtain the optimum

set of descriptors. Predicted values of ON for different compounds are also shown in Table 2.1. It is important to mention that the ON predictions result in larger errors in the regions of lower ON due to the smaller number of measured data points used in this region for the development of the models. In industrial practice, this region is less important because the amounts of compounds with ON's lower than 40 are very low, and will not contribute much to the total ON of the fuel. For fundamental studies, however, it is often important to be able to estimate the ON's of these compounds because they may be present in large amounts for a given chemical reaction. It is still very important to realize that ON values that are in the very low ON range or those that may be extrapolated to negative numbers may not be very accurate. The trends, however, are still captured by the model and can be very useful in determining how beneficial a particular reaction is in the overall reaction scheme.

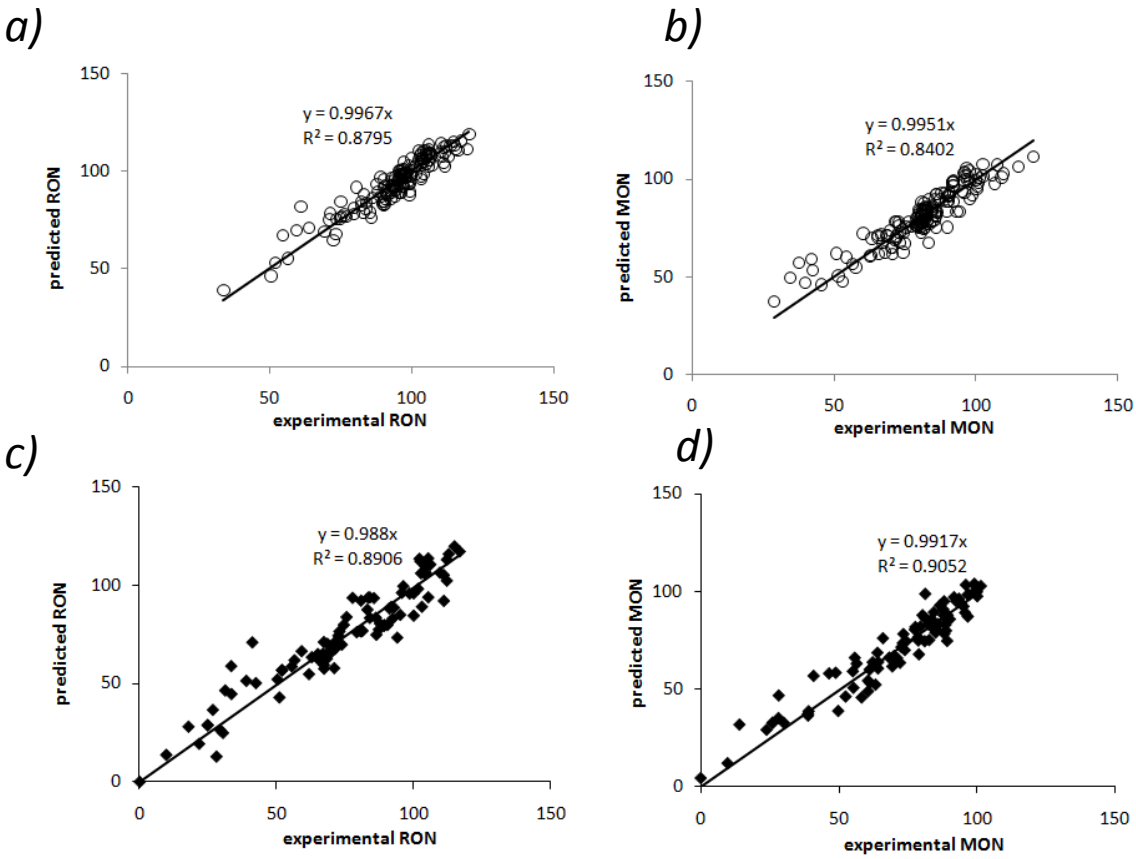


Figure 2.3 Predicted *versus* observed RON and MON octane values for olefins and aromatics (a,b), and n, iso, and cycloparaffins (c,d).

2.5.3. Prediction of Threshold Sooting Index (TSI)

In addition to CN and ON, the smoke point (SP), which is the maximum smoke-free laminar diffusion flame height, has been employed widely to evaluate the tendency of different fuels to form soot. This tool is most commonly utilized for kerosene, but also has been utilized for diesel fuels.[18,19] Researchers have tried to relate smoke points of pure compounds to their molecular structure. It was found that the inverse of smoke point, which measures the potential of a fuel to form soot, increases from n-paraffins to isoparaffins to alkylbenzenes to naphthalenes.[20,21] Since smoke points vary with experimental conditions, the concept of a threshold sooting index (TSI), which is calculated from the smoke point, molecular weight, and experimental constants, has been used to compare the soot-formation tendencies of different fuel molecules.[22]

Recent studies have been devoted to the prediction of the TSI of various individual hydrocarbons,[23] using the database compiled by Olson et al.[19] However, the range involved in these predictions is rather limited, covering mostly the kerosene range as TSI is most relevant for this hydrocarbon range. The accuracy of the TSI values greatly diminishes at both extremes, high and low values, due to the nature of the experimental measurement. At very high smoke points, the values of TSI are very small because TSI is inversely related to the smoke point. Consequently, the hydrocarbons with high smoke points are all very close together on the TSI scale, so small deviations in TSI correspond to large deviations in smoke point. At the other end of the scale, very small smoke points produce large TSI values, with small deviations in the smoke point producing large deviations in the TSI. For these reasons, it is expected that TSI values are more accurate in the middle of the scale, where the instruments and

the correlation are much more precise. TSI values were predicted with an identical methodology to the previous models with CN and ON. The model depicted in figure 2.4 utilized 15 descriptors, and had a RSM error of 3.98 with a cross validation error of 5.31. The predicted threshold soot indices (TSI) of different hydrocarbon compounds are tabulated in Table 2.1, together with cetane and octane numbers.

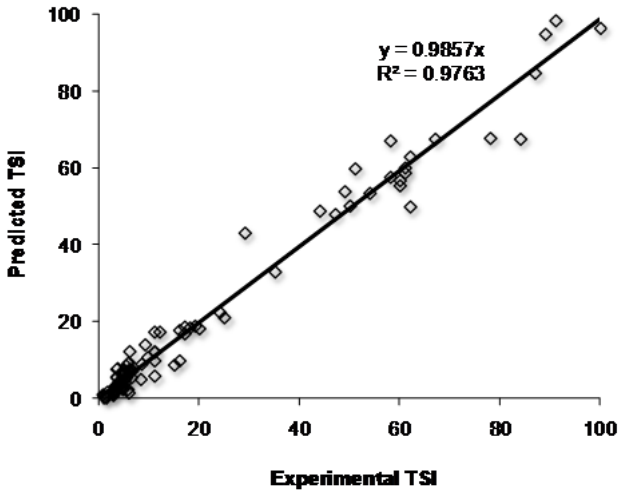


Figure 2. 4 Predicted *versus* experimental values for TSI

2.6. Correlation between Particulate Matter (PM) emissions and fuel properties

Besides the fact that these fuel properties must be at a certain minimum number in order to meet current EPA regulations, there are other important results that can be obtained from these fuel properties. As mentioned in the introduction, TSI provides an indication of how much PM a particular fuel will produce. The primary reason for the high CN regulations is the fact that the unburned hydrocarbons resulting from low CN fuels produce PM or soot, which is harmful to the environment and human health. As described above, CNs of individual compounds heavily depend on their molecular structures. For example, in an attempt to demonstrate the relationship between paraffinic molecular structure and soot formation in the high temperature range corresponding to the in-cylinder flame zone, Nakakita et. al [24] have carried out an investigation to measure the soot yields of isomeric hexanes in a shock tube. The temperature dependence of the yield of soot formation was found to follow a bell-shaped curve, with a maximum at about 2000°C for all four isomers. These maximum yields are summarized in Figure 2.5. It is seen that the soot production increases in the following order:

cyclohexane > 2,2-dimethylbutane > 2-methylhexane > n-hexane.

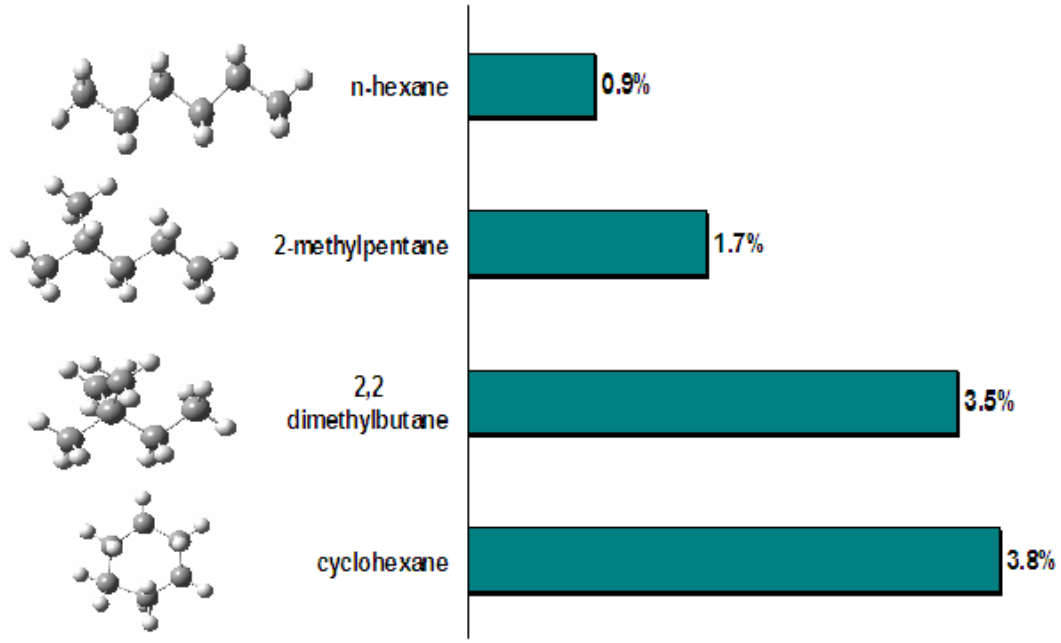


Figure 2. 5 Comparison of soot yield for various hexanes. Adapted from ref 24.

Similar to the soot formation in the high temperature range, PM precursor formation at intermediate temperatures is also influenced by paraffinic molecular structure. It was proposed that the soot formation yield decreases in the order: cycloparaffin > 2-branched isoparaffin > 1-branched isoparaffin > normal paraffin. This trend is opposite to the cetane number trend, in which naphthenes have the lowest CNs and normal paraffins have the highest CNs.

One might be tempted to conclude that soot formation always decreases with increasing CN. However, Androulakis et al.[25] have clearly demonstrated that CN alone may be misleading. They conducted experiments with model feeds fed in a high-speed diesel engine with fuels of varying overall compositions, but practically the same CN. Compositions of the fuels investigated are summarized in Figure 2.6. The first fuel is denoted as TF-1 and has a composition similar to current market diesel fuel, although

with increased levels of two-ring aromatics. Except for TF-8, the CNs of all other fuels are in a similar range, but the compositions vary considerably. The PM emissions from the advanced high-speed direct injection (HSDI) diesel engines for different fuels were measured and the results are shown in Figure 2.7. It was observed that, under high and medium load conditions (2800 rpm/60% and 2200 rpm/40% loads), PM emissions from TF-1 and TF-3, which contain more aromatics, were 60%-70% higher than those from the paraffinic fuels TF-5, TF-7, and TF-8. When comparing the PM emissions from TF-5 and TF-7, which have almost equivalent CNs, cycloparaffins (naphthenes) are seen to have a higher PM formation tendency than isoparaffins or n-paraffins. As more aromatics and naphthenes are introduced, the amount of PM will increase, even while keeping the same CN, in good agreement with previous observations.[26] An exception was observed for TF-8 that contained the largest amount of n-paraffins. It does not yield the PM reductions that one may have expected. In fact, the very high CN of TF-8 (CN = 80.5) results in a significantly decreased ignition delay. Consequently, combustion is initiated before sufficient fuel-air mixing has occurred. This could be altered, however, by changing the engine parameters. The general trends identified from the study of PM emission HSDI diesel engines are: higher aromatics, naphthenes, CN, and density all lead to increased PM. These results increase the importance of utilizing other fuel properties in the design of a given fuel that will provide a better indication of the fuel tendency to form PM than CN alone.

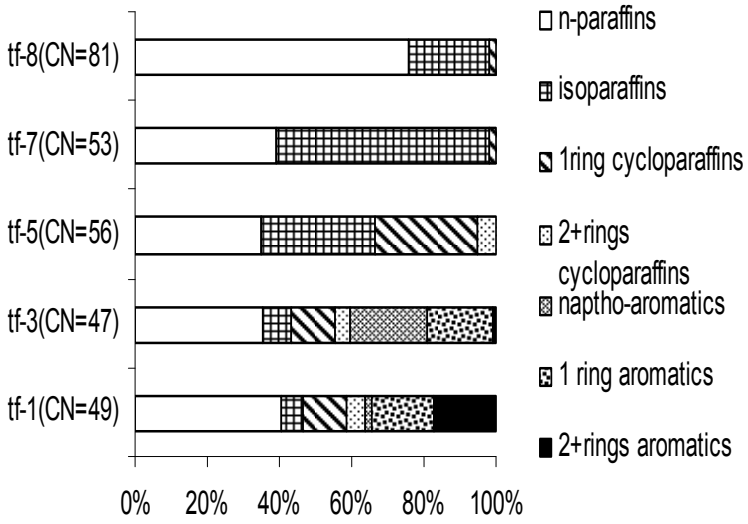


Figure 2. 6 Molecular composition of matrix fuels. Adapted from ref. 25**.**

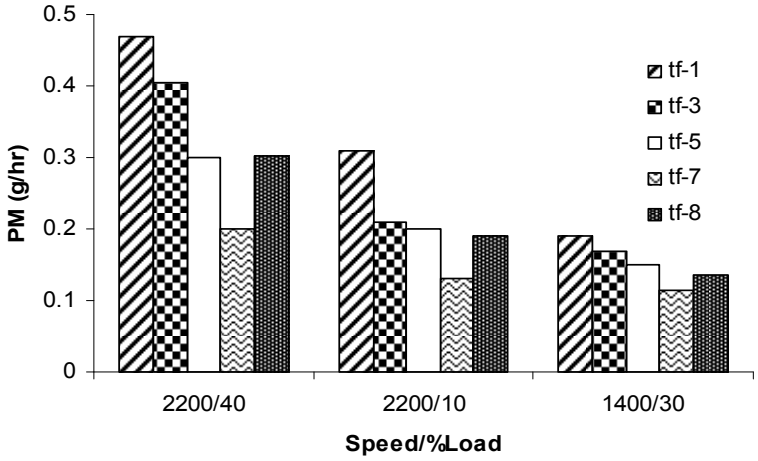


Figure 2. 7 Engine-out exhaust PM results from tests of several fuels at fixed speed/load conditions of an advanced, high-speed, direct injection diesel engine. Adapted from ref. 25

The purpose of this example is to show that PM emissions are a function of many parameters, and one alone may not be the best estimate. Furthermore, a simple property such as TSI inherently captures many properties of the molecule. TSI is a complicated measurement of the fuel to not only form soot via pyrolysis, but also oxidize. The ratio of soot formed via pyrolysis and oxidation will be much different in a laminar flame as opposed to a diesel or kerosene engine. As temperature increases, both fuel oxidation and pyrolysis increases, but oxidation increases more dramatically. Because of this, there is a need to separate the two events, and be able to distinguish a molecule's tendency to oxidize from its tendency to form soot via pyrolysis. This will be the focus of the next chapter.

References

1 I.T. Joliffe *Appl. Statist* **1982**, 31(3), 300.

2 M. Kagami, Y. Akasaka, K. Date, T. Maeda *SAE-Paper* 841082, **1984**.

3 S.L. Lee, P. H. Desai, C. C. Jonhnson, M.Y. Asim *Fuel Reformulation* **1993**, 3(3), 26.

4 K. Parikh *Bull. Catal. Soc. India* **2004**, 3, 68.

5 A. Roj, K. Karlsson *Fuels Reformulation* **1998**, 46.

6 M. Wilson, I. Fisher, J. Kriz *Ind. Eng. Chem. Prod. Res. De.* **1986**, 25(4), 505.

7 H. Yang, Z. Ring, Y. Briker, N. Mclean, W. Friesen, C. Fairbridge *Fuel* **2002**, 81(1), 65.

8 N. Ladommatos, J. Goacher *Fuel* **1995**, 74(7), 1083

9 P. Ghosh, S. B. Jaffe *Ind. Eng. Chem. Res*. **2006**, 45(1), 346.

10 J. D. Taylor, J. Michael in "Compendium of Experimental Cetane Number Data", **2004**. Golden, Colorado: National Renewable Energy Laboratory, 48.

11 R. C. Santana, P. T. Do, W. E. Alvarez, J. D. Taylor, E. L. Sughrue and D. E. Resasco *Fuel* **2006**, 85, 643.

12 P. Ghosh, K. J. Hickey, S. B. Jaffe *Ind. Eng. Chem. Res.* **2006**, 45(1), 337.

13 R. Meusinger, R. Moros *Chem. Intell. Lab. Syst.* **1999**, 46, 67.

14 T. A. Albahri *Ind. Eng. Chem. Res.* **2003**, 42, 657.

15 D. Billingsley, L. Gordon, Z. Tzanzalian in "Octane Prediction of Gasoline Blends Using Neural Nets", **1995**, Nashville, NPRA Computer Conference.

16 P. C. Anderson, J. M. Sharkey, R. P. Walsh *J. Inst. Pet.* **1972**, 59, 83.

17 E. J. Y. Scott *Proc. API Di*V. *Refin.* **1958**, 38, 90.

18 O. L. Gulder *Combust. Flame.* **1989**, 78(2), 179.

19 D. B. Olson, J. C. Pickens, R. J. Gill *Combust. Flame.* **1985**, 62(1), 43.

20 R. A. Hunt Jr *J. Ind. Eng. Chem* **1953**, 45 , 602-6.

21 R. L. Schalla, G. E. McDonald *J. Ind. Eng. Chem.* **1953**, 45 , 1497.

22 H. F. Calcote, D. M. Manos *Combust. Flame* **1983**, 49(1-3), 289.

23 S. Yan, E.G. Eddings, A.B. Palotas, R.J. Pugmire, A.F. Sarofim *Energy Fuel* **2005**, 19 (6), 2408.

24 K. Nakakita, K. Akihama, W. Wssman, J.T. Farrell *In. J. Engine Res.* **2005**, 6(3), 187.

25 I.P. Androulakis, M.D. Weisel, C.S. Hsu, K. Qian, L.A. Green, J.T. Farrell *Energy & Fuels* **2005**, 19,111.

26 Y. Akasaka, Y. Sakurai *Trans. JSME.* **1997**, 63 (607), 1091.

CHAPTER 3

3. Development of a Novel Micropyrolysis Index (MPI) to Estimate Sooting Tendency of Fuels

3.1 Overview of applicability towards molecular engineering strategy

As explained in previous chapters, fuel properties and their prediction provide guidance for the entire molecular engineering strategy. For the case of particulate matter emissions, however, no property has been developed which separates the fundamental nature of a molecule to form soot via pyrolysis. For this rare case, in order to develop strategies to improve the sooting tendency of a fuel, the property itself must first be developed. The aim of this chapter is to develop this property, coined the Micropyrolysis Index (MPI). MPI is then predicted via QSPR and subsequently compared with other properties CN and TSI. The end benefit is twofold, a deeper understanding of the relationship between molecular structure and pyrolytic sooting tendency, as well as a property which can now be optimized through the molecular engineering strategy.

3.2. Introduction

Particulate matter (PM) emissions from soot can cause lung and heart diseases[1-6] and can potentially lead to 60,000 premature deaths per year in the US.[7] In addition, PM emissions contribute to smog, reduce visibility, affect local climate, and could also

play a significant role in the global climate.[8-11] Public concern about these serious health and environmental impacts has resulted in stricter EPA standards towards the amount of fine particulates in emissions.[12]

While the amount of particulate matter emissions that a given fuel will produce is dependent on parameters such as engine type and operating conditions, the sooting tendency associated with the chemical composition of the fuel is a critical factor. A reliable method for quantification of the sooting tendency of pure fuel components and their mixtures can be of significant help to understand and control PM emissions from different fuels. Quantitative values of sooting tendencies would also be important in upgrading of fuels to improve and model the sooting tendency.[13] In fact, some recent studies have made use of such numbers to create models which predict sooting tendencies under specific conditions.[14,15]

For diesel fuels, the cetane number (CN) is often mistakenly taken as an indication of the amount of PM emissions that a given fuel will produce when burned in a diesel engine. However, this has been shown to not be the case [16,17] as the PM emissions have been shown to be highly dependent on the aromatic content and operating parameters, even when the CN is kept constant. One other method which is commonly used to estimate PM emissions, especially for jet engines, is the smoke point, which is the maximum diffusion flame height obtainable before the flame begins to produce smoke. Because these measurements vary from instrument to instrument, an effort was made to correlate the various measurements by fitting them with apparatus-specific constants and defining the threshold sooting index (TSI). This also allowed the incorporation of smoke point measurements obtained by varying the fuel mass

consumption rate rather than the fuel height into the TSI database. Regrettably, these measurements have been shown to have precision uncertainties of up to ±15% [18] for those measurements obtained by measuring smoke height and ±7% [19] for those measurements obtained by fuel mass consumption. Furthermore, the TSI may be more or less representative of the amount of soot that a given fuel may produce depending on the engine operating parameters as the sooting tendency largely varies with the richness of the flame and many other parameters.

One aspect that may be important to consider when evaluating a technique for determining sooting tendencies in pure compounds and prepared mixtures is the amounts of fuel required to obtain a single measurement. The current techniques require amounts that may be prohibitively large for laboratory research scale. For instance, one CN measurement requires on the order of 1L of fuel. While TSI and IQT (ignition quality test) require considerably lower amounts, e.g. on the order of 20mL, they may still be significantly large for lab studies. For example, in a catalyst development study of fuel upgrading conducted in a typical laboratory reactor, collecting several mL of liquid for a single TSI or IQT measurement may take several hours. As a result, the database of pure compounds can be limited due to the large volumes needed in order to conduct a single measurement.

Another method that has recently been developed[20] involves the maximum soot volume fraction measured by laser induced incandescence in methane doped flames. This test has been named yield sooting index (YSI), for which considerable improvement has been made on the precision of the measurements to ±3% for aromatic doped flames. Furthermore, these results roughly correlate with the TSI measurements

conducted by varying the mass flow rate of the fuel, but not as well with the flame height measurements. It is also claimed that because the measurements were conducted in a methane flame, the values are more representative of an alkane fueled flame, a considerable improvement over TSI measurements of pure compounds, because aromatics behave much differently in pure aromatic flames than in mixtures.

The fuel in the TSI and YSI tests is partially oxidized and partially pyrolyzed to form soot, with little information separating the two events. For this reason, we have attempted to develop a method in which the conditions are fixed and only the soot-forming pyrolysis is monitored and so the intrinsic sooting tendency of a given hydrocarbon can be analyzed. The chemistry involved with pyrolysis in oxygen-free environments is also much simpler, as the ability of molecules to oxidize, the heating value, etc. need not be taken into account. Consequently, it would be very valuable to have a fuel property which could give an indication of the nature of a particular fuel to form soot via pyrolysis which is independent on the oxygen/fuel ratio of the flame.

In designing the method presented in this contribution we stipulated that it should be much more precise than traditional smoke point methods, it should require small sample volumes so that it can be utilized on a lab scale and with expensive model compounds, and it should require common lab equipment so that it can easily be implemented and reproduced in existing labs. Based on these requirements, we have developed a simple method that measures a newly defined fuel property that we have called the micropyrolysis index (MPI), which satisfies all of the aforementioned conditions.

In this contribution we describe the experimental details of the MPI method and report measurements on pure hydrocarbon compounds. The MPI values are compared with the corresponding TSI measurements. In addition, a quantitative structure-property relationship (QSPR) has been developed between the molecular structure of each pure compound and the measured MPI. From this relationship, MPI values of unmeasured pure compounds have been estimated, leading to a large database expansion and the possibility of developing trends for various families of compounds.

3.3. Experimental

3.3.1. Carbon deposition

All experiments were conducted by pyrolyzing 20μL of a vaporized liquid sample across a hot bed of 300mg α-Al_2O_3 beads (Purchased from Atlantic Equipment Engineers, particle size 30-50 mesh, 99.9% purity). A schematic of the reactor system can be seen in Fig. 3.1. The alumina bed was placed at the desired height in a ¼" OD quartz tube and held up with 15mg of quartz wool. The reactor was placed in a Thermcraft Incorporated electric furnace (model# 114-12-3ZV) controlled with an Omega® temperature controller, model CN 3251, to keep the temperature constant at 850°C. This temperature was chosen because it is a high enough temperature to pyrolyze hydrocarbons, but low enough to avoid alumina sintering and utilize common lab equipment. For the injection, 20 μL of the desired hydrocarbon sample was placed in a Hamilton 100 μL SampleLok gas-tight syringe (part# 81056) with a seven inch needle. The syringe was first filled with 20μL of air, then 20μL of sample, followed by 20μL of air, and then closed off from the surrounding environment. The two air pockets

were used in order to ensure that no sample was left in the needle before or after the time of injection. A gas-tight syringe was used in order to avoid losses of sample by vaporization before the injection. The seven inch needle was used to ensure that entire sample was in the heating zone of the reactor when it left the syringe, so that no condensation could occur. A helium flow rate of 25ml/min was maintained through the system as the sample was heated to 850^{o}C.

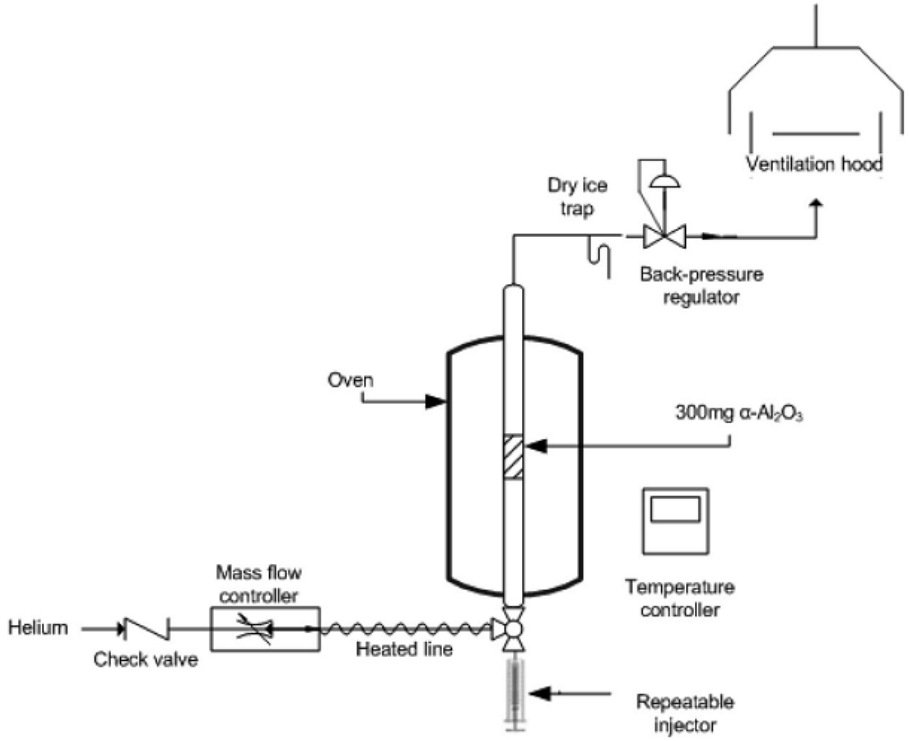


Figure 3. 1 Schematic description of the apparatus used to obtain MPI values by pyrolysis of a 20μL liquid sample across an α-Al_2O_3 placed in a ¼ in. o.d. quartz tube, held at 850 °C. A He flow rate of 25mL/min was maintained through the system, and a backpressure regulator was used in order to maintain a pressure of 10 psig.

A Tescom® backpressure regulator (model# 44-2361-24) was used in order to maintain a constant system pressure of 10 psig, and to prevent any oxygen back-diffusion into the reactor. A period of 30 min was allowed for the temperature of the catalyst bed to stabilize at the desired value. Once the temperature of the alumina bed

was stabilized, the sample was injected at a constant rate over thirty seconds. This controlled injection was accomplished by using a Hamilton repeatable dispenser (part# 83700) set to inject at a rate of 2μL/second. Once the sample was injected on the alumina bed, the bed was maintained at 850^{o}C for 10 min to ensure that any light volatile hydrocarbons had passed through the reactor. After 10 min, the reactor was allowed to cool to room temperature under the same He flow rate and pressure in order to eliminate any back-diffusion of oxygen that could oxidize some of the deposited carbon. After the reactor was cooled to room temperature, the dry ice trap, and the line from the reactor to the backpressure regulator were cleaned with acetone in order to eliminate any tar buildup.

3.3.2. Temperature Programmed Oxidation (TPO)

After the sample was cooled to room temperature, the alumina bed with a given amount of deposited carbon was transferred to a clean reactor bed. The carbon was then placed in a TPO system in order to quantify the amount of carbon deposited on the alumina during the injection. The TPO system is typically used to quantify coke deposits in heterogeneous catalysts and consists of a quartz tube containing the sample that is placed in an electric furnace while 5% O_2/He stream flows through the sample at a rate of 80ml/min. The temperature of the oven is then linearly heated to 900^{o}C at a constant rate of 10^{o}C/min. The exit gas is sent through a methanator containing a 5%Ni/Al_2O_3 catalyst and a side-stream of H_2 to convert all of the CO and CO_2 into CH_4, which can be detected by the sensitive FID detector. The area of the C peak is then compared with that of a reference peak resulting from a pulse of 100μL of CO_2 in order to quantify the amounts of deposited C. This setup is preferred because of the high

sensitivity of the FID detector, but other systems and detectors, such as MS, or TCD, etc. might also be used. Only the carbon on the alumina was quantified because the goal of this work is to measure the kinetic tendency of a compound to form soot via pyrolysis. The alumina acts only as a mechanism of heat transfer, so some carbon will be deposited on the quartz wool as well as the walls of the reactor. Because such a small fraction of the injected carbon deposits on the alumina, the kinetic tendency of a compound to produce soot is captured by quantifying only the carbon deposited on the alumina as long as all of the parameters discussed in section 3.3.4 are carefully controlled.

3.3.3. Definition of MPI

We define the micropyrolysis index MPI as the amount of C deposited from injection of 20μL of the sample, normalized to two reference compounds. The first one is n-octane, for which an arbitrary value of 5 was assigned, and the second is decahydronaphthalene (decalin), which was assigned a value of 20. All others were taken in reference to these values. MPI gives an indication as to how much soot a given fuel produces on a volumetric basis, and is very practical from a fuels standpoint, but it may sometimes be misleading if one wants to study the chemistry because different amounts of C are being injected in each fuel due to the differences in density. In that sense, a value normalized by the number of moles of carbon injected would a give better idea of the sooting tendency of each atom of C injected. For this reason, another number may be calculated from MPI results where the number of C moles deposited on each sample are divided by the number of moles of C injected. This value typically follows very similar trends to MPI, but small differences may be observed when

considering similarly-sooting molecules. This fraction of injected carbon which deposits on the surface will likely be different for different systems, but the observed trends should be quite similar.

3.3.4. Effect of Injection Speed, Temperature, and Pressure

In order for MPI measurements to be reproducible, three factors must be carefully controlled: speed of injection, temperature, and pressure. While it is acknowledged that small deviations in these variables will likely occur as the method is repeated in other systems, the soot formation tendency of each sample with respect to that of a reference compound (hexane and decalin) should remain quite constant. What is essential, however, is that these parameters do not vary from run to run for a particular system. First, the amount of carbon deposited on the α-Al_2O_3 is highly dependent on the injection rate for multiple reasons. By varying the injection rate, both the evaporation rate and residence time through the sample can vary, leading to large differences in the observed MPI. For this reason, each sample must be injected at reproducible rates. Second, small deviations in temperature may greatly influence the rate of pyrolysis. For this reason, it is essential that the temperature of the catalyst bed is stable for the duration of the run. In most systems, additional time is required for the catalyst bed temperature to come in equilibrium with the furnace wall temperature as measured by the thermocouple. This time may vary from system to system, but can easily be measured by conducting a blank run with a thermocouple inside the catalyst bed. Third, an important variable that must be maintained constant in all measurements is system total pressure. A simple backpressure regulator can be used to maintain system pressure at 10 psig. By increasing or decreasing the system pressure, one can

manipulate the amount of carbon that deposits on the alumina. If less sensitive detectors, such as TCD or MS are used, one may need to increase the pressure of the system slightly to produce more carbon per run. One further advantage of the backpressure regulator is the elimination of any possible back diffusion of oxygen from the environment that may partially oxidize some of the deposited carbon. It is essential that a dry ice trap is placed before the backpressure regulator in order to prevent any unwanted pressure increases that may be brought about by tar-like pyrolysis products building up inside the backpressure regulator. Because the MPI is a kinetic measurement, it is essential that these three variables are carefully controlled. By changing the residence time through the reactor or the pyrolysis rate, drastic differences may be observed in the amount of soot deposited on the alumina.

3.3.5. Repeatability

As long as the aforementioned parameters are controlled, MPI measurements can be very precise. Standard deviations of 0.11, 0.22 and 1.02 MPI were observed for sooting values of 3.3 MPI, 32.4 MPI, and 94.7 MPI, respectively. This level of reproducibility is very high compared with typical uncertainties obtained for the TSI method (e.g. 7% [19] to 15% [18]). It is also comparable to the more precise YSI method, for which an estimated ±3% inaccuracy has been reported.

3.4 Results and Discussion

3.4.1. Effects of molecular structure on MPI

Table 3.1 summarizes MPI and mol C deposited/mol C injected values obtained on a series of hydrocarbons. Clear trends are immediately apparent. For instance, it is observed that alkanes exhibit significantly lower MPI values than isoparaffins and naphthenic compounds. Similarly, for a given family of hydrocarbons, the MPIs clearly increase with the number of carbons in the molecule.

It is well known that the tendency for particulate formation from hydrocarbons increases in the order: n-paraffins<isoparaffins<naphthenics<aromatics; indeed, the MPI values reported in Table 1 are in very good agreement with this trend. The increase in MPI with increasing chain length could also be anticipated and has been observed with TSI [15]. One factor that is easily noted is the large effect that the degree of branching has on the MPI (e.g. hexane<2-methylpentane<2,2-dimethylbutane).

Table 3. 1 MPI values of several hydrocarbons (n-alkanes, isoalkanes, and cycloalkanes) in the C_6-C_{11} range.

name	carbons	skeletal	MPI	mol C deposited/ mol C injected
hexane	6	n-alkane	3.3	8.73E−04
2-methylpentane	6	isoalkane	6.5	1.43E−03
2,2-dimethylbutane	6	isoalkane	7.0	1.54E−03
cyclohexane	6	cycloalkane	10.8	1.81E−03
methylcyclohexane	7	cycloalkane	14.2	2.32E−03
ethylcyclopentane	7	cycloalkane	15.6	2.53E−03
1,1-dimethylcyclopentane	7	cycloalkane	19.2	3.11E−03
octane	8	*n*-alkane	5.0	1.09E−03
1,3-dimethylcyclohexane	8	cycloalkane	16.0	2.58E−03
2,2-dimethylheptane	9	isoalkane	8.4	1.61E−03
tert-butylcyclohexane	10	cycloalkane	20.5	3.07E−03
decalin	10	cycloalkane	20.0	2.68E−03
undecane	11	*n*-alkane	7.3	1.38E−03

Since the density of isoparaffins is significantly lower than that of n-paraffins, MPI and the molar ratio of C deposited/injected show considerable differences. To appreciate the need for taking into account both MPI and the molar ratio of C deposited/injected, one can compare undecane and 2,2-dimethylpentane. They both form comparable amounts of soot on a volumetric basis, but when one considers the actual moles of C that were injected, the branched molecule is seen to produce significantly more deposits, as one could have anticipated.

It is well known that during combustion naphthenic compounds produce more soot than paraffins due to the hydrogen abstraction reactions that can take place at high temperatures with the ensuing production of aromatics, which in turn are effective producers of soot. On the other hand, the explanation for the sooting trends associated

with the naphthenic ring size and alkyl substituents is somewhat less straightforward. One can clearly see from the data in Table 3.1 that increasing the degree of branching and increasing the number of tertiary bonds in the molecule result in increases in MPI.

Overall, the trends exhibited by MPI for non-aromatic compounds seem to be consistent with those generally accepted for soot formation. For example, cyclopentane rings appear to have similar or even larger MPI values than similar cyclohexane compounds with the same number of carbon, as can be noted by comparing the MPIs of ethylcyclopentane and dimethylcyclopentane with that of methylcyclohexane. The high sooting tendency of C_5 naphthenic rings can also be explained in terms of hydrogen abstraction. Through this reaction path a cyclopentane ring can lead to cyclopentadienyl radicals. Two of these radicals can then recombine to form naphthalene[21], which is a high-sooting molecule.

3.4.2. Comparison with TSI

As noted in the introduction, TSI values give estimates of the sooting tendency of a flame with oxygen, and the amount of soot produced is highly dependent on the oxygen/fuel ratio. Moreover, another aspect which varies in the TSI measurements is the flame temperature. This could lead to increased nonlinearities when mixtures of pure compounds are considered. Further complications of TSI are brought about by its definition, i.e., TSI=a(MW/SP) +b [18]. In this equation, the molecular weight is introduced to offset the inherent smoke point increase brought about by increased molecular weight and is mostly due to the larger air/fuel ratio required for stoichiometric combustion. While this effect can be relevant to some engines, this

further complicates the chemistry and may not be very relevant when dealing with true fuel mixtures.

One other effect of TSI which may be misleading is that it is inversely proportional to the smoke point. This means that when dealing with any compound that has a high smoke point (e.g. alkanes), the TSI values will be very low, making it difficult to differentiate between fuels in this range, which may make up a large portion of many fuels. On the other end of the spectrum, aromatics have very low smoke points, which lead to very high TSI values. This means that a very small error, even a fraction of a mm, when reading the smoke point could lead to huge errors in TSI. Furthermore, flame temperature may have a dramatic effect on TSI values. As an example of this, Olson *et al.* studied the emissions temperatures of several model hydrocarbon diffusion flames [19]. It was found that the emission temperatures of cyclohexane, methyl cyclohexane, ethyl cyclohexane, and isooctane were all 1460K, while the emission temperatures of n-paraffins were significantly higher. This indicates that multiple phenomena are involved when measuring the TSI of pure compounds. It is well known that iso-alkanes and naphthenics have a higher tendency to produce soot under pyrolysis than n-paraffins, but this rate also is highly dependent on flame temperature. If n-paraffin flame temperatures are higher, the observed difference between sooting tendencies of the different groups may not be so straightforward. This can be illustrated by comparing the TSI values with MPI values obtained from pure pyrolysis at a uniform temperature as shown in Fig. 3.2. Note that the MPI values for iso-alkanes and naphthenic compounds shift to higher values when compared with the corresponding TSI values. This shift can be explained by differences in flame

temperatures of the three groups, which merge the TSI values closer together while MPI values distinguish the groups better. The naphthenic compound which appears to have a very high TSI value is decalin, which as indicated by Olson *et al*., has a uncharacteristically high emissions temperature when compared with substituted cyclohexanes as it is a very stable naphthenic, and was found to have emissions temperatures closer to those of aromatics. The differences between aromatic measurements between MPI and TSI will be discussed later in section 3.3.5. Overall, the scale of MPI seems to differentiate much better between low sooting non-aromatics and stoichiometric differences need not be accounted for as no oxygen is involved, leading to a much more straightforward fuel property.

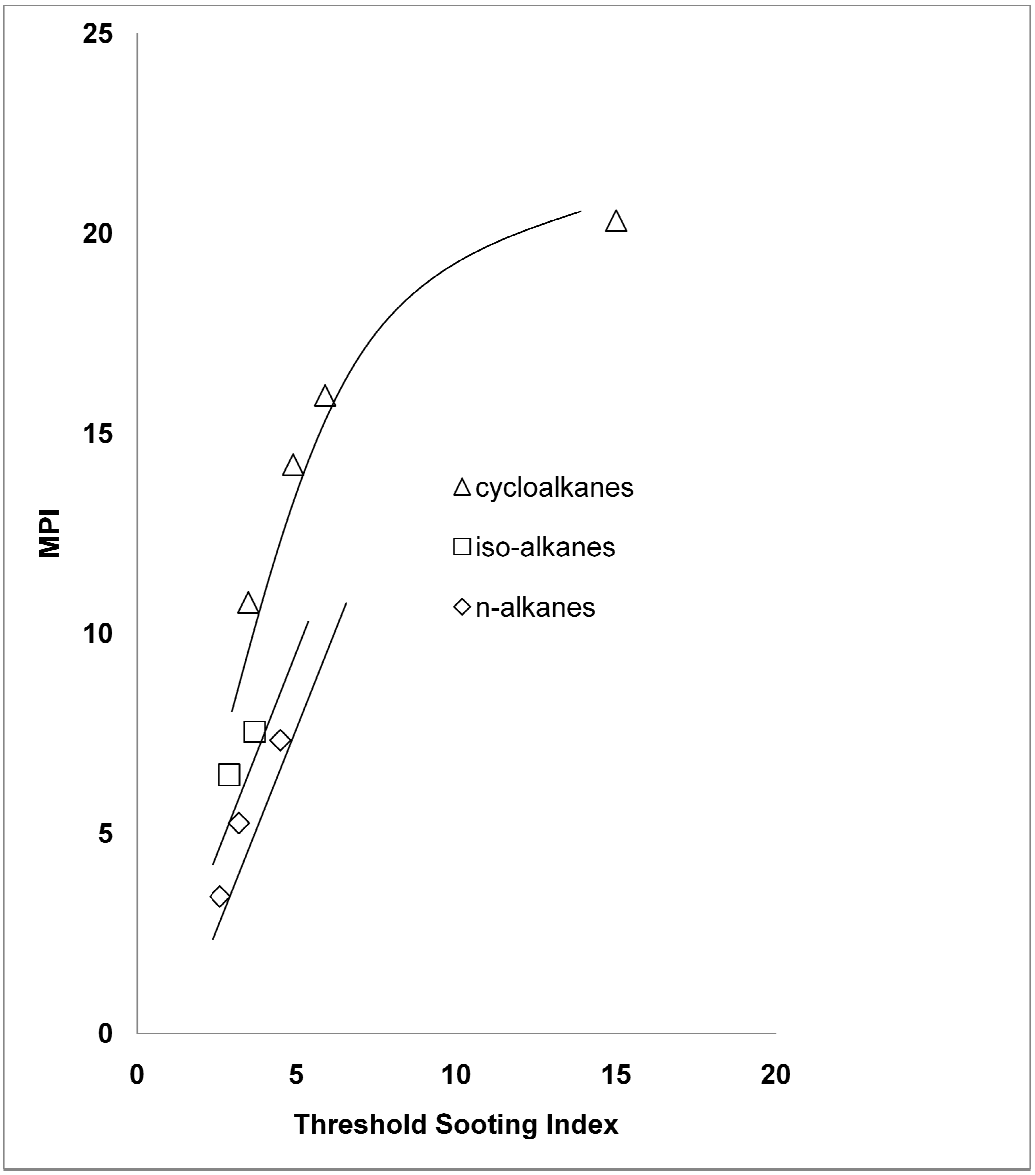


Figure 3. 2 Comparison of MPI values obtained in this work with TSI values from the literature.[19]

3.4.3. MPI of oxygenates

With the growing interest in renewable energy sources, the sooting tendencies of oxygenates must be well understood. It is clear that MPI values of oxygenates are lower than those of the corresponding oxygen-free hydrocarbons. For example, this trend can be seen by comparing the MPI of n-octane with that of octanol. Octane has an MPI of 5 while octanol has an MPI of only 3.1. This difference is likely due to the radical scavenging ability of the alcohol to eliminate radicals which are the precursors of soot. The sooting tendency of oxygenates will be the focus of future studies using MPI, since this method has the ability to probe the effects of oxygen-containing compounds on soot formation or soot reduction without the presence of oxygen in the surrounding atmosphere which further complicates the chemistry. This effect of oxygen will be discussed in greater detail in chapter 7.

3.4.4. MPI of aromatics

When comparing the sooting tendencies of pure aromatics, one must take caution. Aromatics in mixtures typically produce a great deal of soot when combusted in diesel or jet engines due to the fact that the formation of the first aromatic ring is the rate limiting step in soot formation. Aromatics are also very stable, so it is very unlikely that their C-C bonds will break apart at considerable rates under these pyrolysis conditions, but rather fragments of other compounds in the fuel will attach to the aromatics to form large particles. For this reason, a small amount of aromatics can lead to very large increase in soot when added to fuel mixtures. However, when tested as pure components the aromatics can only form soot by reacting with themselves, and this rate will be highly dependent on the stability of the side chains on the aromatics. An

example of this is shown in Fig. 3.3. It can be seen that the rate of soot formation for pure components is dependent on the stability and number of carbons in the side chains, which are subject to pyrolysis. For this reason, molecules with less stable side chains are more likely to produce greater amounts of carbon deposits. By contrast, in mixtures the trend is reversed as the aromatics that form the most soot are those that had less side chains. This is because other molecules in the mixture could connect the aromatics and form soot more quickly. Because these measurements are done on a volumetric basis, the amount of aromatic rings introduced to the system typically decreases with the addition of side chains, which also will likely influence the sooting tendency in dilute mixtures for a particular volume of aromatics injected.

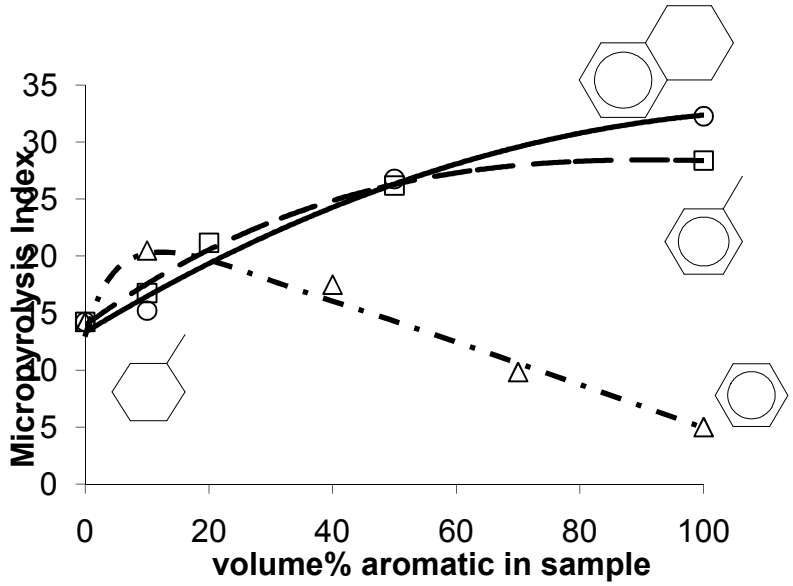


Figure 3. 3 Effect of aromatic content in mixtures. Aromatics tetralin, toluene, and benzene were blended with methylcyclohexane in various volume percentages. The resulting effect on MPI is shown.

From the practical point of view, mixtures with small percentages of aromatics may be more representative of an actual fuel (diesel, gasoline, or kerosene) than a pure aromatic mixture. Furthermore, it is proposed that mixtures with small percentages of aromatics are the most accurate for measuring the effects of aromatics on soot formation. In order to determine the effect of aromatics in a mixture, we extrapolated the line from 0-15% aromatic content to 100% aromatics. We conclude that this is a much more accurate representation of how aromatics will influence the sooting tendency of a fuel than obtaining an MPI value of the pure aromatic compound.

The role of aromatics is different in the MPI method from the standard TSI. For TSI, oxygen is involved, which may partially oxidize some of the aromatics, making them much less stable. However, in MPI under the pyrolysis conditions alone the aromatic rings will not break in significant amounts. An example of this is shown by the MPI of pure benzene. Pure benzene alone forms far less deposited carbon than any of the other aromatics. When present in a small amount in mixtures, however, benzene produces significant amounts of carbon. This is one other inherent advantage of MPI, in which only the pyrolysis is studied. For example, the TSI values of benzene, toluene, and tetralin are 29, 44, and 61 respectively[19]. This indicates that pyrolysis plays the most important role in soot formation in flames, but by introducing oxygen the chemistry becomes much more complex. Furthermore, when introducing oxygen to aromatics, the flame temperatures and point in the flame where soot inception begins will likely change, but the effects will be dramatically different depending on the conditions. Because of these issues, TSI values for pure compound reflect both of these issues, which explain the lack of correlation between MPI and TSI values of pure

aromatics, as seen in Fig. 3.4. Aromatic species typically have MPI values greater than 30, with the exception of pure benzene (not shown). For all of the non-aromatic species, the MPI correlates with the TSI quite well as described above, but this correlation breaks apart at high sooting values. For this reason, it is proposed that the sooting tendency of a particular aromatic is more accurately estimated by investigating the effect that this compound has on the MPI of a mixture of non-aromatics.

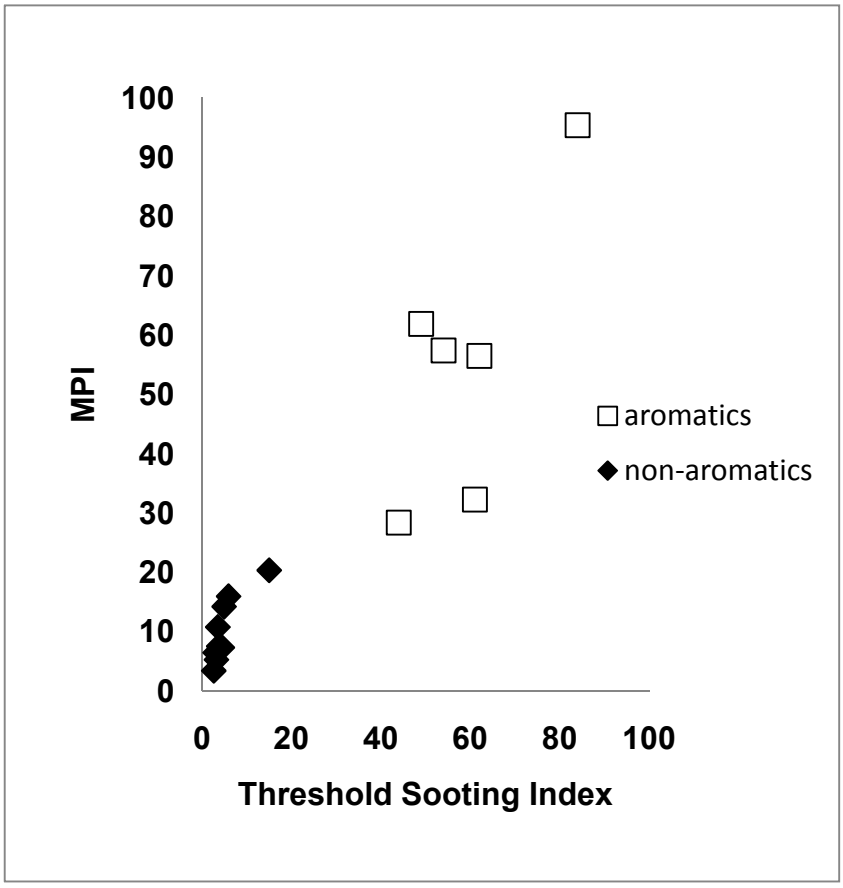


Figure 3. 4. Comparison between MPI values obtained in this work and TSI values from the literature.[19]

3.4.5. Development of QSPR models to estimate MPI

Quantitative Structure Property (QSPR) relationships have been used in the past to predict the values of many important fuel properties such as Octane Number[13],CN[13,22], and TSI[23,13]. QSPR relations provide a very powerful tool in fuel upgrading. Once a property is predicted, direction to desired molecules is provided as the database of fuel property values is expanded through QSPR estimation. This information helps to determine which compounds should be maximized, and which ones should be reduced in a particular fuel upgrading. The main challenge here is the limited amount of experimental data available. Furthermore, as described in the aromatic blending section, different factors influence the amount of soot that aromatics will produce when compared with non-aromatics. This means that different molecular descriptors must be used in order to quantify the MPI for aromatics. This work is in progress in our lab, as the aromatic database is being expanded.

In this contribution, for all of the non-aromatic compounds, a model was created in order to estimate the MPI of a pure compound which has not been previously measured. In order to accomplish this estimation, 13 non-aromatic compounds were measured and correlated with molecular descriptors to the MPI of each compound. The molecular descriptors were calculated and correlated with MDL® QSAR software (version 2.2.0.0.446 (SP1) from MDL Information Systems, Inc.). This software calculates over 400 molecular descriptors of each molecule. A genetic algorithm was used in order to determine the descriptors which best described MPI by minimizing Friedman's lack-of-fit scoring. These descriptors were then correlated to MPI through an ordinary multiple regression model which involved 3 descriptors. Although many

types of models were created, the ordinary multiple regression model was chosen based on its ability to capture the trends observed in MPI without over-fitting the data. Table 3.2 shows the equation used to predict MPI as well as the information encoded in the descriptors which were chosen. In prediction studies like this, it is typically recommended that a subset of data, not included in the model, be compared with the predicted values in order to validate the model and ensure that the data was not over-fit. However, in this case, due to the small number of compounds used in the database, traditional model verification techniques could not be used as each data point was

Table 3.2. Equation used and molecular information encoded in the descriptors used to predict MPI of unmeasured molecules.

$$MPI = -7.445k_1 + 11.33x_0 + 20.42x_{ch}^5 - 6.29804$$

descriptor	molecular information encoded
k_1 (kappa 1 shape index)	number of carbons, degree of branching, degree of cyclization
x_0 (zero-order chi index)	degree of skeletal branching
x_{ch}^5 (fifth-order chi chain index)	degree of substitution on a ring and degree of cyclization in a molecule

crucial. For this case, the leave-one-out method was used to find the best model. This technique involves building a model based on each compound except one in the database, and then predicting the value of the last compound. This technique was repeated for each compound in the database, and the errors were summed as a form of cross validation. This technique works very well when the amount of data is limited, but as the database is expanded, the traditional method should be used. The total cross

validation sum of squares added to 19.52, corresponding to an average cross validation RMS error of ±1.22MPI, which is higher, but in the same order of magnitude as the value of ±0.79MPI average RMS error predicted in the final model. An increase in the cross validation error is to be expected, especially with the limited number of data points in use. A parity plot of the predicted vs. experimental numbers is shown in Fig. 3.5. Note that the error is well dispersed, and does not deviate to one side or the other. This is critical in order to ensure that the correct trends have been captured. Also, based on the cross validation results, as well as several parity plots for different groups which were plotted, one can conclude that the model does not over-fit the data, and predictions from this model can be used to calculate MPI values in this range.

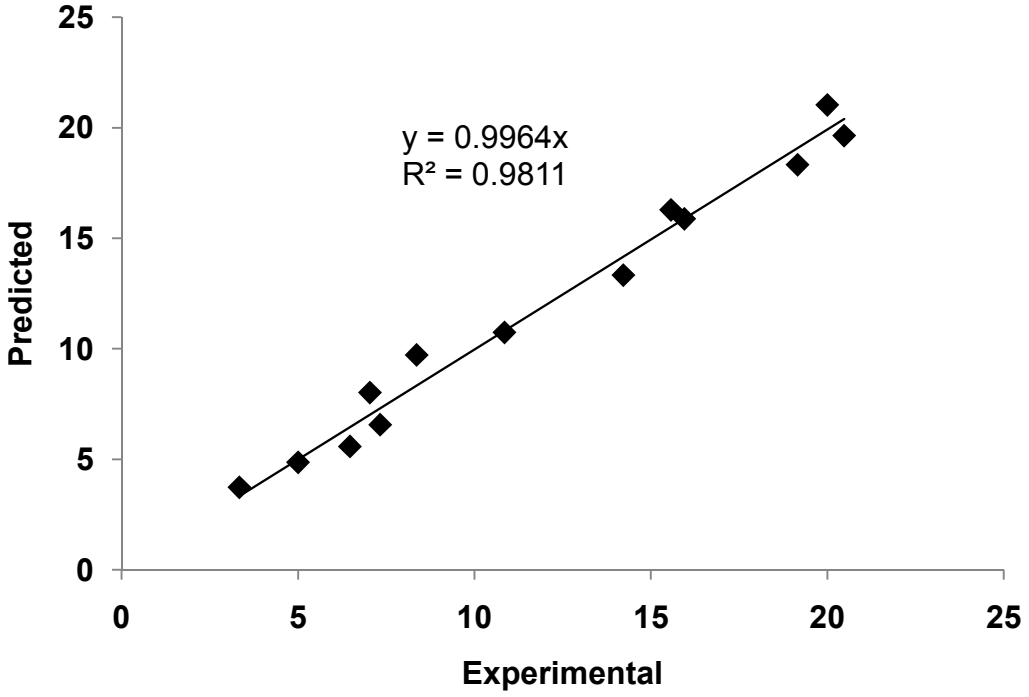


Figure 3. 5 Parity plot of predicted vs. experimental values of MPI through the use of QSPR.

3.4.6. Results from predicted MPI values

The results from MPI prediction can be of great value. One example can be seen in Fig.3.6, where the MPI values of various groups of compounds are plotted as a function of the number of C atoms. One can clearly see that the trends discussed earlier are captured by the predictions. As branching increases, the MPI increases, as would be expected for the pyrolysis of a mixture. Also, the addition of a ring increases the MPI even more, as expected. With this tool, one can calculate the estimated MPI for a variety of compounds and can clearly see the trends as molecular structure varies. This tool can be of great use for a variety of applications, including fuel upgrading. Tables 3.3 a and b show predicted MPI values compared with suggested experimental TSI values from Olson *et al*.[19] for several pure compounds. The trends discussed in section 3.4.2 are shown to hold for these data when compared in a much larger range of data as can be seen in Fig. 3.7. It can clearly be seen that MPI differentiates more than TSI for the various groups of hydrocarbons. This is a very important observation as one can now study the effect of pyrolysis alone, which compliments sooting tendency measurements which involve oxygen and flames. This is very important as the influence of oxygen and flame temperature on the actual sooting tendency of a fuel will vary largely depending on the combustion properties such as the oxygen/fuel ratio, etc... This gives an even greater value on the ability to differentiate between the effects of oxygen and flame temperature with the ability of a compound to produce soot solely via pyrolysis. For a given set of molecules with the same TSI value, the MPI values follow the trend n-alkanes<iso-alkanes<cycloalkanes.

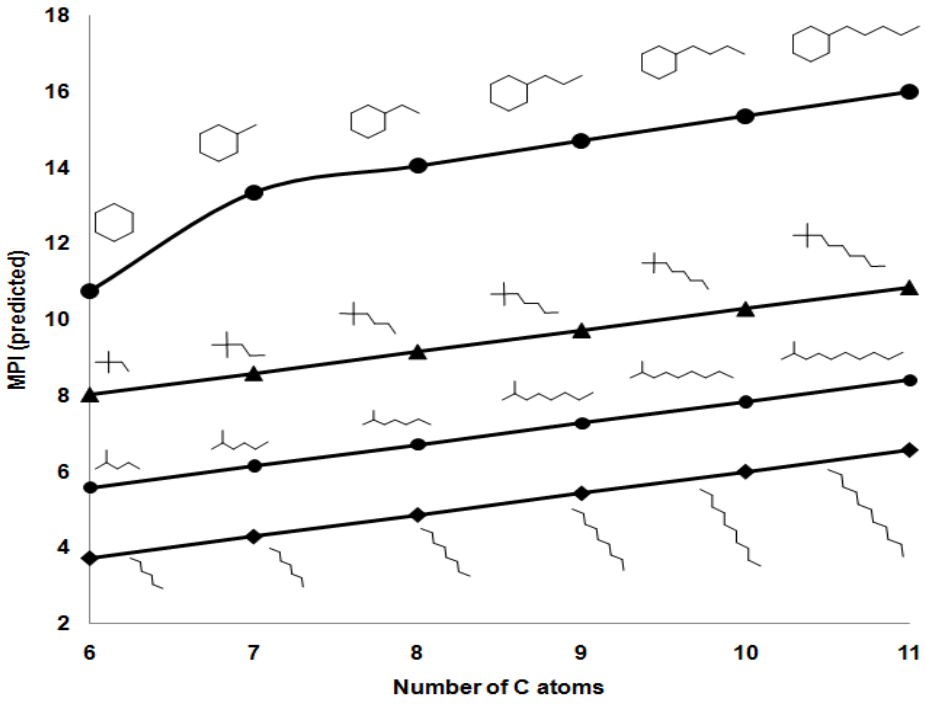


Figure 3. 6. MPI predicted values as a function of number of carbon atoms for various classes of non-aromatic hydrocarbons.

Table 3. 3 Experimental TSI values and predicted MPI values for several pure hydrocarbons.[a]

a

group	name	MPI (predicted)	TSI (from the work of Olson et al.[20])
alkanes	*n*-butane	2.6	1.4
	n-decane	6	4.2
	n-dodecane	7.1	5.1
	n-heptane	4.3	2.6
	n-hexane	3.7	2.6
	n-nonane	5.4	3.1
	n-octane	4.9	3.2
	n-pentane	3.2	1.5
	n-tetradecane	8.3	5.4
	n-tridecane	7.7	5.2
	n-undecane	6.6	4.5
	n-propane	2	0.8
iso-alkanes	2,2,4-trimethylpentane	11	6.4
	2,2-dimethylbutane	8	3.7
	2,2-dimethylhexane	9.2	4.5
	2,2-dimethylpropane	7.5	3.5
	2,3,3-trimethylpentane	11	5.7
	2,3,4-trimethylpentane	10.4	5.7
	2,3-dimethylbutane	7.4	3.2
	2,3-dimethylhexane	8.6	3.8
	2,3-dimethylpentane	8	3.5

b

group	name	MPI (predicted)	TSI (from the work of Olson et al.[20])
iso-alkanes	isopentane	5	1.6
	2-methylpentane	5.6	2.9
	3-methylpentane	5.6	3
	2-methylhexane	6.1	3.2
	3-methylhexane	6.1	3.2
	2-methylheptane	6.7	3.5
	3-ethylhexane	6.7	4
	3-methylheptane	6.7	3.7
	4-methylheptane	6.7	4
	isononane	7.3	3.8
	2,4-dimethylpentane	8	3.6
	2-methyl-3-ethylpentane	8.6	4.4
cycloalkanes	cyclohexane	10.7	3.5
	cyclooctane	12.2	5.9
	methylcyclohexane	13.3	4.9
	cyclopentane	13.5	3.5
	ethylcyclohexane	14	5.4
	methylcyclopentane	15.5	5
	1,3-dimethylcyclohexane	15.9	5.9
	trans-decalin	21	15
	bicyclohexyl	22.9	12

[a] Pure TSI values were obtained from the literature.[20]

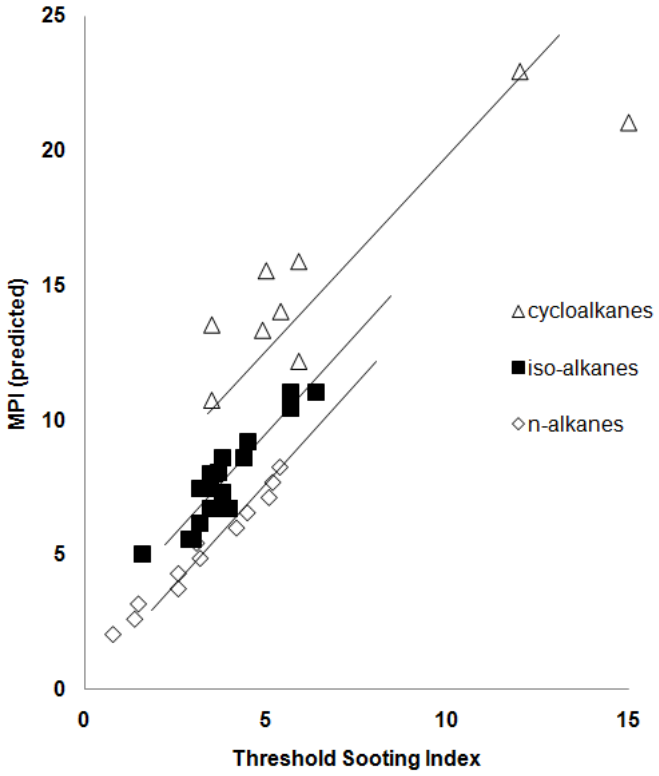


Figure 3. 7. Predicted MPI values vs. experimental TSI values obtained from the literature.[19]

3.4.7. Comparison between predicted MPI values and Cetane Number

As discussed earlier in the introduction, Cetane Number is often mistakenly taken as an indicator of the sooting tendency of a particular fuel. The reason for this assumption is that fuels which are more stable and less likely to combust upon compression typically contain a large degree of aromatics and highly branched compounds which result in both a low CN and a high sooting tendency. For this reason, it is generally perceived that decreasing CN will necessarily result in increasing sooting tendency. What are not so obvious are the opposite trends observed with increasing carbon numbers in many cases. By increasing the number of carbons in n- and

isoalkanes the CN increases, but at the same time the sooting tendency also increases. These trends can be seen in Fig. 3.8a, where predicted MPI values are compared with CN data found in

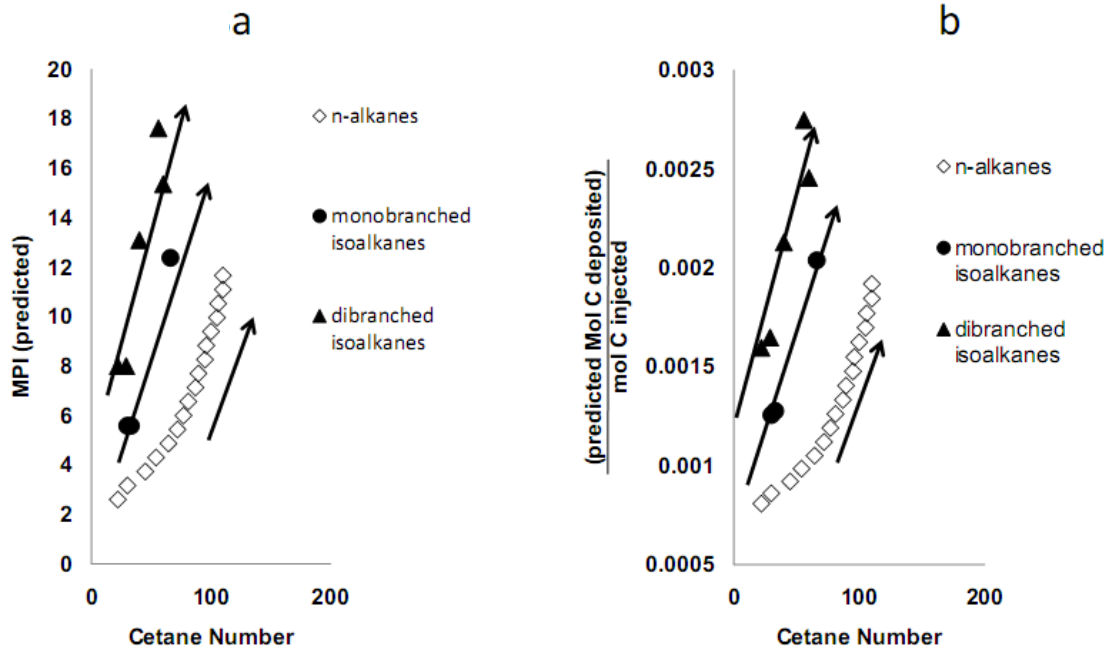


Figure 3. 8. (a) Comparison between predicted MPI and experimental CN values obtained from literature[22] for n-alkanes and isoalkanes. (b) Comparison between the (moles of carbon deposited)/(moles of carbon injected) and CN. Arrows indicate the direction of increasing number of carbons/molecule.

the literature.[22] Arrows indicate the direction of increasing number of carbons. Among the separate groups, CN increases with increasing sooting tendency due to the higher reactivities of the larger molecules, but one can clearly see the distinction between the separate groups, with MPI differentiating more clearly between the branched molecules for a particular cetane number. One could quickly assume that the increasing in MPI for larger hydrocarbons would result from a higher density of the fuel, that is, one is

injecting more carbon atoms which can form more soot. However, if we calculate the amount of carbon deposited per mole of carbon injected similar results are still obtained. To estimate the mole-based MPI, we first calculated the moles of carbon deposited on the surface from MPI values based on the moles of carbon which correspond to the MPI values of the references, 5 and 20. After these values were found, the moles of carbon injected for each pure compound could be calculated from the density, molecular weight, and number of carbons of each molecule. Results can be seen in Fig. 8b, with the overall trends being identical to those found when comparing CN to MPI alone.

In contrast, when considering cycloalkanes, the trends among the various molecular groups may not be so obvious; for instance, increasing the number of carbons may actually decrease CN in some cases. This can be seen in Fig. 9a. Again, the arrows indicate the direction of increasing number of carbons. While CN trends do not remain constant across the different groups, predicted MPI values can be interpreted much more easily. For this case, the 1-ring cycloalkanes were all n-alkyl monosubstituted cyclohexanes (cyclohexane, methylcyclohexane, ethylcyclohexane, and propylcyclohexane). In this case, the CN increased with increasing number of carbons (or length of the alkyl substituent, as did the MPI, as should be expected. For the two-ring substituted cycloalkanes, however, this trend is not so obvious. The 2 ring cycloalkane molecules shown in Fig. 9 are trans-decalin, 1-propyldecalin, 1-butyldecalin, and 1-octyldecalin. In this case, even though the branch is linear, increasing numbers of carbons results in decreasing CN values. This trend is not observed with the predicted MPI values, as sooting tendency increases with an

increasing number of carbons. That is, increasing the number of rings, the number of branches, or the number of carbons in the molecule increases the sooting tendency, even when it does not correlate with CN. As in the previous set of figures, when comparing MPI and CN on a per-carbon-mol injected basis, the same trends are observed (See Figs 3.9a and b). These results provide further evidence that CN alone does not provide a good estimate of a particular fuel's sooting tendency.

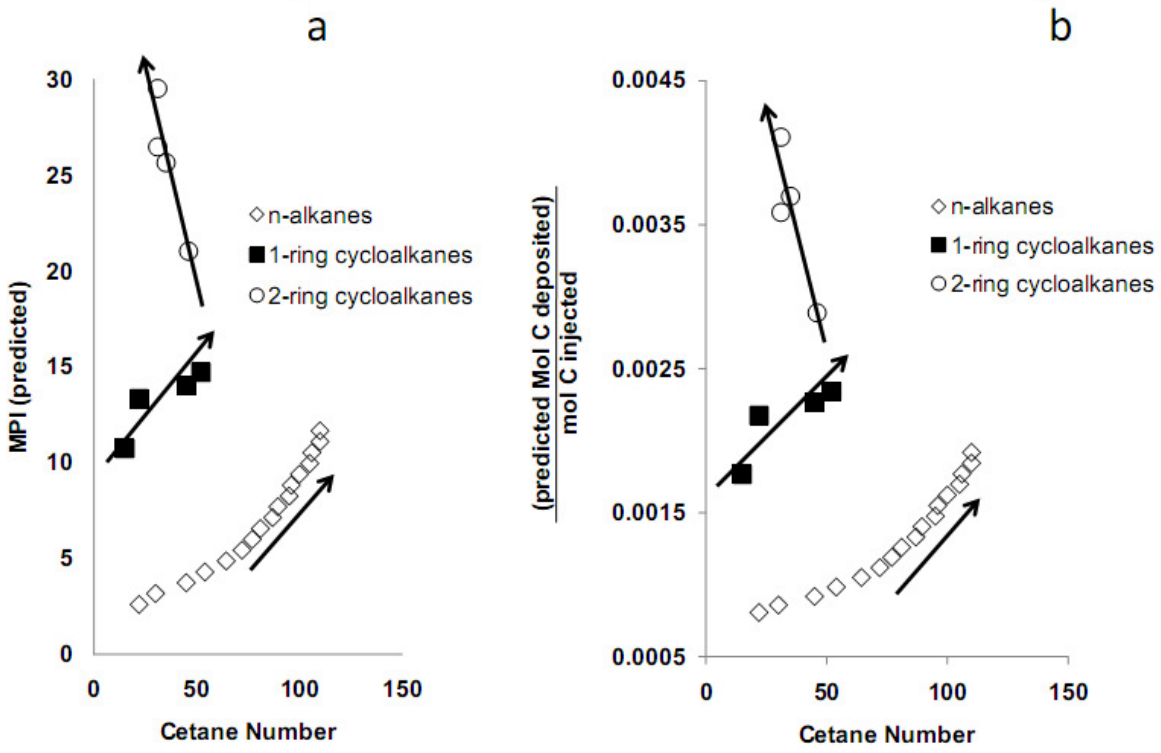


Figure 3. 9. (a) Comparison between predicted MPI and experimental CN values obtained from the literature[22] for n-alkanes and cycloalkanes. (b) Comparison between the (moles of carbon deposited)/(moles of carbon injected) and CN. Arrows indicate the direction of increasing number of carbons/molecule.

3.4.8. MPI measurements of real fuel mixtures

A valuable feature of MPI is its ability to measure real fuel mixtures. To test this feature, we obtained several samples of real fuels from ConocoPhillips. The NOISE analysis (provided by ConocoPhillips) of each fuel along with its extrapolated MPI value can be seen in Table 3.4. The MPI values were calculated by diluting each sample to 10%volume in n-heptane, and measuring the MPI of this mixture. The pure MPI values were then found by extrapolating a line from 0-10% sample in n-heptane to 100%; this would be the case if a pure sample were injected

Table 3.4. MPI and compositional analysis of several real fuel mixtures

	composition (wt %)						
sample	*n*-alkanes + isoalkanes	total cycloalkanes	compounds containing 1 aromatic ring	compounds containing 2 aromatic rings	substituted cyclohexanes	cycloalkanes with 2 or more rings	MPI (extrapolated)
A	26.50	60.29	12.89	0.31	33.40	26.90	65.9
B	32.19	67.81	0.00	0.00	64.00	3.80	34.6
C	39.62	48.17	12.20	0.00	44.48	3.69	43.4
D	37.12	43.62	19.16	0.10	38.76	4.85	50.8

and no nonlinearities would exist. This approach was taken in order to eliminate any nonlinearities due to high concentrations of aromatics as discussed in section 3.4.4. This is a good approach if the actual fuel composition is unknown and only the sooting tendency is to be estimated. In this case, larger concentrations of sample could be used as long as the total aromatic content in the sample does not go over~20% by volume. The observed MPI values indicate that MPI scales with aromatic content, but the presence of both large aromatic and naphthenic rings also play an important role. For instance, sample B contains no aromatics, and consequently has the lowest MPI value. As aromatic content is introduced in sample C, the MPI value increases substantially,

but heavier naphthenics play a significant role as well. This is indicated by the differences in samples A and D.

On the other hand, by comparing samples C and D, one can see that if the total cyclane content is kept constant, but the mono-aromatic content is increased, the MPI value increases. What is not so obvious is that when comparing samples C and A, by keeping the mono-aromatic content somewhat constant, but replacing a fraction of the small naphthenics and paraffins with large naphthenics, an even larger increase in MPI can occur. This means that observing only the aromatic content of the fuel can lead to skewed interpretations of its sooting tendency.

3.5. Conclusions

The Micropyrolysis Index (MPI) proves to be a valuable tool for estimating the sooting tendency of a particular fuel component. Some advantages over more traditional measurements of sooting tendency are:

a) Only pyrolysis is involved in the measurement, so this method is independent of stoichiometric oxygen ratios and flame temperatures, making it much more representative of a particular compound in a mixture, as well as very promising for fundamental studies.

b) Only small sample volumes are required, making this method accessible for laboratory scale studies, from which small sample volumes are available.

c) Reproducibility is much improved compared to the traditional TSI method, and equipment commonly found in conventional labs may be utilized to obtain the MPI values.

This provides an extremely valuable measurement with the purpose of guiding the molecular engineering strategy. Strategies may now be developed in order to minimize the MPI of the resulting products, thus improving the health and environmental properties of the fuel.

3.6 Acknowledgment:

Financial support from the Oklahoma Center for Advancement of Science and Technology and ConocoPhillips is gratefully acknowledged. Discussions with Walter Alvarez at ConocoPhillips were very helpful during the development of this study as well.

References

1 D. W. Dockery, C.A. Pope III, X. Xu, J.D. Spengler, J.H. Ware, M.E. Fay, B. G. Ferris Jr., F.E. Speizer *N. Engl. J. Med.* **1993**, *329,* 1753.

2 J.M. Samet, F. Dominici, F.C. Curriero, I. Coursac, S.L. Zeger *N. Engl. J. Med.* **2000**, *343*, 1742.

3 K. Katsouyanni,G. Touloumi, E. Samoli, A. Gryparis, A. Le Tertre, Y. Monopolis, G. Rossi, D. Zmirou, F. Ballester, A. Boumghar, H.R. Anderson, B. Wojtyniak, A. Paldy, R. Braunstein, J. Pekkanen, C. Schindler, J. Schwartz *Epidemiology* **2001**, *12*, 521.

4 C.A. Pope III, R.T. Burnett, M.J. Thun, E.E. Calle, D. Krewski, K. Ito, G.D. Thurston *J. Am. Med. Assoc.* **2002**, *287*, 1132.

5 J. Kaiser *Science* **2000**, *289*, 422.

6 J. Schwartz *Environ. Health. Perspect.* **2000**, *108*, 563.

7 J. Kaiser *Science* **1997**, *277*, 466.

8 J. Hansen, L. Nazarenko *Proc. Natl. Acad. Sci.* **2004**, *101*, 423.

9 M.Z. Jacobson *Nature* **2001**, *409*, 695.

10 M.O Andreae *Nature* **2001**, *409*, 671.

11 M.Z.J. Jacobson, *Geophys. Res.* **2002**, *107,* (D19) [Article Number 4410].

12 M.D. Avakian, B. Dellinger, H. Fiedler, B. Gullet, C. Koshland, S. Marklund, G. Oberdorster, S. Safe, A. Sarofim, K.R. Smith, D. Schwartz, W.A. Suk *Environ. Health Perspect.* **2002**, *110*, 1155.

13 P. Do, S.P. Crossley, M. Santikunaporn, D.E. Resasco *Catalysis (Special Periodical Reports)*; Royal Society of Chemistry: Cambridge

14 C.W. Lautenberger, J.L de Ris, N.A. Dembsey, J.R. Barnett, H.R. Baum *Fire Safety J.* **2005**, *40*, 141.

15 Y. Yang, A.L. Boehman, R.L. Santoro *Combustion and Flame* **2007**, *149*, 191.

16 I.P. Androulakis, M.D. Weisel, C.S. Hsu, K. Qian, L.A. Green, J.T. Farrell *Energy & Fuels* **2005,** *19,* 111.

17 N. Nakakita, K. Akihama, W. Weissman, J.T. Farrell *International Journal of Engine Research*, **2005**, *6(3)*, 187.

18 H.F. Calcote, D.M. Manos *Combust. Flame*, **1983**, *49*, 289.

19 D.B. Olson, J.C. Pickens, R.J. Gill *Combust. Flame*, **1985**, *62*, 43.

20 C.S. McEnally, L.D. Pfefferle *Combustion and Flame* **2007**, *148*, 210.

21 C.S. McEnally, L.D. Pfefferle, B. Atakan, K. Kohse-Hőinghaus *Progress in Energy and Combustion Science* **2006**, *32*, 247.

22 R.C. Santana, P.T. Do, M. Santikunaporn, W.E. Alvarez, J.D. Taylor, E.L. Sughrue, D.E. Resasco *Fuel* **2006**, *85*, 643.

23 S. Yan, E.G. Eddings, A.B. Palotas, R.J. Pugmire, A.F. Sarofim *Energy Fuels.* **2005**, *19*, 2408.

CHAPTER 4

4. Development of Strategies for Upgrading of Conventional Fuels

4.1 Introduction

The strategies created according to the methodology outlined in chapter one are the end product of the molecular engineering strategy. These have been developed to produce novel solutions which solve a variety of problems. Although the motivation for the strategies may seem to be widely varied, the underlying strategy utilized to develop them is the same. This is to understand the fundamental reactions occurring on the catalyst surface, and link those to fuel properties in order to determine which properties should be maximized.

Three strategies will be discussed, hydrogenation of multi-ring aromatic compounds, selective ring opening of naphthenics to produce high octane gasoline, and selective ring opening to produce high cetane diesel fuel. These strategies are highly interrelated. Hydrogenation of aromatic rings is the first step of the overall process, which produces naphthenic compounds. In order to minimize secondary cracking, an acid catalyzed ring contraction step is then employed. The resulting naphthenic compounds can then be utilized to produce either diesel or gasoline fuel, depending on where the ring is selectively opened. The resulting properties are highly dependent on the selectivity to where the ring is opened, as can be observed in figure 4.1 starting with the model compound naphthalene. By opening the ring selectively at substituted positions, a high cetane diesel fuel may be obtained, while opening selectively at

unsubstituted positions results in high octane gasoline fuel. This figure represents the reactions which will be considered in this chapter, which eventually lead to novel catalytic strategies built on fundamental knowledge.

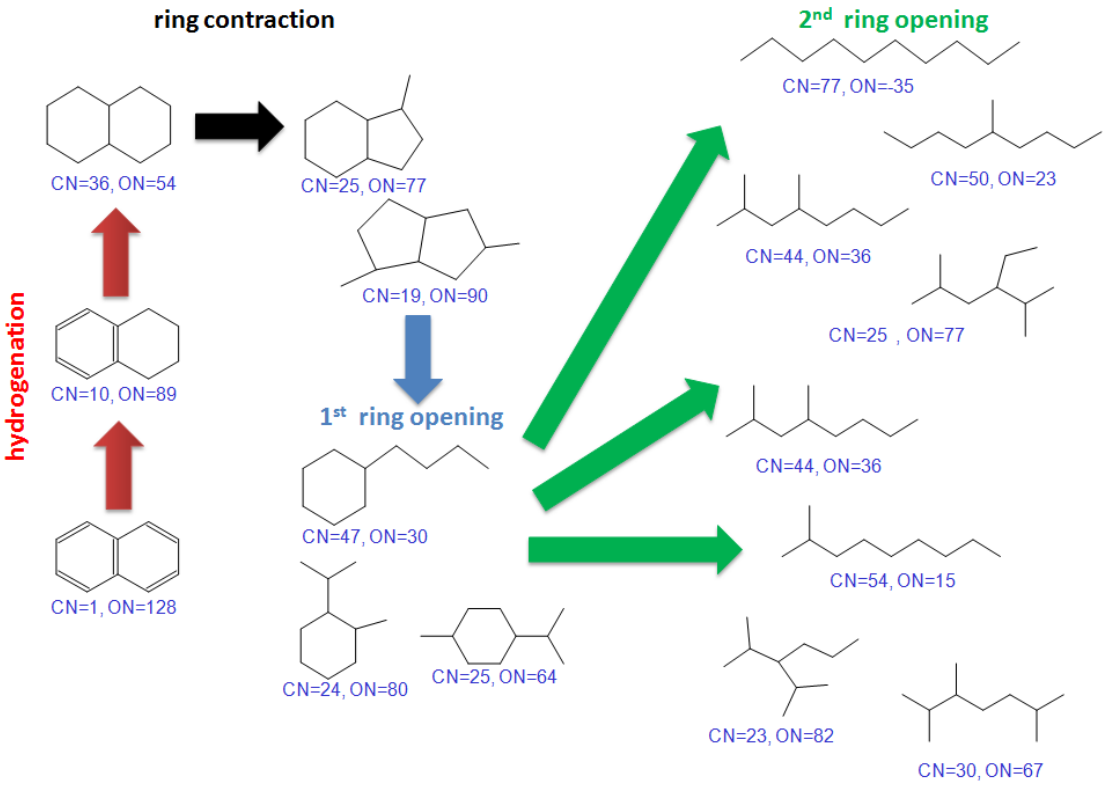


Figure 4. 1 Overview of catalytic steps involved in the upgrading of diesel and gasoline fuels

Fuel properties associated with hydrogenation of aromatic rings are well understood, that is the cetane number dramatically increases with hydrogenation while the ON dramatically decreases with hydrogenation. Hydrogenation is necessary, however, for both fuels as even in the case of gasoline a limit is placed on the aromatic content allowed due to health and environmental concerns. Because the fuel properties resulting from hydrogenation of aromatics are well known, the focus for this study will

be to understand the kinetics and degree of inhibition by other compounds present in light cycle oil streams containing nitrogen and sulfur containing compounds. This will be accomplished through the use of kinetic fittings in order to determine the rates of each reaction, as well as the adsorption constants. A quantitative structure property relationship will then be utilized to relate the structure of the nitrogen containing compounds with their adsorption strength, and thus their ability to competitively adsorb on the surface of the catalyst.

For the next two examples, selective ring opening (SRO) will then be compared for the two cases of improving octane or cetane number. As can be observed in figure 4.1, this is highly dependent on where the ring is selectively opened. By understanding the fundamental surface reactions involved in this pathway, strategies are then developed in order to target the selective cleavage resulting in either high CN or ON products.

4.2 Influence of Nitrogen Containing Compounds and Number of Aromatic Rings on the Inhibition of Hydrogenation Activity over Sulfided $NiMo/Al_2O_3$.

4.2.1 Introduction

A combination of depleting petroleum resources and increasingly stringent environmental concerns on produced fuels provides a unique challenge for refiners. A depleting reserve has caused an increasing trend towards the processing of heavier

petroleum crudes which inherently contain a large amount of heavy aromatic compounds.[1] In addition, increasingly stringent clean fuel regulations[2-7] require the end fuels to have a lower total aromatic content than in the past. Because of these challenges, hydrotreating reactions of heavy oil cuts have recently received considerable interest. This is especially true for the case of diesel fuel, as very high efficiencies in hydrodearomatization (HYD) and hydrodesulfurization (HDS) must be obtained in order to meet on-road diesel specifications. For this to occur, a thorough understanding of the reactions and competition between molecules on the catalyst surface must first be obtained.

A fundamental phenomenon which is not well understood is the effect of competitive adsorption between molecules on the catalyst surface. One is the influence of competitive adsorption among various polycyclic aromatic compounds, and another is the competitive adsorption of nitrogen containing compounds with HYD and HDS reactions. Both of these reactions have been investigated to some extent, but each case has been lacking some practical aspect.

Our group has shown in the past that there is a strong inhibition between 3, 2, and 1-ring aromatic compounds over noble metal catalysts in a flow reactor.[8] This has not been conducted, however over a commercial hydrotreating catalyst. An interesting study has been conducted over $CoMo/Al_2O_3$ by Korre and Klein[9] in a batch reactor which indicates the presence of competitive adsorption among the aromatic compounds. In practice, however, hydrotreating reactors are operated continuously, and Nickel based catalysts are more commonly employed.

The inhibiting effect on hydrogenation from nitrogen containing compounds is also very important, and somewhat poorly understood. Interesting information implying the inhibition effect from nitrogen containing compounds has been conducted in the past,[10-12] but a systematic study which includes ammonia as well as other nitrogen containing compounds has not been conducted. Furthermore, there has not been an effort to understand the fundamental phenomenon which is responsible for the competitive nature of nitrogen containing compounds. For these reasons, a commercial NiMo hydrotreating catalyst has been employed under realistic flow conditions in order to better understand the effects of competitive adsorption in a hydrotreating reactor.

4.2.2. Experimental

4.2.2.1 Reactor Tests[13,14]

The commercial NiMo/alumina hydrotreating catalyst *Criterion 424* used for all experiments contained 6 wt%Ni and 18 wt% Mo. The catalytic activity was measured in a continuous flow reactor at a temperature of 345°C and a total pressure of 70 atm, with a H_2/HC molar ratio in the range 20–130 and at different contact times. Before each run, the catalyst sample was physically mixed with 5 cc of inert alumina and placed in the center of the reactor between layers of 3 mm glass beads. The catalyst was pre-sulfided in flow of 10% H_2S in H_2 at 200 and 370°C.

Table 4. 1 Feeds utilized in this study (adapted from ref 13,14)

							nitrogen doped feeds				
	feed no. (wt%)										
	1	2	3	4	5	6	7	8	9	10	11
tetralin (monoring)	5			5	5	5	5	5	5	5	5
naphthalene (diring)		3		3		3					
phenanthrene (triring)			2		2	2	2	2	2	2	2
quinoline							1000ppm				
tetrahydroquinoline								1000ppm			
indole									1000ppm		
indoline										1000ppm	
ammonia											85ppm

a) dodecane was used as a solvent

Several different feeds were used in this work (see Table 4.1) A model feed was prepared by blending various amounts of tetralin (TL; Acros, +98%), naphthalene (NP Aldrich, +99%), and (phenanthrene (PHE Aldrich, 98%) with 500 ppm of dibenzothiophene (DBT Aldrich, 99%) and 500 ppm of 4,6-dimethyldibenzothiophene (4,6-DMDBT; Aldrich, 99%) in 90 wt.% of dodecane (DO; Aldrich, 99%). Nitrogen compounds containing feed were prepared by adding 1,000 ppm of quinoline (Q; molar fraction = 0.00176); 1,2,3,4-tetrahydroquinoline (THQ molar fraction = 0.00171); Indole (IN; molar fraction =0.00194), Indoline (HIN; molar fraction = 0.00191) and 85 ppm NH3 (molar fraction = 0.00114), respectively, to the model feed, respectively. The products were trapped with chilled water and analyzed online by a HP6890 gas chromatograph with an FID detector using an HP-5 column. The data were collected at Time-on-stream (TOS) = 5h because of the stability and reproducibility of the data at this TOS. Experiments were undertaken at pre-determined conditions (flow-rate = 10 cc/h and particle diameter\0.64 mm) where no significant mass transfer effects were expected.

4.2.2.2 Kinetics[13,14]

The generalized Langmuir–Hinshelwood model for hydrogenation suggested by Kiperman [15][9] was used to fit the data obtained in this study.

$$r_{ij} = \frac{k_{ij} K_i K_{H_2} \left(P_i^{n_1} P_{H_2}^{n_2} - P_j / K_{\mathrm{eq}} \right)}{\left(1 + \sum_m K_m P_m^{n_3} \right)^{\mathrm{Z}}}$$

Where r_{ij} (mol $g_{cat}^{-1} h^{-1}$) is the rate of conversion of compound *I* to compound *j*, *P* (atm) is the partial pressure, k_{ij} is the kinetic rate constant, K_{eq} is the equilibrium constant and K_m (atm^{-1}) is the adsorption parameter of individual compounds. Usually n_1 can be taken as 1, Z represents the number of surface sites required for reaction, n_3 is ½ for atomic adsorption of H_2, and m is 1 for molecular adsorption. The equilibrium constants were obtained using HSC-Chemistry-5.0® software (Reg. USPTO, Outotec). The nonlinear parameter estimation of the kinetic model was performed with the Powell version of the Levenberg-Barquardt algorithm. The differential equations were solved using the EPISODE package of Scientist.®

4.2.2.3 Theoretical calculations

Electronic structures of studied organonitrogen compounds were calculated using density-functional-theory (DFT). The molecules were optimized using Gaussian 03W (DFT/B3LYP/STP-3G), and the Mulliken charges on the nitrogen atoms were

subsequently calculated. These were utilized for structure property correlations as will be discussed below.

4.2.3 Results and discussion

4.2.3.1 Competitive adsorption among aromatic rings

While it has been proposed that aromatic hydrocarbons hydrogenate in the order of aromaticity, that is, the compounds with a greater number of aromatic rings have the highest adsorption strength on the surface, and thus hydrogenate first, this has not been verified under realistic hydrotreating conditions with a $NiMo/Al_2O_3$ catalyst. Perhaps the best description of this inhibition activity can be taken from Beltramone *et al.*[13] As can be observed below in figure 4.2, addition of a small *amount* of di and tri ring aromatic compounds severely inhibits the conversion of tetralin over the surface

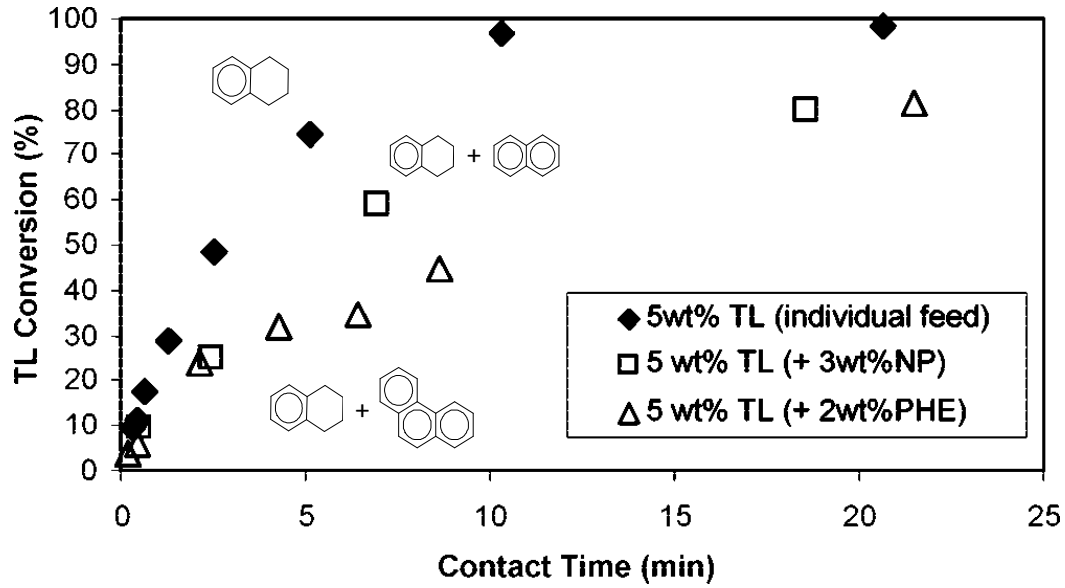


Figure 4. 2 conversion of tetralin over $NiMo/Al_2O_3$ at 100psig, 345°C. Model feeds 1,4, and 5 (see table 4.1).Adapted from Ref 13.

In a similar fashion, naphthalene conversion is only decreased in the presence of phenanthrene, and phenanthrene conversion is only mildly affected by naphthalene. Both multiaromatic ring compounds are not influenced by the presence of tetralin. This alone provides strong evidence for the competitive adsorption phenomenon previously outlined. A more clear case can be made, however, when one compares adsorption constants resulting from the kinetic fitting of not only the feed molecules, but also the products produced. These can be observed below in figure 4.3.

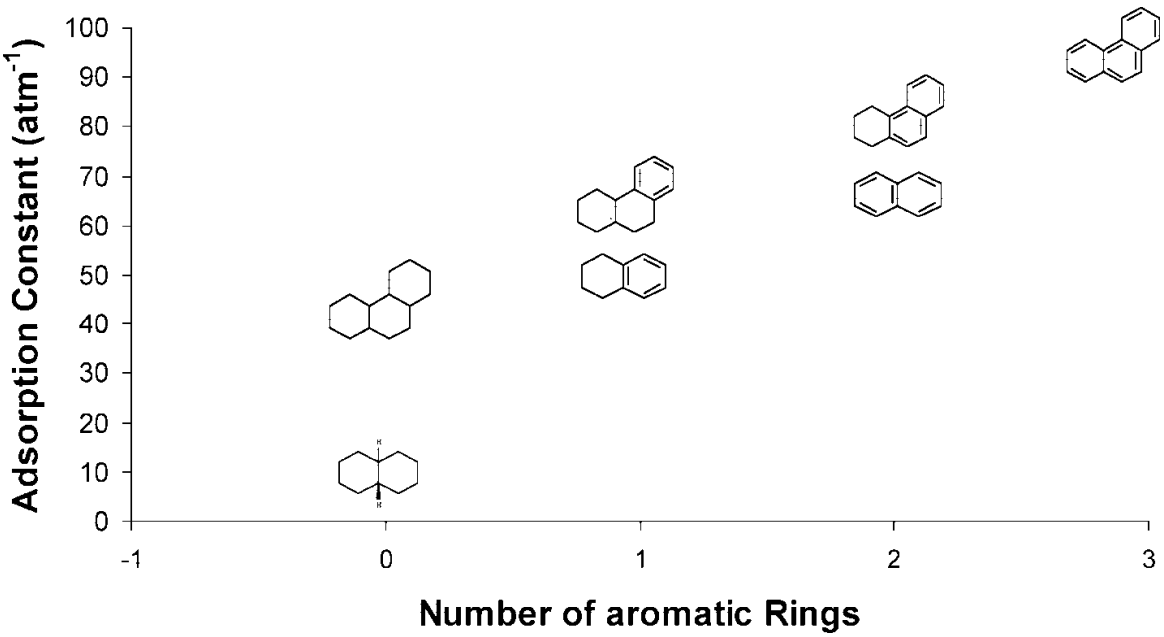


Figure 4. 3 Adsorption constants K (obtained from the kinetic fittings) as a function of the number of aromatic rings. Adapted from ref 13.

Through this graph, the influence of aromatic rings and naphthenic rings on adsorption is very clear. Naphthenic rings provide a marginal increase in adsorption,

while aromatic rings provide a much more pronounced increase for every case. This provides a clear example of the competitive nature of multiple aromatic rings.

4.2.3.2 Competitive adsorption among nitrogen containing compounds

The effect of nitrogen inhibition was studied in an identical manner to the investigation of competitive adsorption among polyaromatic hydrocarbon groups. For this case, as can be observed in Table 4.1, the ratio of aromatic and sulfur containing compounds was maintained while small amounts of nitrogen containing compounds were introduced to the system. Nitrogen containing compounds of various molecular weights and various degrees of basicity were compared, and the results were subsequently fit with the previously described Langmuir Hinshelwood kinetic model. The results for the inhibition of tetralin and phenanthrene doped with 1000ppm, or in the case of ammonia 85ppm, of nitrogen containing compounds can be observed in figure 4.4a and b.

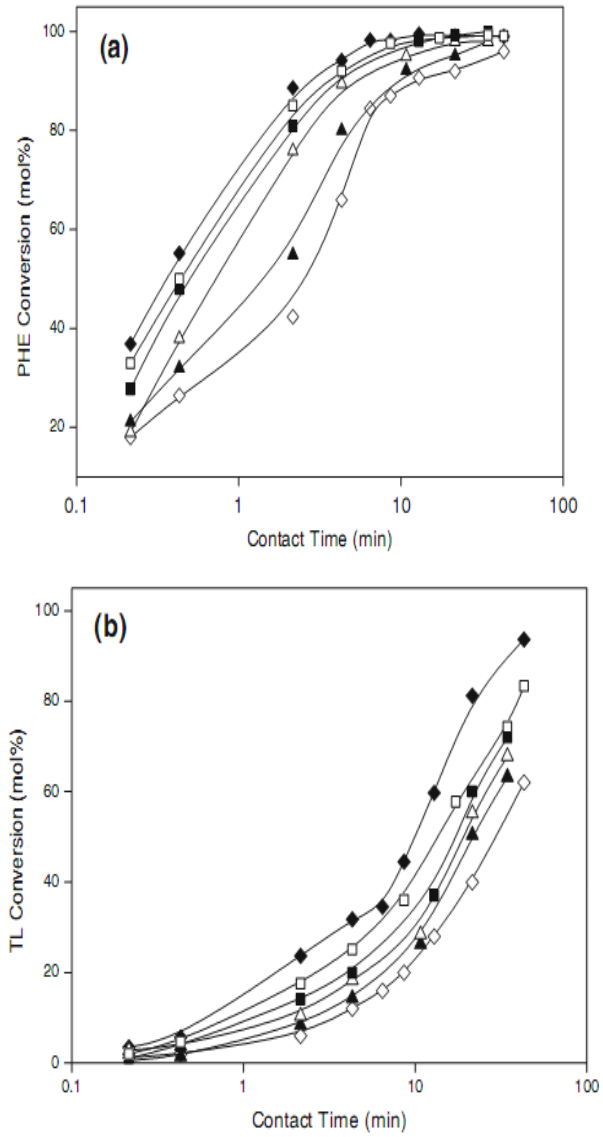


Figure 4. 4 Influence on nitrogen containing compounds on conversion of (a) phenanthrene and (b) tetralin. Symbols represent feed 5 (no dopant →solid diamonds), feed 7 (1000ppm Quinoline→open squares), feed 8 (1000ppm tetrahydroquinoline→ closed squares, feed 9 (1000ppm Indole→open triangles), feed 10 (1000ppm Indoline→ closed triangles, and feed 11 (85ppm ammonia→ open diamonds). *Note: Log scale used for clarity*

One can clearly observe the strong competitive nature of the nitrogen containing compounds. Even the strongly adsorbed phenanthrene is inhibited by each of these compounds even in small amounts. This indicates that the adsorption constants of these

nitrogen containing compounds are extremely high with respect to polycyclic aromatic species. As before, a thorough analysis of reaction kinetics can be utilized to help explain this phenomenon. By comparing the adsorption constants of each of the nitrogen derived species, one has the ability determine the fundamental nature of the molecule responsible for the strong adsorption on the surface. The kinetic adsorption constants for the nitrogen containing compounds are in Table 4.2.

Table 4. 2 Adsorption constants of various nitrogen containing compounds.

Compound	Adsorption constant (atm^{-1})
Quinoline	500
TetrahydroQuinoline	1,450
Indole	1,200
Indoline	1,500
Propylaniline	2,000
Ethylaniline	2,000
Ammonia	3,129

The first observation from these constants is that they are extremely high in comparison with the aromatic hydrocarbons discussed in section 4.2.3.1. For most of these compounds, the adsorption constant is an order of magnitude greater than those for the strongly adsorbed phenanthrene. The next step is to determine what molecular feature is responsible for this phenomenon.

This phenomenon can be explained through a simple structure-property relationship. As discussed in section 4.2.2.3, density functional theory calculations

were conducted in order to obtain the optimum structure and electronic configuration of the nitrogen containing compounds. Mulliken charges are the partial charges attributed to atoms on the molecule when computed according to a population analysis of the wavefunctions. The Mulliken charges of the nitrogen atoms were compared with the experimental adsorption constants, with the results shown in figure 4.5.

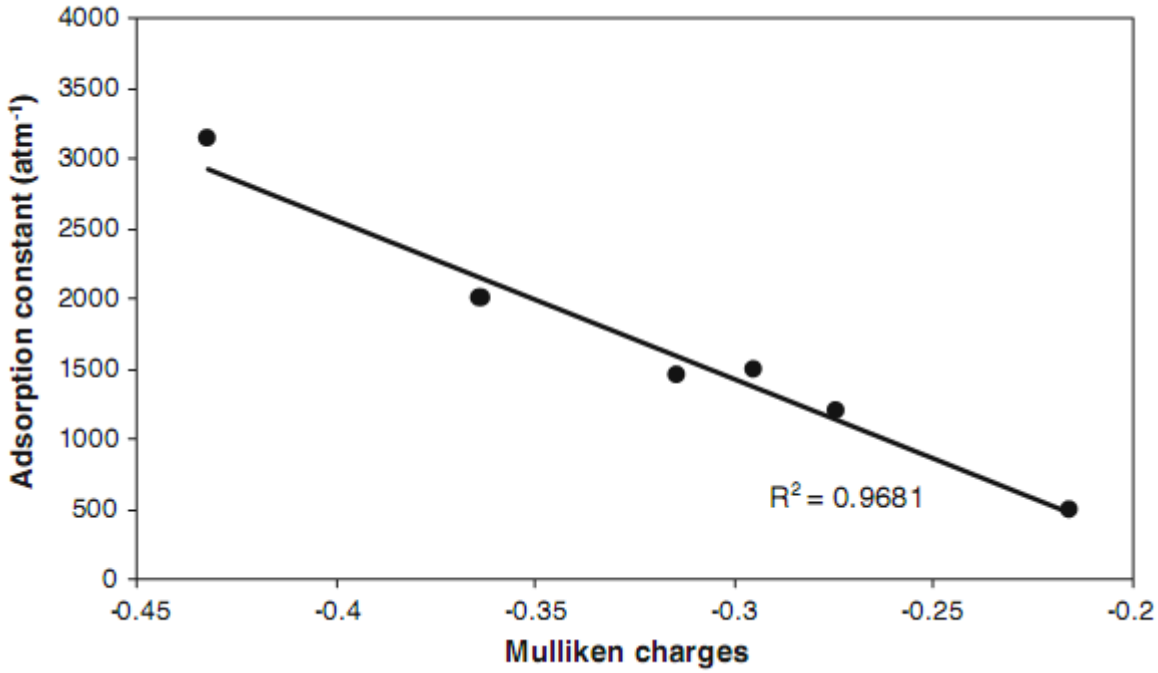


Figure 4. 5 Correlation between the adsorption constant of the organonitrogen compounds and the negative Mulliken charges on the nitrogen atoms as calculated with DFT.

The agreement between the partial charges on the nitrogen atoms with the adsorption constant is remarkable. This provides strong evidence that the underlying factor attributed to the adsorption constant of nitrogen compounds over nickel hydrotreating catalysts can be explained simply by the partial charge on the nitrogen

atom of the molecules. Although this charge was calculated via an expensive computational method, the relationship is one of the most fundamental correlations between a property and molecular structure which can be derived, with an extremely high return. With this methodology, one could estimate the adsorption constant under these conditions of nitrogen containing compounds under these conditions while knowing only the partial charge on the nitrogen atom.

4.2.4 Conclusions

Several important conclusions can be drawn from this study.

1) The adsorption strength, and therefore reactivity of multiring aromatic compounds increases on the order tetralin<naphthalene<phenanthrene, indicating the strong influence of the number of aromatic rings in a molecule on the adsorption over a nickel based hydrotreating catalyst.

2) The adsorption constant of nitrogen containing compounds can be explained by the increasingly negative partial charge on the nitrogen atoms as calculated via DFT.

4.2.5 Applications to molecular engineering strategy

This section provides an example of the molecular engineering strategy, although the focus was heavily on understanding what happens on the catalyst surface, and very little emphasis was placed on the optimization of fuel properties. Fuel

properties are still what drives this example, and the reason why they were not emphasized is because the result is rather trivial. Hydrogenation of aromatics increases CN and decreases ON at the expense of hydrogen as was seen in figure 4.1. The desired result is to maximize hydrogenation conversion, and gain fundamental knowledge to improve the efficiency of the process. Through this, a maximum in fuel properties will be obtained.

This example serves as one where fuel property prediction plays the most minor role. As this chapter progresses, a perpetually increasing emphasis will be placed on fuel property prediction for the guided development of fuels. This provides a nice transition to chapter 5, where QSPR's will be utilized to not only predict fuel properties of interest, but also catalytic behavior.

4.3 Aromatics removal in gasoline while minimizing ON losses

4.3.1 Introduction

Aromatics removal in gasoline provides a unique challenge to refiners, as aromatics contain exceptional octane numbers. Simple removal of aromatics to their corresponding naphthenics provides an enormous drop in octane number. This can be observed in figure 4.6, as aromatics are hydrogenated to their corresponding naphthenics, a significant decrease in octane number is always observed.

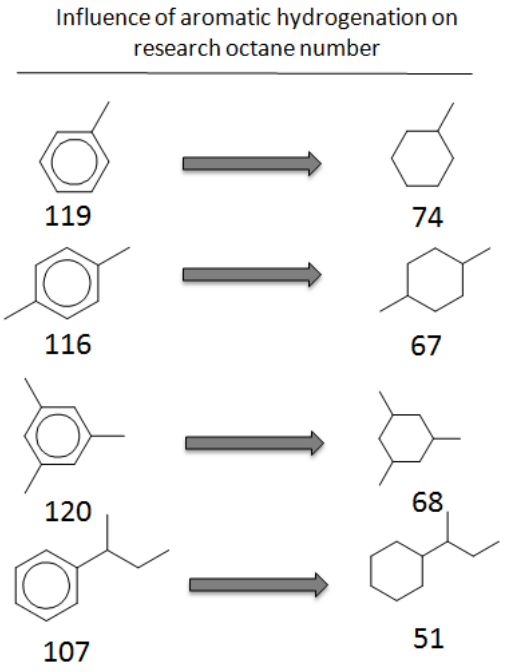


Figure 4. 6 RON values of mono-ring aromatic hydrocarbons before and after hydrogenation

This scenario provides extreme potential for the molecular engineering strategy, as novel catalytic strategies can be developed in order to remove aromatics while minimizing losses in octane number. An overview of potential ON improvement strategies will first be discussed, followed by the actual implementation of the most promising strategy for octane improvement.

4.3.2 Overview of potential catalytic strategies for ON improvement

As a first step, one should investigate how selective ring opening alone will impact octane number. Utilizing methylcyclohexane as a model compound, this can be

investigated by looking at the various ring opening products of methylcyclohexane, as well as the properties which would result. These can be observed in figure 4.7 as the RON of the various ring opening products can be compared with that of methylcyclohexane. It can clearly be observed that octane number varies dramatically depending on where the ring is selectively opened. This aspect is overwhelmed, however, by the fact that each of the potential products has an octane number which is significantly lower than the initial feed of methylcyclohexane. Although this is only one compound, this provides an indication that selective ring opening alone may not be the optimum strategy for further improving octane number.

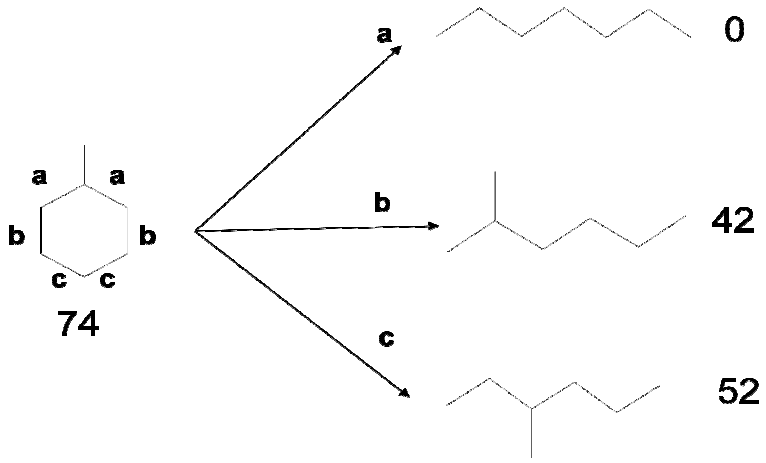


Figure 4. 7 Influence of position of selective ring opening on research octane number for selective ring opening of methylcyclohexane.

As an alternative approach, one may consider an acid catalyzed ring contraction step. This serves two purposes, it may increase the degree of branching on the ring, while at the same time making the ring more prone to selective ring opening without excessive cracking to low value products. As an illustration of the fuel properties which

may result from a ring contraction step, methylcyclohexane again will be utilized as a probe molecule. The RON of methylcyclohexane, as well as its potential ring contraction products can be observed below in figure 4.8.

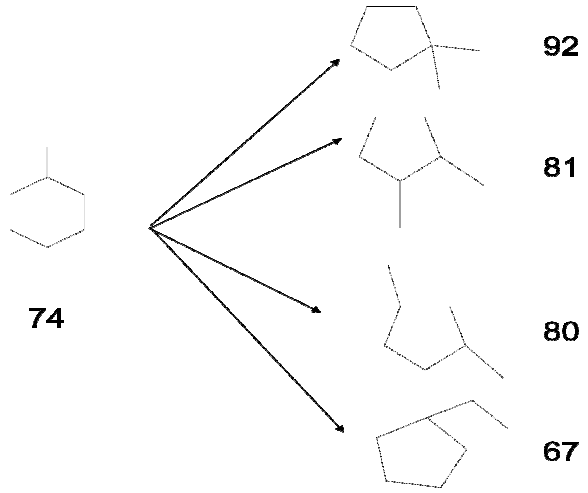


Figure 4. 8 RON values for potential ring contraction products resulting from methylcyclohexane

As can be observed in figure 4.8, each product except for ethylcyclopentane has an octane number which is significantly higher than the feed. This provides great promise for an acid catalyzed ring contraction step as a potential route for improvement in ON.

Although ring contraction is quite promising for improvement of octane number, advantages are quite marginal, and it is worth investigating if these ring contraction products can be improved further. As mentioned above and illustrated in figure 4.7, direct ring opening of methylcyclohexane is not beneficial, regardless of where the ring is opened. Ring opening of the ring contraction products, however, can result in increasingly branched alkanes with much improved octane numbers. This is illustrated

for the case of 1,2 dimethylcyclopentane in figure 4.9. While opening the ring at position a or b clearly has a detrimental effect on octane number, the opening at position c produces a significant advantage. This gives motivation for selective ring opening, as selective cleavage at position c would result in products with notably higher octane numbers than those of hydrogenation alone.

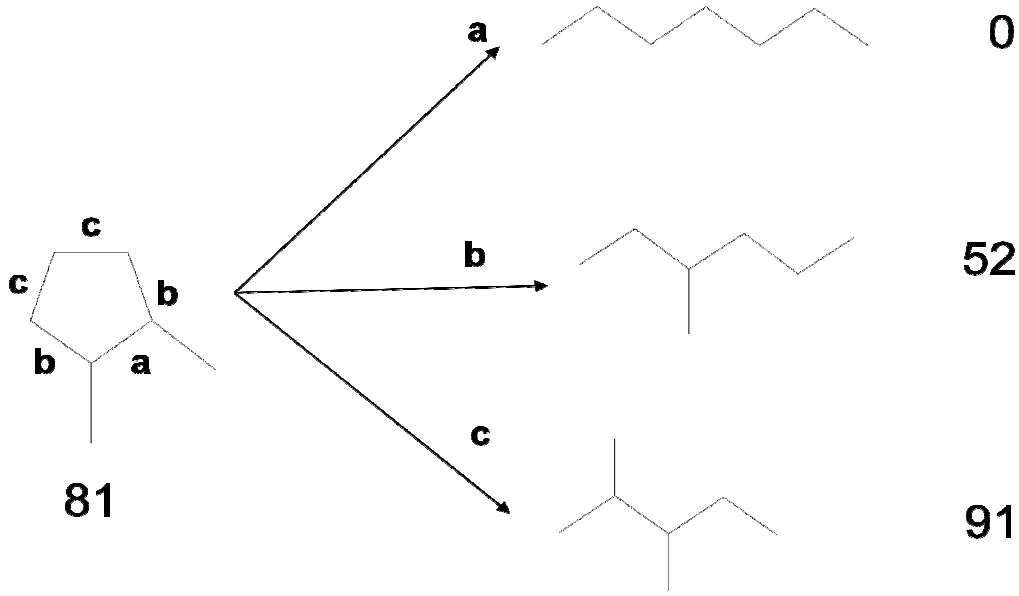


Figure 4. 9 RON resulting from the selective ring opening of 1,2 dimethylcyclopentane

In order to selectively open the ring, and avoid excess cracking, McVicker *et al* found that Iridium based catalysts were the most selective for opening the ring of naphthenics while minimizing secondary cracking when compared with Pt, Ni, and Ru.[16] Furthermore, a member of our group, Phuong Do, subsequently found a dramatic influence of support for ring opening selectivity of substituted cycloalkanes over Ir based catalysts.[17] This effect can be observed in figure 4.10. For the model compound

1,3 dimethylcyclohexane, cleavage at unsubstituted vs. substituted positions was found to be much greater for Ir/SiO_2 when compared with the supports Al_2O_3 and TiO_2. This was attributed to an increased tendency to form a dicarbene intermediate on the surface, thus resulting in selective cleavage at unsubstituted positions. For this reason, Ir/SiO_2 was selected as the most promising catalyst for providing further improvements in ON after the ring contraction step.

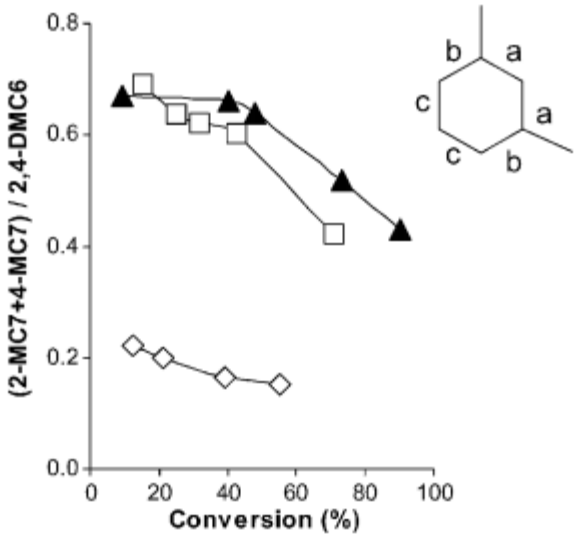


Figure 4. 10 Ratio of cleavage at substituted positions on the ring to unsubstituted positions on the ring as a function of conversion over Ir based catalysts in a flow reactor at 593 K and 3540 kPa. The hydrogen/hydrocarbon ratio was maintained at 30. The ratio on the y-axis represents cleavage at positions (*a*+*b*)/*c*. Open diamonds represent a support of SiO_2, closed triangles represent Al_2O_3, and open squares represent TiO_2. Adapted from ref 17.

This provides an indication of the true power of combining model compound studies to understand the fundamental surface intermediates with fuel properties. A potential reaction strategy of ring contraction followed by selective ring opening over Ir/SiO_2 has been developed as a way of increasing the ON of the model compound

methylcyclohexane before any reactions have even been conducted. This is the true value of fuel property prediction, and an example of how it can provide guidance for the development of catalytic strategies.

4.3.3 Implementation of catalytic strategy for improvement of ON.

Because of the guided nature of the molecular engineering approach, ring contraction and selective ring opening at unsubstituted positions have already been selected as the best strategy for maximizing ON of hydrogenated aromatic compounds. What is left is to determine the optimal approach for these reactions. This study was conducted by Malee Santikunaporn while at OU.[20] For the ring contraction step, Pt/HY was utilized. It was observed in previous studies that the addition of Pt enhances catalyst lifetime and reduced secondary cracking. This is due to the increased rate of hydrogen transfer brought about by the Pt[18] as well as the decrease in acid site density.[19] In order to determine the best overall strategy for octane improvement, while utilizing methylcyclohexane as a probe molecule, three potential approaches were investigated. A schematic of these three approaches is outlined in figure 4.11.

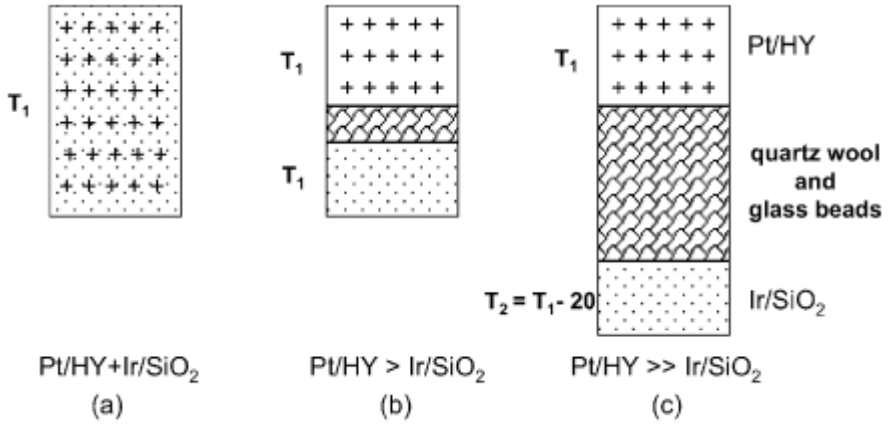


Figure 4. 11 Schematic reaction system configurations. Adapted from ref. [20]

These configurations outlined in figure 4.11 obviously should produce marked differences in the resulting fuel properties. For configuration (a), the Ir/SiO_2 bed will be in potential contact with some of the unconverted feed methylcyclohexane, resulting in some degree of direct ring opening. This approach does not conceptually appear to be the best due to the properties of the products which would result as indicated by figure 4.7. Configuration (b) separates these two events by placing the Ir/SiO_2 bed after the Pt/HY bed. This should result in improved properties when compared with configuration (a). Configuration (c) introduces the potential advantage of performing the ring opening step at 20°C cooler than the initial ring contraction step. This idea arises from the fact that cyclopentane rings have an added amount of ring strain, and thus ring open much more readily than cyclohexane rings. Because of this, by decreasing the temperature slightly, selective ring opening of the ring contraction products may be maintained while minimizing undesirable secondary cracking.

The results of these three strategies on RON and MON can be observed below in figures 4.12 (A) and (B). For this case, due to the highly nonlinear blending rules of ON for mixtures, ON was estimated utilizing the method outlined by Ghosh *et al*[21] which was developed for blends and has a standard error of ~±1octane number. This method was described in chapter 2 section 2.4.2. The result of the reaction results is very promising. One can clearly observe that catalytic bed arrangements (b) and (c) both provide a substantial advantage over the equilibrium obtained through ring contraction alone. The productivity of the catalyst bed arrangements appears to follow the order (a)<(b)<(c), most likely due to the aforementioned hypothesis for each case.

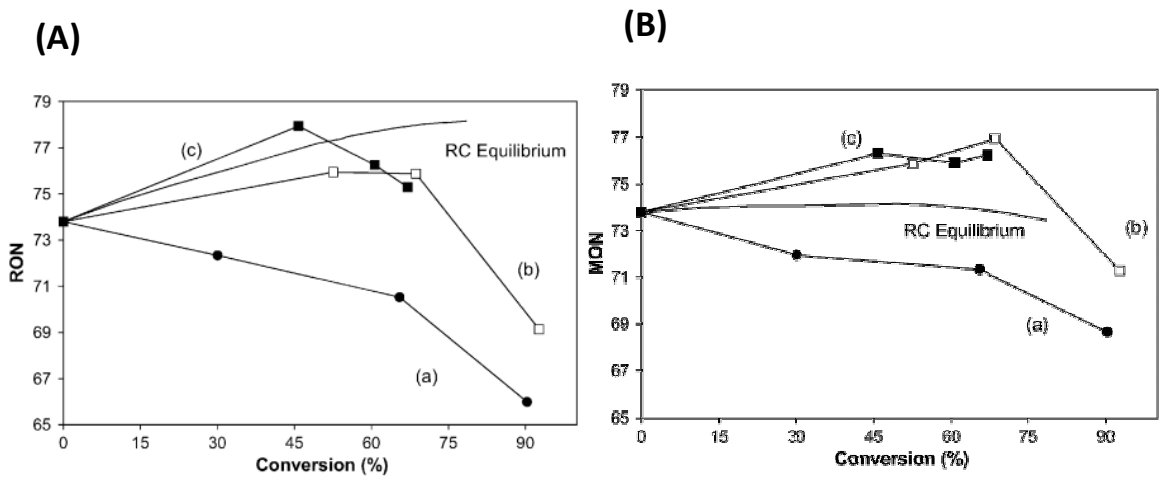


Figure 4. 12 (A) RON and (B) MON of the product mixture resulting from conversion of methylcyclohexane following the reactor bed configurations outlined in figure 4.11. Total pressure = 2MPa; H_2/feed molar ratio=40. Adapted from ref.20.

4.3.4 Conclusions

Due to a combination of fuel property prediction with fundamental model compound studies, a novel catalytic strategy was developed which could provide great promise for upgrading of gasoline fuels while at the same time meeting environment demands for reducing aromatic content. This provides an excellent example of how model compounds can be combined with fuel properties in order to develop catalytic strategies which are effective, but also built on a fundamental foundation.

4.4 Insight gained towards improvement of CN of diesel fuels

An identical approach to that taken for the improvement of ON can be utilized in order to improve the CN of diesel fuel. Fuels which have a high ON typically have an inherently low CN, and vice versa. This can be observed through the schematic overview of this chapter depicted in figure 4.1. For the case of CN improvement, the opposite bonds for ring cleavage should now be targeted. Instead of preferential cleavage at unsubstituted positions via the dicarbene mechanism, cleavage at substituted positions via the metallocyclobutyl mechanism should be maximized. According to figure 4.10, Ir/Al_2O_3 should now be the preferential catalyst of choice as it has a higher tendency to break at these positions while minimizing secondary cracking.

While the fundamental approach to this problem is very similar, the underlying practical question is somewhat different. For the improvement of CN, the molecular weight range will be quite different. Diesel fuels contain a heavier cut of hydrocarbons,

and many compounds in the diesel range may have multiple aromatic rings if one wishes to utilize some of the heavier cuts of crude oil such as light cycle oil. While the first step towards improving the properties of polycyclic aromatic compounds towards the production of diesel fuel is obviously hydrogenation, as outlined in section 4.2, the sequential steps are not clearly defined. If one starts with decahydronaphthalene, as in figure 4.1, it is widely accepted that opening of the first ring will result in an increase in CN. The opening of the second ring, however, is the subject of debate as the properties which result can vary wildly depending on the selectivity to where the ring was opened and the degree of secondary cracking.

This leads to the fundamental question of whether or not the opening of the second ring is beneficial or not. This will be the focus of chapter 5, with a further increased emphasis placed on the usefulness of structure property models.

4.5 Conclusions

Thus far, we have outlined three examples of how the molecular engineering strategy can be employed in order to develop catalytic strategies to improve the properties of conventional fuels. Each sequential example has an increased emphasis placed on fuel properties, and their prediction. At the same time, these examples are highly correlated, as hydrogenation is the preliminary step for the other two reactions. The improvement of ON and CN are very much related as well, as selective ring opening is employed in both cases, with only the position which is opened being the fundamental difference between the two. This serves as an example of how a wide

variety of problems can be approached through the use of the same fundamental strategy.

References

1 V.A. Gembicki, T.M. Cowan, G.R. Brierley *Hydrocarbon Process* **2007**, 86, 41.

2 S. Brunet, D. Mey, G. Perot, C. Bouchy, F. Diehl *Appl Catal A Gen* **2005**, 278, 143.

3 K.G. Knudsen, B.H. Cooper, H. Topsoe *Appl Catal* **1999**, 189, 205.

4 C. Song *Catal Today* **2003**, 86, 211.

5 T.V. Choudhary, J. Malandra, J.Green, S. Parrott, B. Johnson *Angew Chem Int Ed* **2006**, 45, 3299.

6 T.V. Choudhary *Ind Eng Chem Res* **2007**, 46, 8363.

7 T.V. Choudhary, S. Parrott, B. Johnson *Environ Sci Technol* ASAP Article. doi: 10.1021/es0720309

8 S. Jongpatiwut, Z. Li, D.E. Resasco, W.E. Alvarez, E.L. Sughrue, G.W. Dodwell *Appl. Catal.,A: Gen*. **2004**, 262, 241.

9 S.C. Korre, M.T. Klein, R.J. Quann *Ind. Eng. Chem. Res.* **1995**, 34, 101.

10 M.J. Girgis, B.C. Gates *Ind Eng Chem Res* **1991**,30,2021.

11 E. Furimsky, F. Massoth *Catal Rev Sci Eng* **2005**,47,297.

12 R. Prins *Adv Catal* **2001**,46,399.

13 A. R. Beltramone, D. E. Resasco, W. E. Alvarez, T. V. Choudhary *Ind Eng Chem Res* **2008,** 47(19), 7161.

14 A.R. Beltramone, S. Crossley, D.E. Resasco, W.E. Alvarez, T.V. Choudhary *Catal. Lett.* **2008**, 123, 181.

15 S.L Kiperman *Stud Surf Sci Catal**1986***, 27,52.

16 G. B. McVicker, M. Daage, M. S. Touvelle, C. W. Hudson, D. P. Klein, W. C Baird, Jr., Br. R. Cook, J G. Chen, S. Hantzer, D. E. W. Vaughan, E. S. Ellis, and O. C. Feeley *J. Catal.* **2002**, 210, 137.

17 P. T. Do, W. E. Alvarez and D. E. Resasco *J. Catal.* **2006**, 238(2), 477.

18 R. Cid and A. Lopez Agudo *React. Kinet. Catal. Lett.* **1983**, 22, 13.

19 G. B.McVicker, O. C. Feeley, J. J. Ziemiak, D. E.W. Vaughan, K. C. Strohmaier,W. R. Kliewer and D. P. Leta *J. Phys. Chem. B* **2005**, 109, 2222.

20 M. Santikunaporn, W. E. Alvarez, D. E. Resasco *Appl Catal A: Gen* **2007**, 325, 175.

21 P. Ghosh, K. J. Hickey and S. B. Jaffe *Ind. Eng. Chem. Res.* **2006**, 45(1), 337.

CHAPTER 5

5. Primary Product Selectivity Prediction over Ir/Al_2O_3 as a Novel Approach towards Fundamental and Practical Problems in Fuel Upgrading.[1]

5.1 Introduction

Hydrogenolysis of naphthenic rings is a potentially valuable step for many applications. One example is the upgrading of light cycle oil (LCO) to produce a more valuable product which can be blended into diesel fuel.[2-5] LCO contains a large fraction of aromatics, which reduces the fuel's cetane number (CN). Thus, in order to improve CN of this fuel and meet environmental regulations, the aromatics can be hydrogenated to their corresponding naphthenes. While it has been suggested that selective ring opening (SRO) can produce linear paraffins with high cetane numbers, we have pointed out[6-8] that this CN increase can only be accomplished via ring opening at substituted positions. However, even the most selective ring opening catalysts, such as Ir/Al_2O_3, do not open the ring at substituted positions with 100% selectivity. Therefore, when looking only at the CN of the products, ring opening may not be worth the investment as only marginal gains in CN may be achieved. But, as we show here, CN is not the only fuel property which may be improved by selective ring opening. The specific gravity of the fuel will slightly decrease as the rings are opened, leading to an increased volume in product. More importantly, the sooting tendency of the fuel can dramatically decrease after further ring opening, leading to a more environmentally friendly fuel.

There are many potential mechanisms for selective ring opening on metals[6-10], and the dominant mechanism can change with various metals, supports, and reaction conditions. Because of this, it would be very valuable to be able to predict the product distribution of a given model naphthenic molecule under specific reaction conditions. This prediction provides important insight towards identifying reaction paths occurring under specific reaction conditions. It also helps determine the value of a particular catalyst towards improvement of ON, CN, specialty chemical production, etc.

In this study, strategies are compared to maximize CN of a fuel while minimizing particulate matter emissions and specific gravity through a combination of hydrogenation followed by selective ring opening. Also, a tool has been developed to predict the primary product distributions obtained when reacting various substituted cyclohexanes over an Ir/Al_2O_3 catalyst under specified conditions. This prediction was made by developing Quantitative Structure Property Relationships (QSPR) between the molecular structure of the feed and various ratios which represent the product distribution. QSPR has been applied previously by our group for the prediction of CN,[7] ON,[6] as well as other important fuel properties. These same techniques are applied here towards the prediction of primary product selectivity, which leads to a very valuable tool with numerous possible applications.

This is an extremely unique application of QSPR's in comparison with the current literature. These studies do not use as complicated and computationally expensive descriptors as are the focus of many recent developments in the chemistry and pharmaceutical fields. On the other end of the spectrum, this does not classify as a high throughput study, where often a single property such as conversion or selectivity

towards a particular product is maximized for hundreds of potential reactions. This study brings with it the unique approach of providing a proof-of-concept for predicting not only the selectivity towards a particular product, but the entire primary product selectivity. In addition, the ability to extract the resulting fuel properties from each of the predicted reaction products is a truly novel and useful approach.

5.2 Effect of selective ring opening on fuel properties

Selective ring opening can have a drastic effect on several fuel properties. The fuel properties of interest in this case are cetane number, particulate matter emissions, and specific gravity. There are two primary routes that one can take when considering ring opening of one ring naphthenic molecules, acid and metal catalyzed ring opening. Acid-catalyzed ring opening results in highly branched products with excessive cracking, so this pathway will not be discussed in this case. The second primary route for ring opening of naphthenics is metal-catalyzed selective ring opening. The selectivity with which a metal breaks a ring depends strongly on many factors, including particle size, support, and metal type.[8] Five-membered rings are much more reactive than six-membered rings due to the increased strain on the molecule. This was illustrated by McVicker *et al.* that alkylcyclopentanes can readily undergo ring opening at a rate nearly 100 times faster than its corresponding alkylcyclohexane (before ring contraction).[5] For this reason, in order to produce high selectivity to ring opening products, it is strongly advisable to precede ring opening of two ring naphthenics by a ring contraction step. Of all catalysts tested by McVicker *et al.,* Ir/Al_2O_3 had the highest selectivity to opening of the ring as opposed to cracking of the molecule. This type of approach is illustrated in figure 5.1 below:

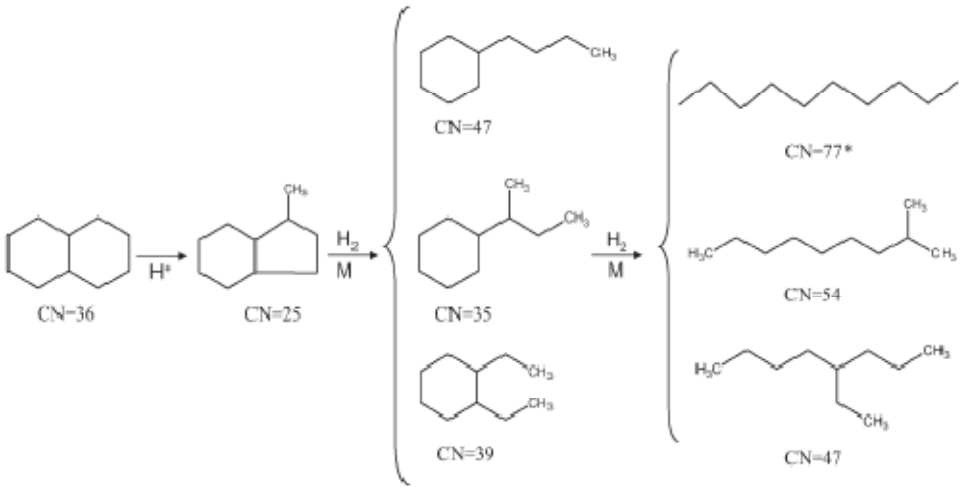


Figure 5.1 Metal Catalyzed ring opening preceded by acid catalyzed ring contraction. Adapted from ref 7

Note that the drastic increases in CN that can occur if the ring is opened selectively at substituted positions. Ideally, decalin would be converted to the non-branched n-decane with 100% selectivity. This has been shown to not be the case, however, and even the most selective ring opening catalysts, such as Ir/Al_2O_3 can cleave the ring at un-substituted positions.[6] It is then important to gain control of the ring opening product selectivities that would result from various single-ring naphthenics. With this knowledge combined with the fuel properties of each product, one could determine if it is beneficial to do ring opening of the second ring or not.

With all of these things in mind, it would be extremely valuable to have the ability to predict the primary product distributions which result from a particular substituted cyclohexane. This was accomplished by measuring the primary product distributions of several model compounds over a particular catalyst, and creating ratios which can be used to represent these product distributions. QSPR models were then

created to correlate these ratios to the molecular structure of the feed, as has already been done by our group for several fuel properties in the past.[6]

QSPR models have been developed to represent primary product distributions for several substituted cyclohexanes over an Ir/Al_2O_3 catalyst. The results provide much improved insight as to reaction mechanisms that occur on the surface, while at the same time providing a valuable tool to estimate the effects that ring opening would have on the desired fuel properties.

5.3 Experimental

Catalytic measurements of primary products were conducted by Phuong Do and Siraprapha Dorkjampa at OU.

5.3.1 Catalyst preparation

For each of the experiments conducted, the catalyst used was a 0.9 wt% Ir/ γ-Al_2O_3 prepared by incipient wetness impregnation as described previously.[6,8] The precursor used was $IrCl_3 \cdot 3H_2O$ obtained from Alfa Aesar. A liquid/solid ratio of 0.9ml/g was used for the γ-Al_2O_3 (HP-140, Sasol). The catalysts were dried overnight at 373K and then calcined in air at 573K for two hours.

5.3.2 Catalyst characterization

CO chemisorption and BET surface area measurements were conducted as previously reported. CO chemisorption was conducted via the dynamic adsorption method in a flow cell. The catalyst was first reduced in H_2 for 1.5h at 723K, and then

cooled to room temperature in He. CO pulses were then sent through the catalyst bed and the *m/e* = 12 signal was monitored via mass spectrometry until the area of each pulse did not vary within ±1%. This final area was taken as the amount of CO in each pulse and the difference between this area and the area of the first injections was taken as the amount adsorbed on the sample. From this method, the ratio of moles of CO/moles of Ir was found to be 0.73. The catalyst support particle size was 150 mesh, and the BET surface area was found to be 250 m^2/g from N_2 adsorption/desorption.

5.3.3 Catalytic activity measurement and data analysis

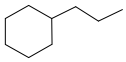
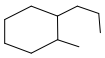
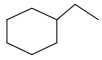
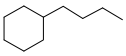
All experiments were conducted in a flow reactor at 603K. The catalyst was reduced for 2 hours in H_2 at 603K prior to feed introduction. In all cases, a hydrogen/hydrocarbon molar ratio of 30 was utilized. The reactor pressure was maintained at 500 psig with a backpressure regulator. The plug flow reactor consisted of a ½ inch stainless steel tube placed inside an electric furnace and the temperature of the catalyst bed was kept isothermal for all runs. Liquid hydrocarbon feed was continuously fed to the reactor with an IscoLC-5000 high-pressure syringe pump. A dry ice and acetone bath maintained at 193K was used to condense all of the products. The liquid samples were then injected into a Hewlett-Packard 5890 plus GC equipped with a FID detector for compositional analysis. Product identification was achieved through the use of a Shimadzu GC-MS-QP5000. Pure component standards were also used in order to attain analytical certainty.

5.4 Results

5.4.1 Selection of molecules and ratios

Fourteen model alkyl-cyclohexane compounds were chosen as representative reaction feeds. The molecules were chosen so that the effect of several factors on the product distribution may be investigated such as the effect of alkyl chain length, number of chains, chain position, and degree of chain branching. The compounds chosen can be seen below in table 5.1.

Table 5. 1 Model compounds utilized in the present study

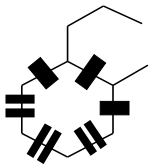
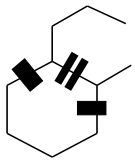
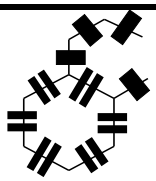
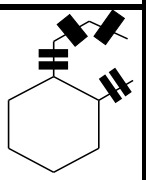
Structure	Name
	1,3-dimethylcyclohexane
	1,2-dimethylcyclohexane
	1,2,4-trimethylcyclohexane
	1-ethyl-2-methylcyclohexane
	1-ethyl-3-methylcyclohexane
	n-propylcyclohexane
	1-propyl-2-methylcyclohexane
	ethylcyclohexane
	methylcyclohexane
	1,3,5-trimethylcyclohexane
	n-butylcyclohexane
	tert-butylcyclohexane
	isopropylcyclohexane
	1,4-dimethylcyclohexane

In order to create models which accurately reflect the tendency of a particular catalyst to cleave each feed molecule in specific positions, the product distributions were measured at very low conversions (4%). This low conversion was chosen so that secondary products could be neglected, which would further complicate the analysis. On the other hand, this conversion is still high enough that analytical certainty and reproducibility still exist as all of the peaks can readily be identified and integrated via

FID-GC. For each case, a minimum of two runs were conducted which measure the conversion very close to 4%, and then the product selectivities were interpolated to determine the selectivity at exactly 4% for each case.

To accurately estimate the cleavage at specific positions both on the ring and on the branches of molecules similar to those measured experimentally, several ratios of various product selectivities were measured. These ratios, shown in Table 5.2, were chosen in order to maximize the accuracy of product selectivity. These ratios are universal enough so that several molecules could be included in each model, but at the same time capture the uniqueness of each molecule.

Table 5. 2 Definition of ratios used to predict product selectivity

Ratio	1	2	3	4
Example				
a= ▬ b= 〓	a/b	a/b	a/b	a/b
Description	substituted cleavage/ unsubstituted cleavage	tertiary-tertiary bond/ tertiary-secondary bond (in the ring)	de-alkylation/ring opening	cleavage of the branch at positions not connected to the ring/ connected to the ring

These ratios contain both statistical and fundamental significance. Through this approach, the product selectivity to each bond can be estimated by utilizing these ratios and some simple algebra. Each of these ratios carries with it mechanistic insight as well. Ratio 1, which is the ratio of cleavage of the ring at substituted/unsubstituted positions, provides an indication of the dominant surface intermediates which are

occurring on the catalyst surface.[5] A high ratio represents cleavage at substituted positions via the proposed metallocyclobutyl intermediate, while cleavage at unsubstituted positions indicates cleavage via the dicarbene mechanism. Ratio 2 provides further insight as to how various functional groups influence the selective substituted cleavage between substituents as opposed to adjacent to only one. Ratio 3 provides an indication of the tendency of the molecule to crack at the branches, which is obviously an undesirable reaction for selective ring opening. Ratio 4 provides an indication of the tendency of a molecule which cracks to undergo terminal cracking as opposed to cleavage of the substituent where it is attached to the ring. This provides an indication as to if the branch itself is adsorbing on the surface of the catalyst, or if the cracking is due to an intermediate where both the ring and branch are adsorbed.

In order to create the most accurate models, some of the ratios were divided by the statistical ratio (i.e. the statistical number of bonds for each group). As an example, the statistical ratio of ratio 1 for 1-ethyl-2-methyl cyclohexane would be 3/3=1 as there are an equal number of both types of bonds for this particular molecule. Models were created for each ratio, as well as each ratio divided by its statistical ratio, and only the best models were used. The results will be discussed in the next sections.

5.4.2. Development of QSPR models to estimate product selectivity

Using the experimental data and ratios shown in the previous section, a QSPR model was created for each of the four ratios in order to predict primary product distributions of unmeasured compounds. Each model was influenced by molecular descriptors which were chosen through the use of a genetic algorithm as well as other

model statistics. Because a small number of experimental data points were used, experimental data along with predicted data are plotted along various groups of molecules, such as increasing branch length, etc. in order to ensure that all trends were captured and no models were over fitting the data. Also, the "leave one out" method was used for cross validation in each case so that all data could be applied to the model. Parity plots for each of the ratios can be observed below in figure 5.2.

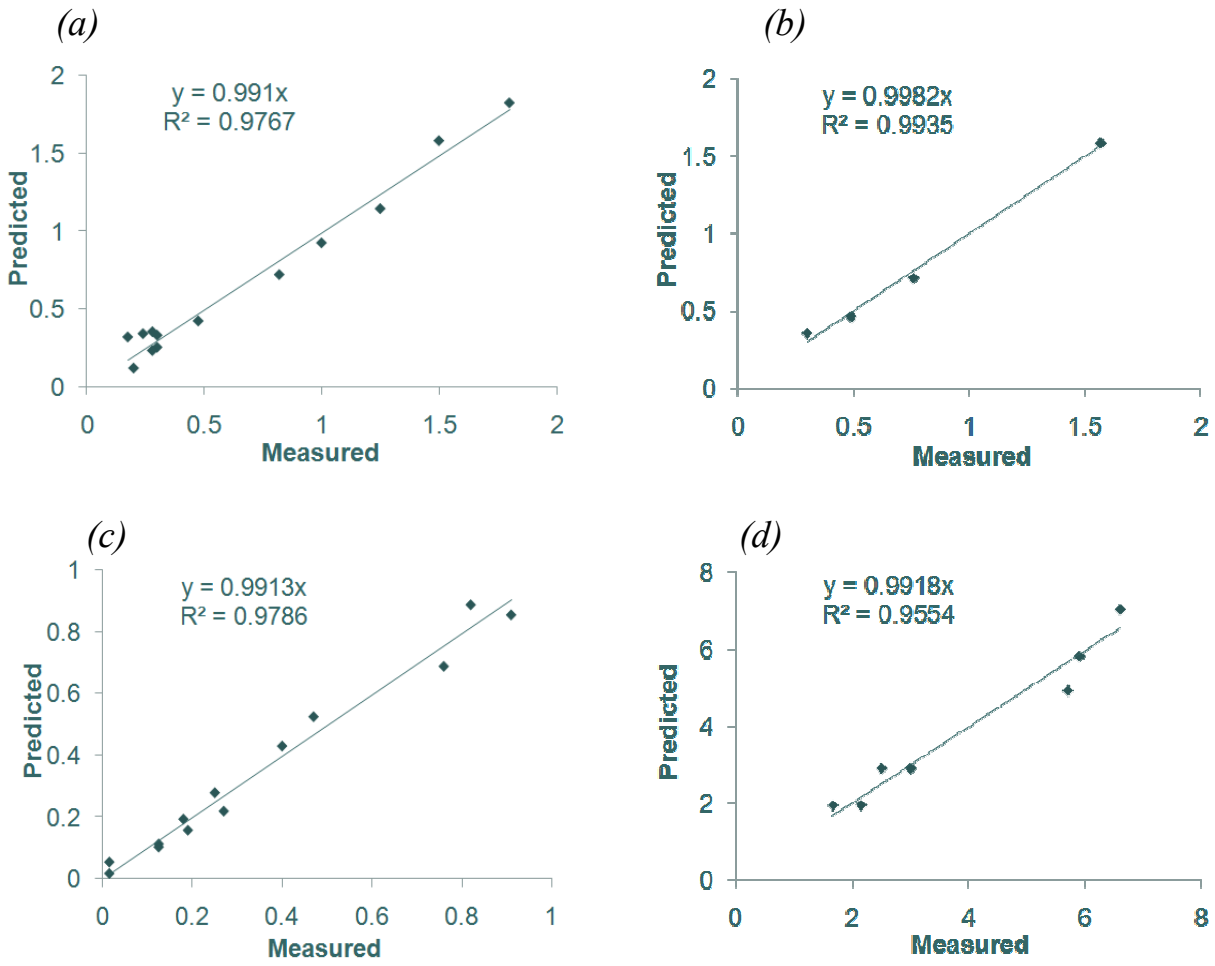


Figure 5. 2 Parity plots for predicted ratios shown in table 5.2. Numerical values which were predicted are *(a)* Ratio1/statistical ratio, *(b)* Ratio2, *(c)* Ratio3, and *(d)* Ratio4/statistical ratio.

Details from the QSAR models can be summarized as follows. For ratio 1, which is an indication of the tendency of the molecule to cleave at the substituted positions (leading in products with a lesser degree of branching), a partial least squares regression model was created which utilized three components. This model was influenced by four molecular descriptors which were chosen as mentioned above. The R^2 value for this model was found to be 0.977. The second model, which essentially measures the tendency of breaking various substituted positions for 1,2 disubstituted cyclohexanes. This ratio decreases as the tendency to break between the two substituents increases. The model selected to predict this ratio utilized one principal component, which was influenced by two molecular descriptors. The R^2 value for this model was found to be 0.994. The third ratio provides an indication as to the tendency of the catalyst to open the ring or to crack the molecule by chopping the branches. This ratio was predicted by utilizing a 3-component partial least squares model which was influenced by four molecular descriptors. The R^2 value was 0.979. The fourth and final ratio provides an indication as to where the catalyst preferentially de-alkylates the branch. This ratio is very important as it provides insight as to how much carbon will actually be lost as light gasses. For this ratio, the best model found was a simple ordinary multiple regression, which utilized two molecular descriptors. The R^2 value for this model was 0.957. Parity plots were created for each model as well to ensure that the error was well dispersed, and did not deviate in any particular trend. This was the case for each of the models.

5.4.3 Results from predicted values

5.4.3.1 Predicted trends in ratios

Predicted initial product selectivities can provide a variety of interesting results. Predicted ratios alone can provide insight as to general trends which are observed as one changes properties of functional groups. As an example, as one looks at ratio 1, which is an indication of the tendency to open the ring next to alkyl substituents as opposed to any unsubstituted position in the ring, one can clearly notice the effect of having two branches on product selectivity. This can be seen below in figure 5.3.

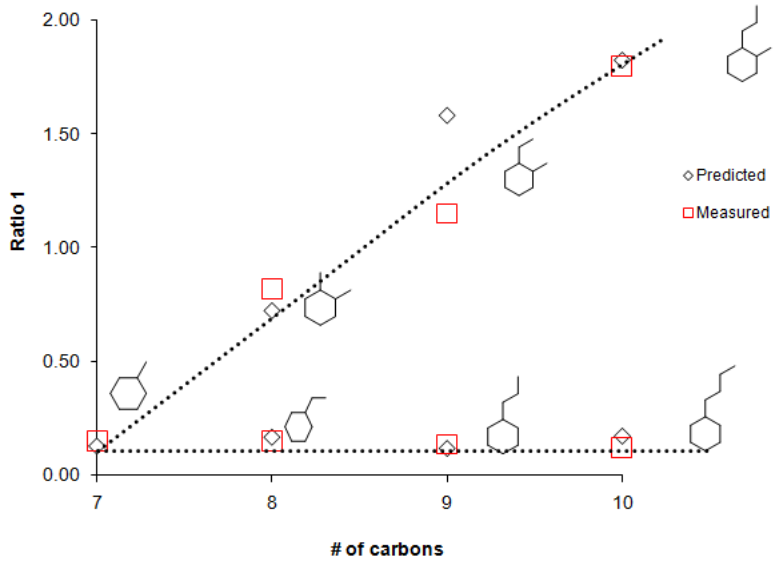


Figure 5. 3 Effect of branch length and position on Ratio 1

One can clearly note that, for monosubstituted cyclohexanes, increasing chain length has virtually no effect on the tendency to cleave at the substituted position, but for 1,2 di-substituted cyclohexanes there is a large effect of chain length. This can be

explained by either the weakening of the bond between the two substituents that results from disubstituted cycloalkanes, or by the influence of the second alkyl group on surface adsorption intermediates. The strong agreement between predicted trends and those observed experimentally should also be noted as this provides an indication that the model is not over-fitting the data.

Ratio 2 provides further insight as to where the molecule breaks for 1,2-disubstituted cycloalkanes. As an example of the information which can be extracted from this prediction, figure 5.4 shows how ratio 2 varies as a function of the number of carbons, and length of branches. A higher value of ratio 2 indicates a lower selectivity towards cleavage between the alkyl substituents. One can clearly see that longer alkyl substituents lead to a higher selectivity towards cleavage between the alkyl groups. This could be explained either by the electronic interaction of the alkyl groups with the ring, or a modified adsorption intermediate resulting from adsorption of the long alkyl chains on the metal surface. Note the smooth trend and agreement between the predicted vs. observed values for this model. This is critical, as this model had only 4 input data points. For this reason, this model should be utilized only with extreme care, and because no branched alkyl substituents were utilized in the model, it should not be extrapolated to estimate selectivities resulting from these types of molecules. This model is extremely useful, nonetheless, as one can clearly predict the tendency of larger alkyl groups to enhance ring opening between them. This is very valuable for the fuel property CN, as cleavage between two linear branches results in the most valuable product, which is the linear paraffin.

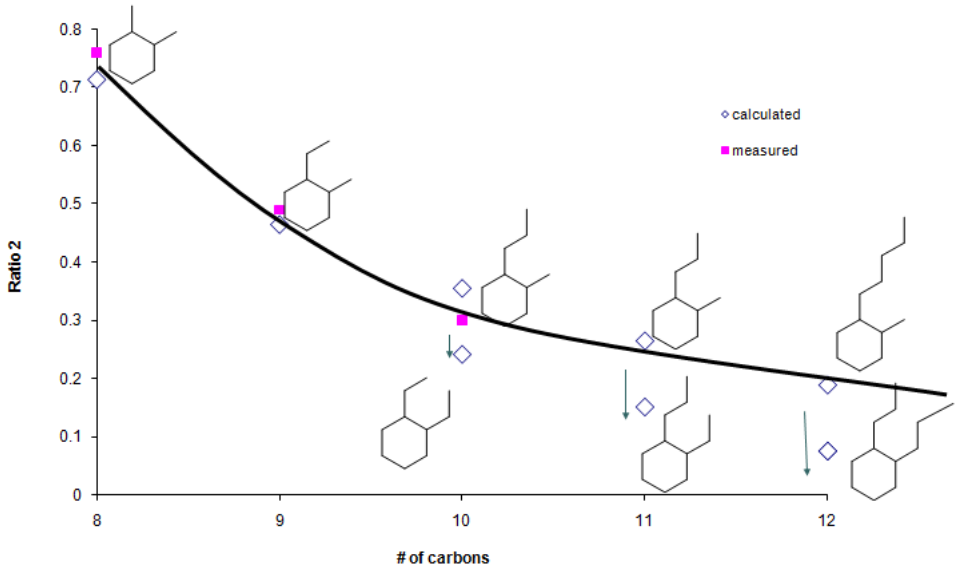


Figure 5. 4 Ratio 2 as a function of increasing number of carbon atoms, and distribution of carbons on the branches.

Ratio 4 is analogous to the ratio of desirable ring opening to undesirable cracking of the alkyl substituents which a molecule may undergo as it is reacted over an Ir/Al_2O_3 catalyst. As one would expect, this ratio of cracking of the alkyl groups to ring opening increases as the length of the alkyl chains increase. This can be observed in figure 5.5.

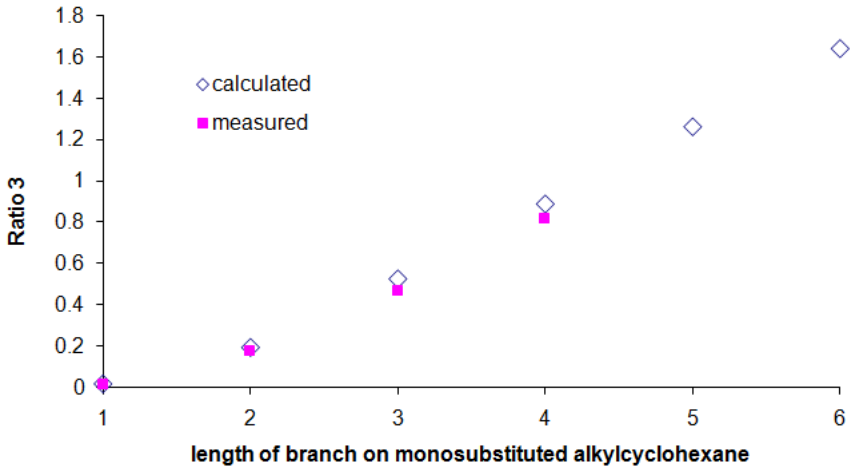


Figure 5. 5 Ratio 3 as a function of length of alkyl branch for monosubstituted cyclohexanes.

As the length of the alkyl branch on monosubstituted cyclohexanes increases, the ratio of cracking dramatically increases as indicated by increase in ratio 3. One may be tempted to conclude that this is only due to increasing ratio of alkyl carbons vs. ring carbons on the molecule. This is not the entire explanation for this phenomenon, however, as shown in figure 5.6, where the statistical ratio of carbons on the branch to carbons in the ring is taken into account. From figure 5.6, it can clearly be observed that there is much more responsible for cleavage than the statistical ratio alone. For methylcyclohexane, the ratio is much less than the statistical ratio, but as the number of carbon atoms increases, this trend shifts. Propylcyclohexane has a ratio which is very close to the statistical ratio of cleavage, but then as the molecules increase further in size, this ratio increases beyond the statistical ratio. This means that the nature of the adsorbed molecules on the surface is changing as a function of carbon atoms in the alkyl group. For methylcyclohexane, the ring is the most dominantly adsorbed molecule, and the ring is likely opened via the selective dicarbene mechanism. As the

alkyl group increases, the adsorption of the alkyl group on the surface plays a stronger role on how the molecule adsorbs on the surface. At longer lengths of carbon atoms, the alkyl group is predominantly adsorbed on the surface, thus dramatically decreasing the selectivity towards dicarbene ring opening. The remarkable aspect here, when compared with figure 5.3, is this seems to have virtually no effect on where the ring is opened. This provides strong evidence that the presence of a second methyl group has a strong influence on the fundamental adsorption intermediates which occur on the surface and therefore lead to ring opening.

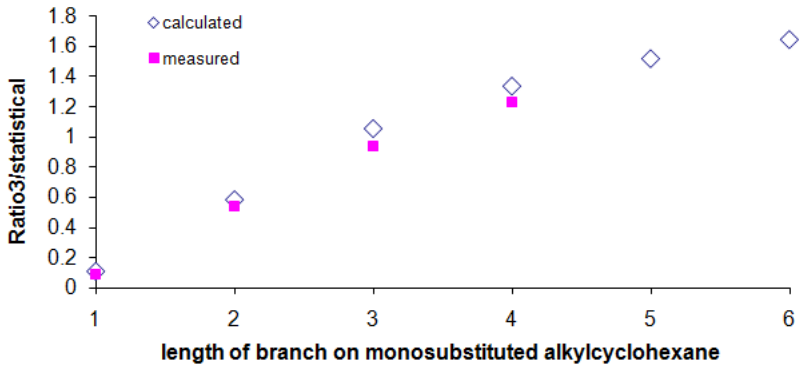


Figure 5. 6 Ratio of cleavage on the branch to cleavage on the ring divided by the statistical ratio of each type of bond available to open for monosubstituted alkylcyclohexanes.

When one does consider more than one substituent, as in the case of 1,2-dimethylcyclohexane, both the degree of cleavage at substituted positions and the degree of cracking increase with an increasing number of carbon atoms. This can be observed for the case of 1-R-2-methylcyclohexane molecules, where the R group is a

linear alkyl group with an increasing number of carbon atoms. The results of the two ratios can be observed below in figure 5.7.

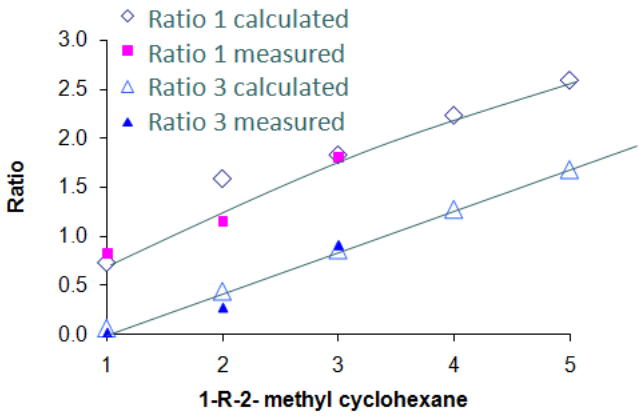


Figure 5. 7. Ratio1 and Ratio 3 plotted against increasing length of linear R group for 1-R-2-methylcyclohexane

This provides an indication as to how the overall fuel properties will be influenced by the increasing chain length on the alkyl substituents. As ratio 1 increases, less branched paraffins will result, indicating a valuable increase in CN. At the same time, one can clearly see that undesirable cracking of the alkyl groups will result due to the increase in ratio 3. This provides the first instance of selectivity tradeoff which is often encountered in the molecular engineering strategy. The resulting influence of these ratios on the fuel properties of the products which result will be the focus of the next section.

5.4.3.2 Incorporation of predicted product selectivities and fuel properties

Perhaps the most valuable information which can be gained through the prediction of primary product selectivities is the resulting impact on desired fuel properties. As mentioned earlier, our group has predicted various fuel properties through QSPR[6]. Through a combination of these two tools, one can predict each of the primary products which will result from reacting the compound over Ir/Al_2O_3, while also having the ability to predict fuel properties of each resulting product. Through this information, estimations on the overall fuel properties resulting from the reaction can be achieved if one assumes linear blending of fuel properties. As an example, we will look at the measured primary product distribution for the reaction of 1-propyl-2-methylcyclohexane. The CN's of each possible liquid phase product were predicted through QSAR, and when summed up over the product distribution, it was estimated that the CN will increase to approximately 42.8. This can be observed in figure 5.8.

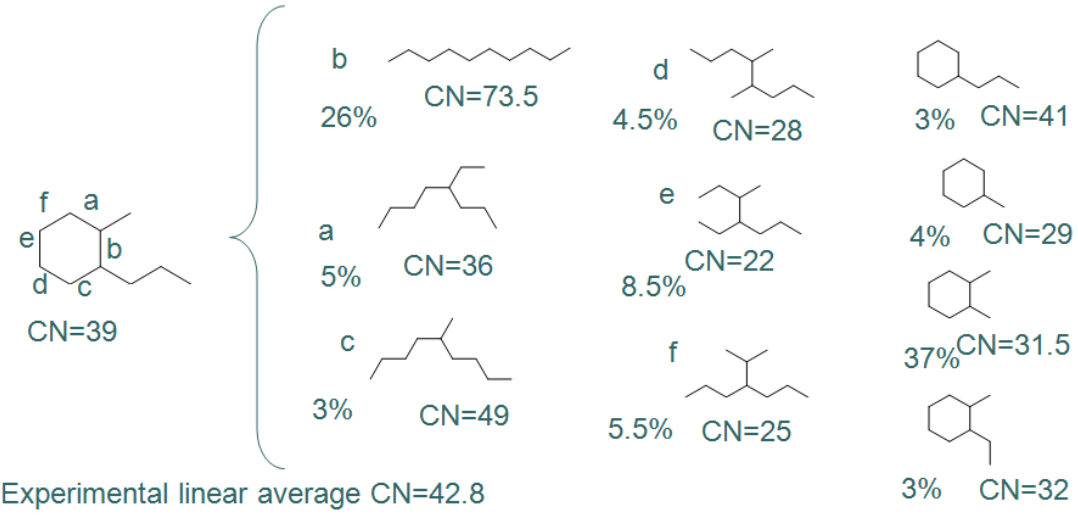


Figure 5. 8 Measured product selectivities and the resulting CN at 4% conversion of 1-propyl-2-methylcyclohexane over Ir/Al_2O_3 at 603K and 500psig of H_2. The linear average CN was obtained by multiplying the product selectivities by each compound's predicted CN, as predicted according to chapter 2.

Figure 5.9 shows the predicted product distribution based on the calculated ratios. The predicted product distribution was calculated by the use of the predicted ratios and some simple algebra while knowing that the sum product selectivities add up to 100%. It can be seen that not every product has been estimated, but rather several like groups can be estimated as indicated by the boxes in figure 5.9. For all products that could not be directly estimated, the selectivities were assumed to be split evenly among the compounds in the group according to their statistical ratios. As an example, the compounds resulting from breaking the ring at points a and c were both assumed to have a selectivity of 4.5%. When one compares the resulting CN estimated from these predicted ratios to that measured experimentally, there is remarkable agreement.

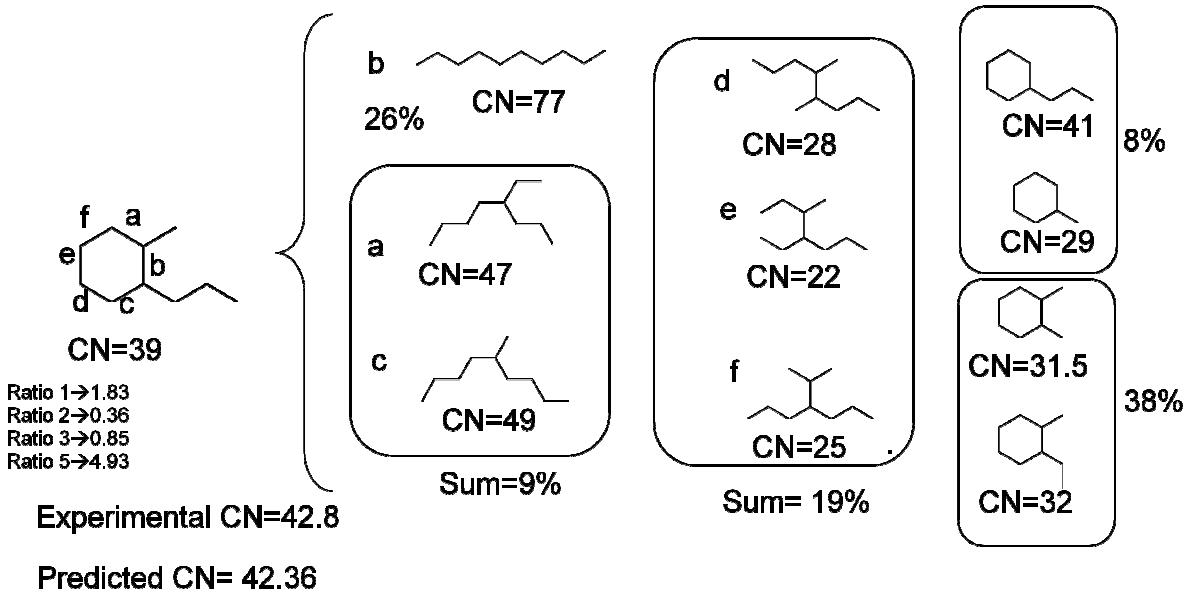
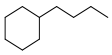


Figure 5. 9 Predicted CN values and predicted primary product distribution to estimate the CN of primary products.

This same methodology can be applied in order to estimate other fuel properties of interest which result from the predicted product distribution. The next step is to

apply these ratios to predict fuel properties of products which have not previously been measured. Results from similar calculations to the one above can be seen in table 5.3. The fuel properties CN, micropyrolysis index (MPI)[11], as discussed in chapter 3, and specific gravity were predicted for each of the feed alkylcyclohexanes as well as each of their potential products. By utilizing these ratios in order to estimate the product distribution, one can estimate the resulting influence on desired fuel properties which will be obtained.

Table 5. 3 Predicted values for CN, MPI, and specific gravity of several substituted cyclohexanes, as well as the linear average of their predicted primary products.

		1-ring naphthenic properties			properties of predicted products		
1-ring naphthenic	**Structure**	**CN**	**MPI**	**Sp. Gr.**	**CN**	**MPI**	**Sp. Gr.**
1-propyl-2-methylcyclohexane		39.1	20.4	0.777	42.7	13.8	0.750
1-isopropyl-2-methylcyclohexane		30.8	22.5	0.785	28.3	14.9	0.744
1,2-diethylcyclohexane		39.0	20.4	0.772	36.5	13.8	0.748
sec-butylcyclohexane		35.3	20.4	0.801	36.1	14.0	0.756
n-butylcyclohexane		47.4	18.3	0.792	40.8	12.8	0.747

These compounds were chosen because they are all the possible one-ring naphthenics which can result from either direct ring opening of decalin, or ring opening of decalin preceded by ring contraction as indicated in figure 5.1. The most obvious difference that can be noticed right away is the inconsistent trend in CN improvement. It can be seen that the CN of the products is higher than that of the one ring molecule for some cases, and less for some cases. One property that consistently improves is the MPI, or sooting tendency of the fuel. The specific gravity of the fuel also consistently

decreases as the final ring is opened. This means that overall, for the ring opening of the second ring of decalin, drastic CN improvements may not be achieved, while the sooting tendency will significantly improve. This makes selective ring opening a means of slightly increasing, or at least maintaining CN while improving both specific gravity and emissions properties of the fuel.

This serves as a truly novel approach towards the utilization of QSPR towards determining not only the selectivity towards a specific molecule, but the entire primary product selectivity which will result. In addition, one can then estimate the fuel properties which would result, not by a simple correlation, but by predicting the fuel properties of the individual molecules which would result. While this study is not robust, as only 14 model compounds were utilized, it serves as an excellent proof-of-concept for future studies based on this fundamental QSPR approach. The advantages if a similar methodology were applied to a greater number of data points, as via high-throughput reactions, would be tremendous, as the amount of practical and fundamental information extracted is invaluable.

5.5 Conclusions

Results from this study indicate that selective ring opening of the second ring of a two-ring molecule, in this case decalin, results in relatively small increases in CN, while improving MPI and specific gravity. Through QSAR analysis, a tool has been developed to predict primary product distributions of several substituted cyclohexanes. The applications of this tool are only beginning to be realized as it can be combined

with fuel property prediction to give insight as to how the fuel properties will change when reacted.

References

1 S. P. Crossley, P. T. Do,S. Dorkjampa, D. E. Resasco (To be published)

2 A. Roj, K. Karlsson *Fuels Reformulation* **1998**, 46.

3 A. Stanislaus, B.H. Cooper *Catal. Rev.-Sci. Eng*. **1994**, 36,75.

4 W.C. Baird Jr., J.G. Chen, G.B. McVicker *US Patent* 6,623,625 **2003**.

5 G.B. McVicker, M. Daage, M.S. Touvelle, C.W. Hudson, D.P. Klein,W.C., Baird Jr., B.R. Cook, J.G. Chen, S. Hantzer, D.E.W. Vaughan, E.S. Ellis, O.C. Feeley *J. Catal.* **2002**, 210,137.

6 P. Do, S.P. Crossley, M. Santikunaporn, D.E. Resasco *Catalysis* **2007**, 20, 33.

7 R.C. Santana, P.T. Do, W.E. Alvarez, J.D. Taylor, E.L. Sughrue, D.E. Resasco *Fuel* **2006**, 85, 643.

8 P. T. Do, W. E. Alvarez, D. E. Resasco *J. Catal.* **2006**, 238(2), 477.

9 G. Maire, G. Plouidy, J.C. Prudhomme, F.G. Gault *J. Catal*. **1965**, 4, 556.

10 F.G. Gault *Adv. Catal*. **1981**,30,1.

11 S. P. Crossley, W. E. Alvarez, D. E. Resasco *Energy and Fuels* **2008**, 22(4), 2455.

CHAPTER 6

6. Transition of the Molecular Engineering Approach towards the Upgrading of Biofuels

6.1 Viability of molecular engineering approach as applied towards biofuel refining.

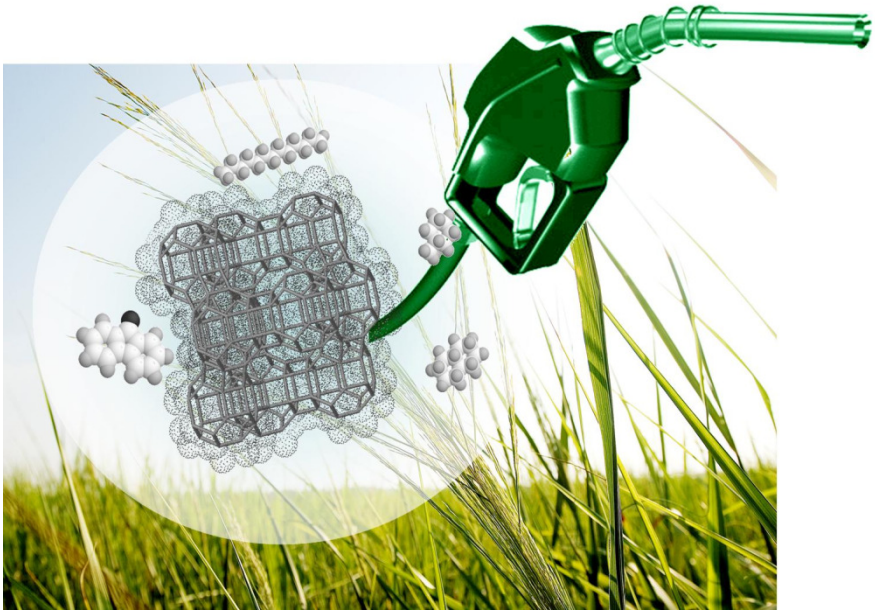


Figure 6. 1 Conceptual schematic of molecular engineering strategy as applied to biofuels.[1]

While during the last few decades we have witnessed significant advances in the production of ethanol biofuel, much less efforts have been directed towards the development of high-tech methods for conversion of biomass into "green" hydrocarbon fuels such as gasoline, diesel, and jet fuel. These fuels are more attractive than ethanol

due to their higher heat content and lower solubility in water. Moreover, they can be fully fungible with petroleum-derived fuels and could be directly incorporated into the existing infrastructure. However, the technological challenges for their production and refining are still enormous. At the same time, these challenges represent excellent opportunities for research and development for the chemical engineering community.

Prof. J. Dumesic (U. Wisconsin) tells us "An important body of fundamental knowledge already exists for catalytic processes involved in the upgrading of petroleum fuels. This knowledge, gained through efforts of researchers over many decades, can serve as the initial basis for biofuel refining. However, the complexity of new biorefining systems has only recently started to become apparent, requiring new and innovative approaches".

The complexity and instability of pyrolysis oils pose huge analytical challenges. Nonetheless, novel analytical techniques and modern instrumentation are making significant progress in this area and are now able to provide detailed information about chemical composition. This information will allow researchers to discriminate among the different chemical groups in the biofuels and could make the development of composition-property relationships possible.

On the side of the researchers are the technological background gained in the area of fossil fuel refining. Against them are the extreme economic pressures to obtain something competitively priced in a minimum amount of time. A better understanding of the fundamental reactions occurring on the catalyst surface will help accelerating the development of effective catalytic strategies for the development of fuels with properties which are acceptable with the current infrastructure.

A rational approach towards this development is through the molecular engineering approach discussed in chapter 1. The approach consists in utilizing model compounds and mixtures of model compounds which represent a more complicated feedstock. The main goal is to understand the fundamental chemistry involved in the reactions, and link this understanding to the practical impact of fuel composition on fuel properties. Some important relationships between the model compounds and their resulting fuel properties of interest are determined on the basis of their molecular structure. A linkage is proposed between the nature of catalyst active sites and the molecular structure of model compounds through the study of selected reactions and careful catalyst characterization. Through these two relationships, one can link the fuel properties of resulting products to specific catalysts and reaction conditions through the structure of model compounds. A number of properties are determinant of the quality of a given fuel. They include octane and cetane numbers, sooting tendency, water solubility, freezing point, viscosity, flash point, cloud point, autoignition temperature, flammability limits, sulfur and aromatic contents, density, boiling temperature, vapor pressure, heat of vaporization, heating value, thermal and chemical stability, and storability. Many of these properties can be modified by catalytic upgrading. In designing a catalytic upgrading strategy, a refiner must know how each of these properties is affected by the structure of the molecule and how a given catalytic conversion of that structure in turn affects the properties.

The main complications of this method arise from the nonlinearities of blending effects. Single model compound studies can be taken as a first approach to provide direction towards optimizing fuel properties, but not the ultimate solution. Surrogate

blends are important to study effects on solubility and competitive adsorption. As one increases the complexity of the system the picture of what is occurring on the surface becomes increasingly murky. However, fundamental studies are highly valuable in providing guidance for development of rational refining strategies rather than purely empirical approaches.

6.2 Potential applications in the upgrading of biofuels

When one applies molecular engineering strategies towards biofuel upgrading, several important opportunities are presented. Each type of biofuel has inherently unique challenges associated with it. Many of these challenges arise from the presence of oxygen in the biofuel molecules. Oxygen can have some positive effects on fuel properties, such as lowering the vapor pressure, decreasing sooting tendency, and improving octane number. However, oxygen can also have a negative impact on critical properties such as blending vapor pressure, storage stability, transport in pipelines, water solubility, corrosion, NO_x formation, toxicity, and heating value. Many of these challenges warrant the need for removal of oxygen from the system to make a more fungible fuel, which is compatible with the current infrastructure. Molecular engineering of biofuels is not the simple deoxygenation, but rather the controlled conversion of the oxygen functionality and how this conversion affects the fuel properties. Through this knowledge, catalysts and processes may be designed to only remove the specific oxygen atoms that pose the greatest problems in fuel applications, while minimizing yield loss and valuable hydrogen consumption. At the same time, the presence of oxygen can be utilized to take advantage of its functionality and condense

small oxygenated molecules with low fuel value (e.g. propanal, acetic acid, furfural, etc.) into heavier hydrocarbon molecules, more appropriate for diesel or gasoline fuels, via organic reactions such as aldol condensation, ketonization, etherification, etc.

6.3 Estimation of biofuels properties

Estimation of properties, which are common for conventional fuels, may pose challenges when dealing with biofuels due to the impact of the oxygenated groups. For this reason, improved methods must be developed to predict fuel properties such as cetane number, octane number, sooting tendency, vapor pressure of biofuels and their blends with petroleum fuels.[2,3] Properties that are typically of minor concern in conventional fuels but have significance for biofuels include water solubility, thermal and chemical stability, corrosivity, and toxicity. Prediction of water solubility is very important, as this property has environmental as well as refining and transport implications. Compounds soluble in water have a greater tendency to negatively impact the environment in lakes and drinking water. Water solubility also hinders storage and conventional pipeline transportation. Because of these inherent issues, the problem of estimating water solubility has been undertaken by a number of groups.[4] Correlations have even been obtained between water solubility and other fuel properties such as melting point, logP (i.e., log of the octanol/water partition coefficient ratio), and molecular weight.[5] Stability can be broken up into various subsets. Oxidative stability, for example, is a cause of concern for olefinic triglycerides and methyl esters. This can be estimated through the rancimat test (EN14212) or oxidative stability index (OSI).[6] Other forms of storage stability, however, are dependent on condensation and

polymerization reactions between functional groups of neighboring molecules.[7] This is a difficult property to access for one compound alone, as it is highly dependent on the fuel matrix.

For example, in the case of pyrolysis oil, which contains many compounds, it would not be practical to evaluate and follow the variation of properties of individual compounds, but rather of all the molecules containing a given functional group. Model studies provide fundamental knowledge about the reactivity of specific functional groups on a given catalyst and the impact of the observed reactions on the targeted fuel properties.

In general, specific functional groups, such as aldehydes and carboxylic acids, which are known to react with each other, can be targeted and converted in order to improve the storage stability. Corrosivity, which is a major issue with pyrolysis oil, can be influenced by both metal content and pH of the fuel. Acidity measurements pH and pKa have been extensively predicted based on QSPR, group contribution, as well as spectroscopic techniques.[8] These types of models are essential for biofuels as many properties of biofuel molecules are unknown, and it may be very difficult to separate and measure them. As an example, fast pyrolysis oil contains over 400 different compounds.[9] Properties for many of these oxygenates have not been previously measured, although they all can have a significant impact on fuel properties.

Ideally, relationships are created such that not only one property, but a number of properties of interest are known for each potential reactant/product in a given reaction to measure the impact of a given conversion. This analysis is critical since it is not uncommon that some desirable properties are improved at the expense of others, as

shown below. In most cases an intermediate solution is reached in which all the target properties are in an acceptable range. An illustrative example can be seen in Figure 6.2 through the conversion of furfural over Cu or Pd catalysts. Furfural is typically derived from dehydration of sugars, but is also present in the product from the fast pyrolysis of biomass.[9] Due to the unstable nature of furfural (as of any other aldehyde), it must be converted to be used as a transportation fuel component. Therefore, the first step is to determine the properties of furfural and those of the potential products that could result from its conversion.

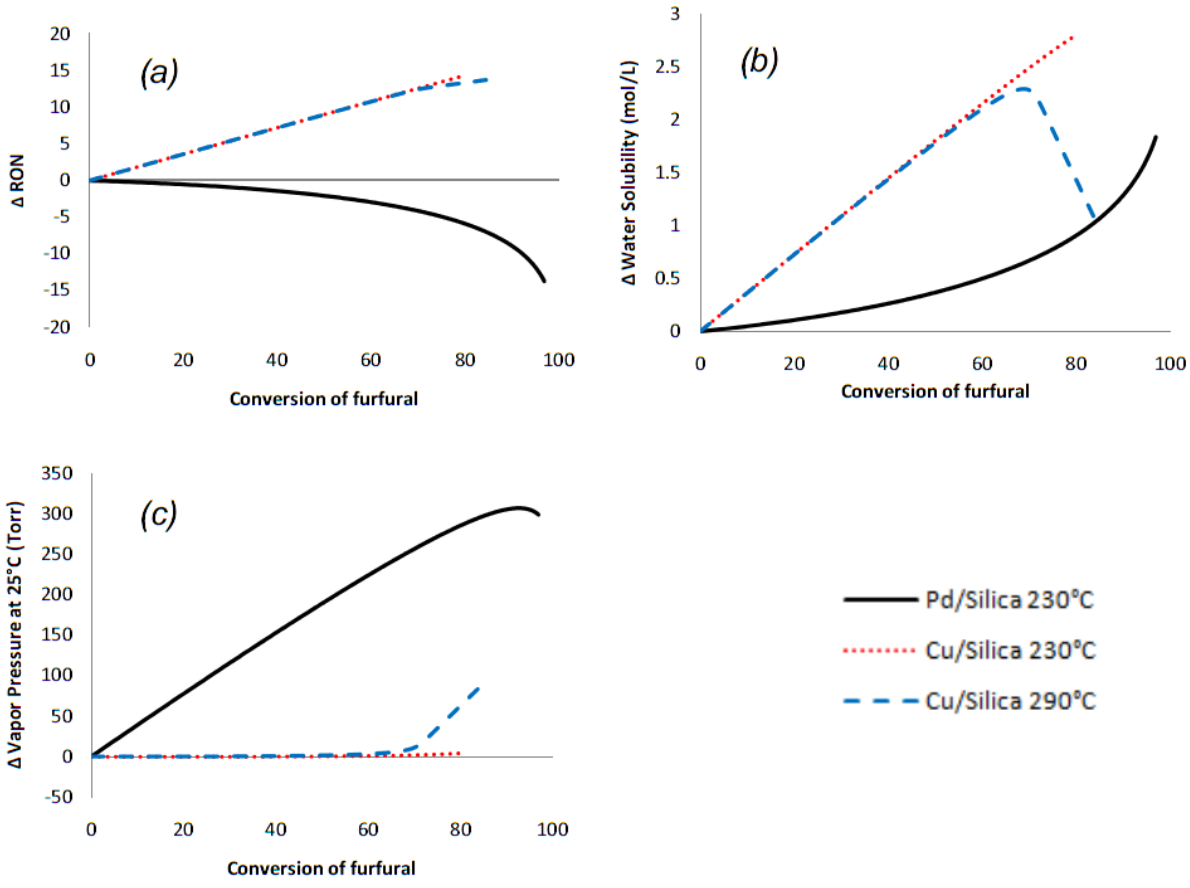


Figure 6. 2 Change in a) Research Octane Number (RON); b) water solubility; c) vapor pressure of products exiting a flow reactor across Cu or Pd catalysts as a function of feed conversion.

For example, the Research Octane Number (RON) of each of the pure molecules was estimated through the use of a linear regression QSPR model by fitting data of 67 oxygenates and hydrocarbons to their molecular structure through the utilization of MDL QSAR software (version 2.2.0.0.446(SP1) from MDL Information Systems, Inc.). The result of this fitting is a model that can predict RON of oxygenate species, based only on molecular structure. The RMS error of the dataset was 6.8, with a cross validation error (leave one out) of 8.9 RON. A parity plot of the QSPR prediction can be observed below in figure 6.3.

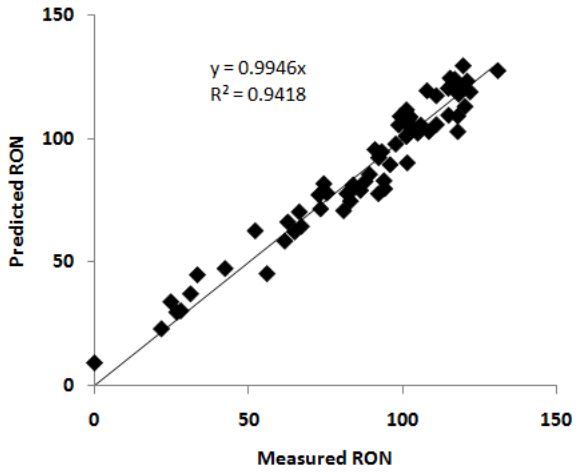


Figure 6. 3 Predicted vs. Observed values for the calculation of RON of oxygenated hydrocarbons.

Likewise, vapor pressure for each compound has been estimated through the use of ACD/Labs Software V9.04 for Solaris. Water solubility was also estimated through a correlation with various other properties of the molecules.[5] These property prediction

capabilities provide guidance on which reactions should be maximized in order to improve the fuel properties of interest.

For example, to illustrate the method, a comparison of changes in properties without considering the non-linearities of the mixtures is made in Fig. 6.2. Gas phase hydrogenation and decarbonylation of furfural were conducted over Pd and Cu at various temperatures in a tubular flow reactor. Properties of the feed and resulting products were estimated assuming linear mixing of the properties of the individual components.

As furfural is converted over either Pd or Cu in the presence of H_2, properties of the compounds exiting the reactor are optimized under different conditions. If one wants to maximize the octane number alone, clearly Cu/SiO_2 is the better catalyst, operating at high conversions. On the other hand, if one considers the water solubility of the resulting fuel, Pd is the better catalyst as its products minimize increases in water solubility. Copper also appears more promising in minimizing light compounds with high vapor pressure as decarbonylation is avoided. This graph also points out the clear tradeoff between vapor pressure and water solubility which is oftentimes encountered while upgrading of oxygenates. Other properties, such as heating value, viscosity, and hydrogen consumption also play crucial roles in determining which catalysts or process condition should ultimately be utilized. This example illustrates that optimization of one property alone is usually not the best option. Property prediction combined with catalytic studies help optimize the process.

In this example, we have compared only two catalysts and two temperatures. Another dimension in the molecular engineering approach could be added by

incorporating high-throughput catalyst design and testing and combinatorial analysis tools.[10] While a higher level of precision will need to take into account the blending effects that may change the resulting properties by intermolecular interactions, analysis of the changes in properties of the individual components is a valuable first approach in defining catalytic strategies.

6.4 Conclusions

In summary, biofuels upgrading offers new challenges to researchers but a great potential economic impact for novel catalysts and processes. Maximum benefit will be obtained from these developments if the rational approach of molecular engineering is employed. In this approach, it is necessary to know how the target fuel properties of interest are affected by the molecular structure of the product, which in turn results from the interaction of the feed and the catalyst under specific process conditions. A detailed fundamental knowledge of these relationships will make the development of biorefining processes much more effective than if empirical approaches are employed.

References

1 D. Resasco, S. Crossley *AIChE CEP* (Accepted)

2 P. Ghosh, K.J. Hickey, S.B. Jaffe *Ind Eng Chem Research* **2006**,45,337.

3 P. Pepiot-Desjardins, H. Pitsch, R. Malhotra, S.R. Kirby, A.L. Boehman *Combust Flame* **2008**,154,191.

4 R. Kuehne, R. Ebert, G. Schueuermann *J Chem Inf Model* **2006**,46,636.

5 W.M. Meylan, P.H. Howard *Perspect Drug Discov*. **2000**,19,67.

6 G. Knothe, R.O. Dunn *J Am Oil Chem Soc.* **2003**,80,1021.

7 J.P. Diebold A review of the chemical and physical mechanisms of the storage stability of fast pyrolysis bio-oils. Report No. NREL/SR-570-27613; National Renewable Energy Laboratory: Golden, CO, **2000**; http://www.osti.gov/bridge.

8 J. Jover, R. Bosque, J. Sales *QSAR Comb Sci.* **2008**,27,563.

9 T.A. Milne, F. Agblevor, M. Davis, S. Deutch, D. Johnson *Developments in Thermal Biomass Conversion* **1997**,1,409.

10 E.G. Derouane, F. Lemos , A. Corma, F. Ramôa Ribeiro *Combinatorial Catalysis and High Throughput Catalyst Design and Testing*. Proc. NATO Advanced Study Institute.vol 560. **2000**.

CHAPTER 7

7. Influence of Temperature and Oxygen Content on Pyrolytic Sooting Tendency as Determined by the Micropyrolysis Index.[1]

7.1 Introduction

The Micropyrolysis Index (MPI) is a tool which has recently been developed in order to determine the pyrolytic sooting tendency of fuels, and distinguish this from oxygenated sooting tendency measurements.[2] This measurement consists of pyrolyzing 20μL of fuel over a bed of α-Al_2O_3 under a flow of He at 850°C. The results have been predicted via QSPR in order to correlate molecular structure to the MPI.

This provides both mechanistic and practical insight, as a fuel property was developed which can be optimized, while understanding the relationship between molecular structure and the tendency to form soot via pyrolysis. It was noted that 850°C was chosen in order to obtain increased repeatability. What has not been conducted to this point is a thorough investigation as to how temperature and oxygen content influence the MPI of a given model compound.

The focus of this study will be to observe the differences in pyrolytic sooting tendency and the nature of that soot as a function of temperature for various model compounds. In order to investigate the influence of aromaticity, toluene and methyl-

dodecanoate were chosen as model compounds. Oxygen incorporation was then investigated for these two classes of molecules. Comparisons were made between dodecane and methyl-dodecanoate in order to study the influence of the ester group on sooting tendency. This gives an indication of the differences in sooting tendency which arise from the transesterification of triglycerides as opposed to hydrotreating. This area has received considerable attention as of late.[3] For oxygenated aromatics, toluene will be compared with benzaldehyde and benzyl alcohol in order to determine the influence of oxygen on the pyrolytic sooting tendency. This series of model compounds is more representative of the lignocellulosic fraction of bio-oil.

7.2 Experimental

7.2.1 Variations from original MPI method

MPI measurements were conducted as reported previously[2] with two notable differences. For high temperature MPI runs (>900°C), the tip of the needle was lowered 1" in order to prevent pyrolysis from occurring inside the needle. Also, a gradient in soot was observed at higher temperature which was not observed at 850°C. For this reason, the 15mg of quartz wool was oxidized via TPO along with the rest of the sample. This allowed for a much more clear repeatability in the measurements.

Because the MPI is an arbitrary number taken from two reference compounds, we chose to investigate the true trends which arise from increasing temperature and

eliminate any misleading conclusions which would arise from comparing it with two other compounds. For this reason, results were reported in terms of moles of carbon deposited on the surface.

7.3 Results and discussion

7.3.1 Influence of temperature on the nature of soot from toluene

While the nature of molecules to form pyrolytic soot on alumina has been previously quantified and analyzed at 850°C, we have not to this point determined much insight as to what these particles look like on the surface, how temperature influences them, and the nature with which they oxidize. This will be investigated first for toluene.

By measuring the sooting tendency via TPO, we are inherently measuring both the amount of carbon on the surface, as well as the nature of carbon on the surface. Results are shown in figure 7.1. The results here are not surprising, as the temperature is increased, the nature of carbon on the surface appears to shift to a "harder" type of coke. Furthermore, the amount of coke on the surface appears to increase exponentially for one 20μL injection. This is not unexpected, as more severe pyrolytic conditions may yield a more graphitic type coke on the surface. The next question is whether this is due to a truly more thermodynamically stable coke, or simply diffusion limitations due to the formation of larger soot particles.

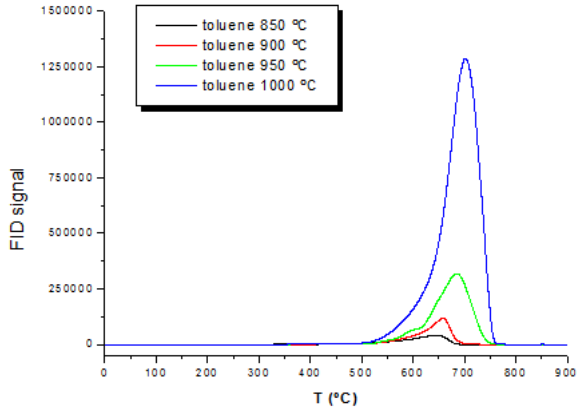


Figure 7. 1 Toluene TPO profiles as a function of temperature.
MPI measurements were obtained from Pilar Ruiz at the University of Oklahoma.

In order to help verify this, SEM (scanning electron microscopy) and same spot TEM (transition electron microscopy) images were employed. First, in order to investigate the nature of particles on the surface, SEM images were taken with the help of Liang Zhang at the University of Oklahoma. Temperatures were compared at 900 and 1000°C. Images can be observed below in figure 7.2. The first observation is that the surface appears much "cleaner" at 1000°C. This indicates that the size of the soot particles increases as the temperature is increased. It should be noted that the MPI method requires a 10 minute devolatilization period after soot deposition, so these particles, once deposited, were subject to 10 minutes of thermal treatment at 900 and 1000°C, respectively. It appears that at 900°C, much of the soot appear as droplets "wetting" the surface of the α-Al_2O_3, which is serving the role of heat transfer medium. At higher temperatures, more uniform spheres are produced. This could be due to

thermal rearrangement of the particles at higher temperatures, or an increased rate of particle growth at the higher temperatures which leads to larger particles.

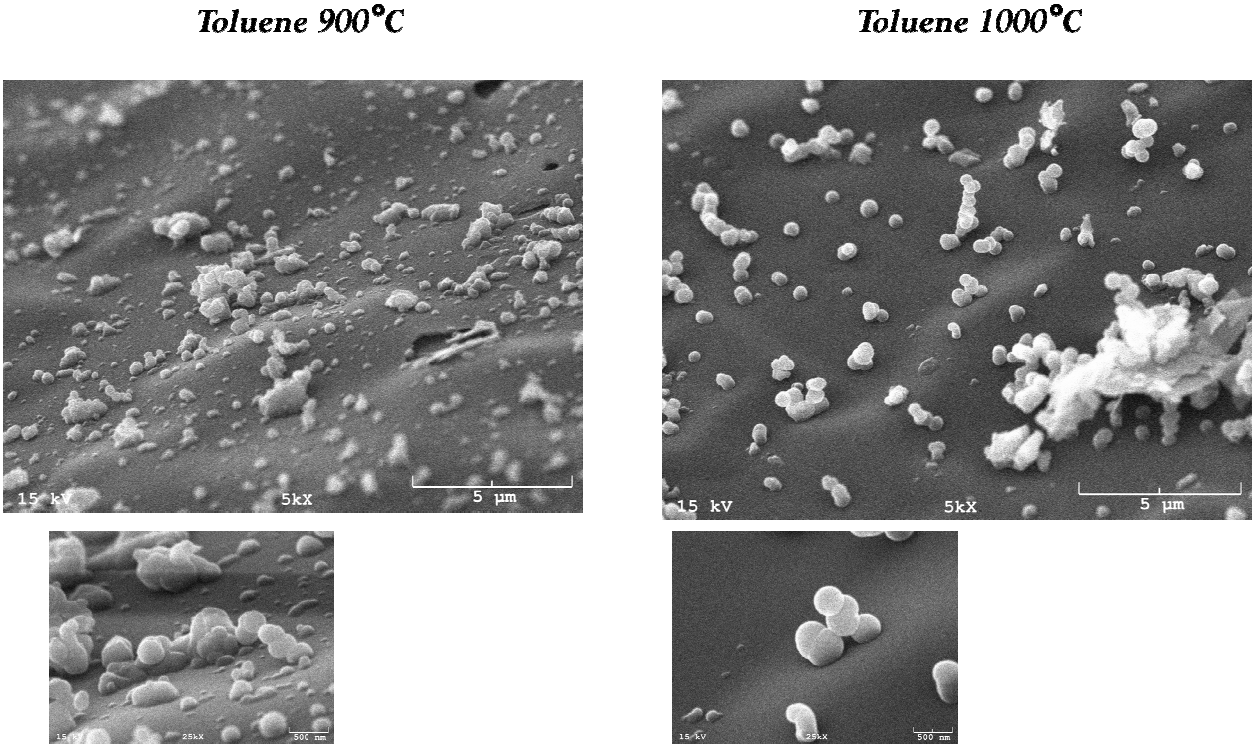


Figure 7. 2 SEM images of MPI soot deposited on Al_2O_3 from 20µL of toluene at 900 and 1000°C.
Images were obtained with the help of Liang Zhang at OU.

This brings up the question as to if the TPO profile shifts are due to a more graphitic type of carbon being formed, or simply larger particles with diffusion limitations. In order to investigate this via imaging techniques, one would need to look at the same particle after partial oxidation. This is not possible with SEM, however, as the particles must be coated with a metal before imaging, thus eliminating the possibility of sequential pretreatment of the samples. A technique which can potentially accomplish this feat, however, it same spot TEM. Through this method, an etched SiN

TEM grid was placed at a 45° angle to the direction of flow in the MPI reactor under conditions identical to those employed for soot deposition. These etched grids allow one to perform a TEM image of a particle, do a subsequent treatment (in this case partial oxidation) and then locate the exact same particle after the pretreatment. This is very similar to environmental TEM, only much more realistic as post treatment steps may be performed ex-situ in more realistic conditions as opposed to in a vacuum. Images of particles taken directly after deposition, and after partial oxidation to 550°C can be observed below in figure 7.3.

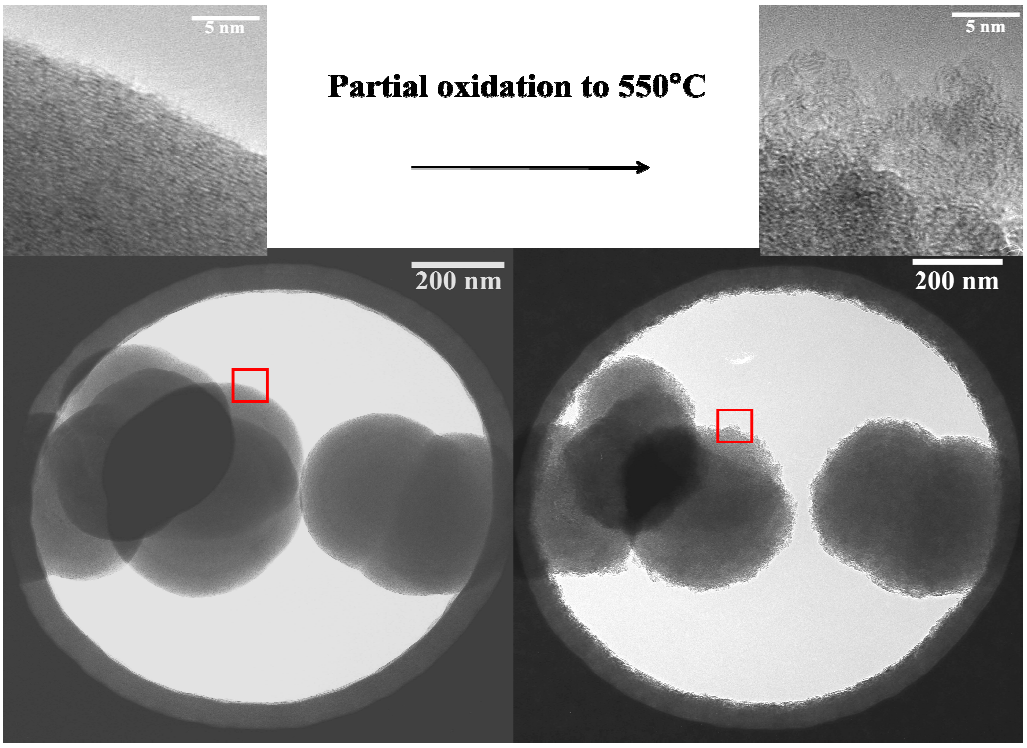


Figure 7. 3 Same spot TEM images obtained for soot deposition from toluene at 1000°C, followed by a partial oxidation to 550°C via TPO. Images were obtained with the help of Liang Zhang at OU.

The major point of interest here is the influence of particle size on the nature of burning. It is very interesting to point out here that the nature of burning appears to be from the outside inwards. This is especially indicated by the zoomed image in the upper right corner after partial oxidation. One can clearly observe the severe amount of disorder introduced at the edge of the particle, with a transition towards a more ordered particle as one goes deeper into the sample. This indicates that with pyrolysis alone, we are not forming a "peanut shell" type of soot burning which has been observed under very lean conditions in diesel engines.[4] Another very interesting result is the carbon film which is deposited around the perimeter of the hole. It is supposed that a carbon film is first deposited on the surface, which then forms small disorganized "droplets" as the curvature is increased. Higher temperatures will result in larger, more spherical droplets. Furthermore, there appears to be a degree of local heating surrounding the particles. This can be observed with the same sample through looking at another hole, as can be observed in figure 7.4.

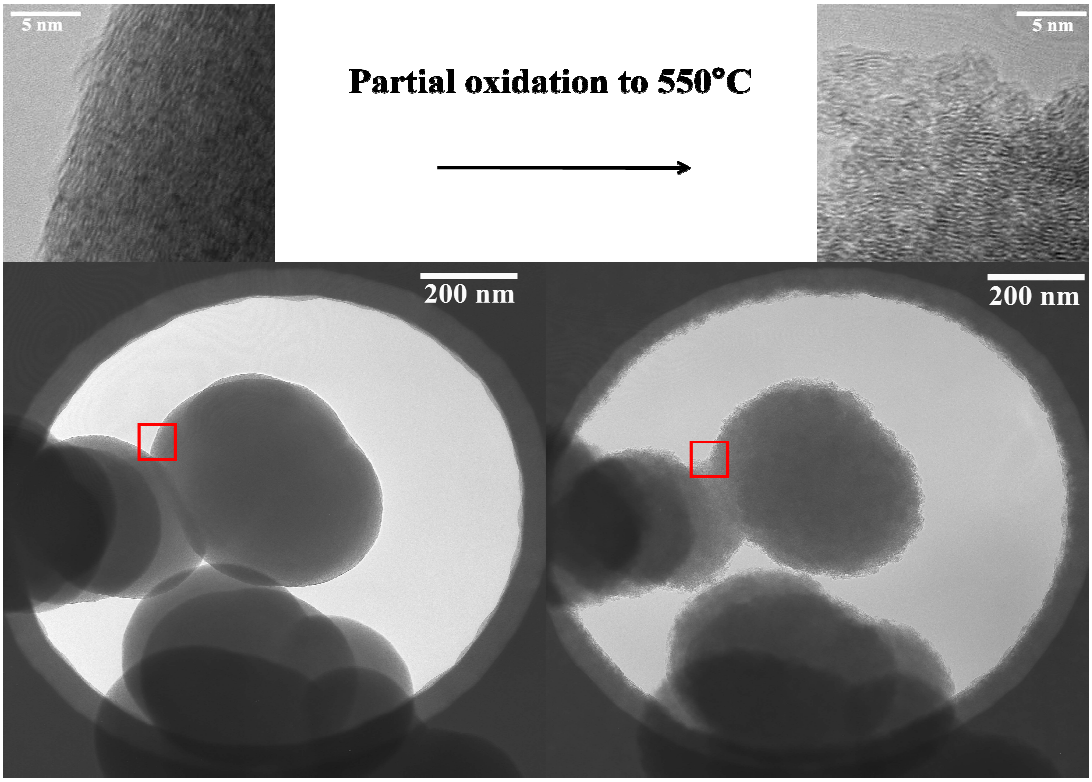


Figure 7. 4 Same spot TEM images obtained for soot deposition from toluene at 1000°C, followed by a partial oxidation to 550°C via TPO. Images were obtained with the help of Liang Zhang at OU.

As the particles are burned, this influences the rate of burning of the carbon surrounding them. This can be indicated by the high degree of burning of the graphite film for the partially oxidized sample, around the soot particles on the left of the hole. Note how the film thickness is much less around the particles when compared with the other areas. This local heating could be influenced by the size of the particles as well. Smaller particles may have a greater curvature, and thus be slightly more reactive than larger particles. This can be observed through the use of figure 7.5.

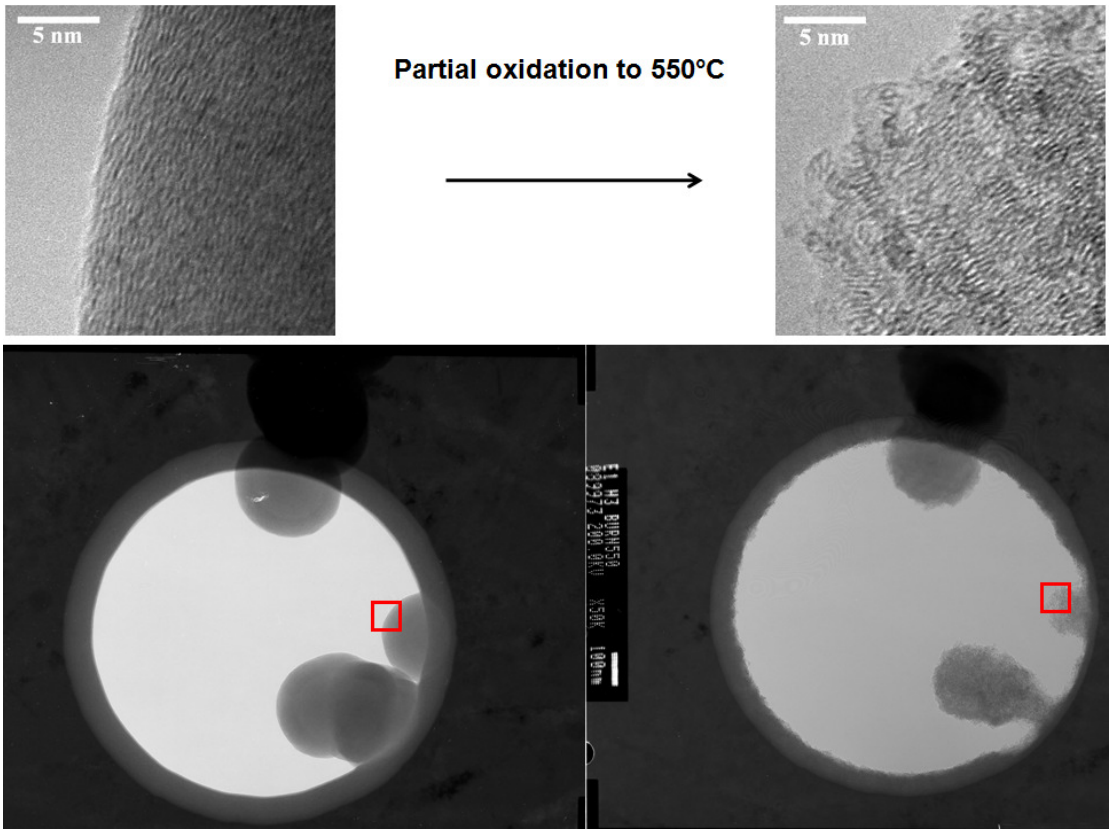


Figure 7. 5 Same spot TEM images obtained for soot deposition at 1000°C, followed by a partial oxidation to 550°C via TPO.
Images were obtained with the help of Liang Zhang at OU.

Here it can clearly be observed that the smaller particles tend to oxidize more readily, and that there is a significant degree of local heating. From this image, one can compare the oxidation ability of the large particle on the top of the hole with the small particle on the right side. The small particle definitely oxidizes more rapidly, and produces a significant amount of local heating, as indicated by the dramatic increase in oxidation on the film as well as the larger particle next to the small one. It should be noted here that, even though the oxidation appears faster for the smaller particles, oxidation of the outside of each of the particles has already begun. This indicates that

oxidation starts from the outside, and then progresses towards the more curved and readily oxidizable inner layers. As the smaller particles are oxidized, they produce a great deal of local heating, potentially contributing to the spike in the TPO profile. This maximum peak height in the TPO, therefore, should provide an indication of particle size distribution.

While TEM images are useful for illustrating ideas, they account for only a small portion of the sample. Bulk techniques, such as TPO, provide a much better idea of what is happening to the entire sample. For this reason, we have chosen n-octane as a probe molecule under the conditions of pyrolysis at 900°C. The reason for this is the shoulders observed for toluene at transition temperatures appear more as large peaks for n-octane. The goal here was to attempt to confirm the hypothesis that this was due to this local heating phenomenon, where the particles all burn, but the smaller ones burn at more rapid rates. Furthermore, if this is true, each of the particles should still burn at 550°C, but the rate at which they burn will just be slower. Results can be observed below in figure 7.6.

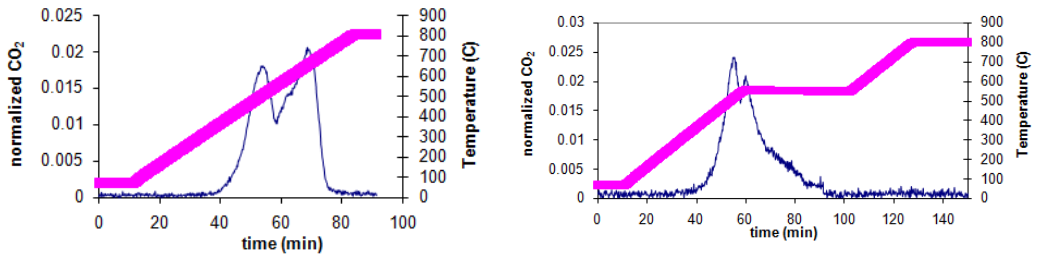


Figure 7. 6 TPO profiles observed for identically prepared samples of n-octane pyrolyzed at 900°C with various heating ramps. Thin blue lines represent the TPO signal, while thick red lines represent the temperature ramp as a function of time.

These graphs clearly support the hypothesized explanation. For graph a), the TPO was performed as normal with a constant ramp rate of 10°C/min to 800°C. Note the two distinct two peaks which result. When one now heats linearly with the same ramp to 550°C, and subsequently holds the temperature for 45 minutes, all of the carbon is still eventually burned, although the rate is much slower. It is also important to note the small increase in CO_2 which was observed initially after the ramp was held constant. This further indicates the presence of local heating. As the temperature is now increased to 800°C, no further CO_2 was observed, indicating that all of the carbon was burned at the slower rate. All of this supports the hypothesis that the carbon burns from the outside in, with maximum peak heights representing local heating due to the rapid combustion of smaller particles. This provides evidence that TPO of MPI carbon may potentially be used to correlate the MPI to particle size distribution, which is an extremely important property for combustion.

7.3.2. Influence of oxygen incorporation on MPI

7.3.2.1 Methyl esters

Methyl esters are known to form a smaller degree of soot than their corresponding alkanes due to the oxygen. OH groups have been suggested to both partially oxidize the soot on the surface and create and scavenge surface radicals, where H_2O may serve as radical scavengers which can prevent surface growth.[5] As an example, the amount of carbon deposited at 850°C is compared in figure 7.7. One can clearly note the decrease

in sooting tendency which is brought about by the methyl ester group. It is observed that the degree of decrease is much larger for the low molecular weight molecules. This is to be expected as there is a greater degree of oxygen in the molecule, and oxygenated groups tend to serve as radical scavengers to prevent soot particle growth. For this reason, the influence of oxygen is greater than the weight percent of oxygen in the molecule. While this is interesting, it is expected.

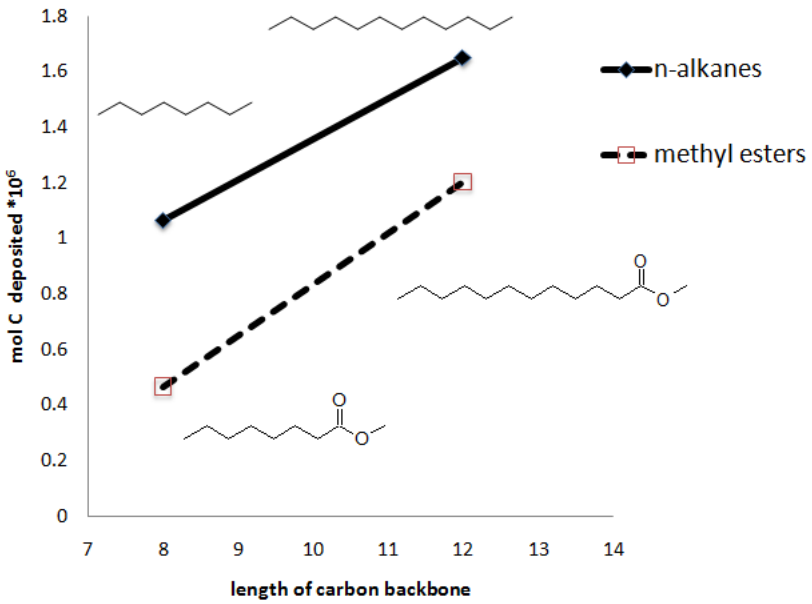


Figure 7. 7 Influence of oxygen on the amount of carbon deposited at 850°C for various alkanes and their corresponding methyl esters.

More interesting results arise from the comparison at higher temperatures, and the resulting nature of the oxidizability of the soot. The results of soot deposited as a result of temperature can be observed below in figure 7.8.

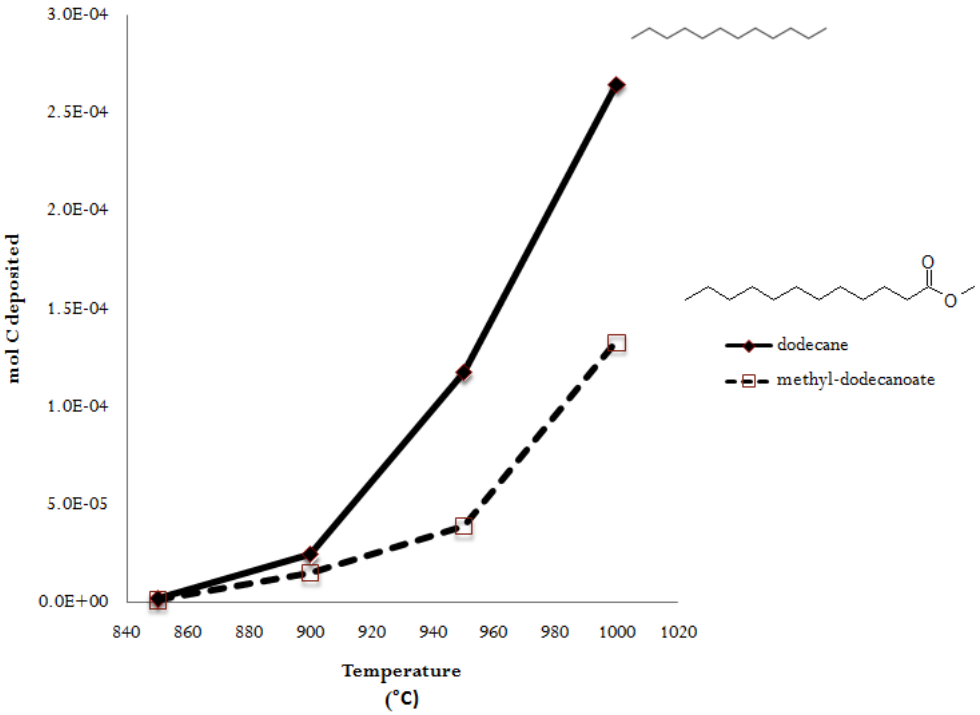


Figure 7. 8 Mol C deposited as a function of temperature for n-dodecane and methyl-dodecanoate.

This graph shows that oxygen significantly decreases soot formation for the entire range of temperatures. In each case, the drop in sooting tendency is significantly greater than the wt% of oxygen in the sample, indicating again the radical scavenging ability.

Perhaps the most intriguing aspect of these measurements is not the total amount of carbon which was deposited on the surface, but the nature of that carbon. The best method for analyzing this is through the TPO profiles. TPO profiles as a function of temperature for dodecane and methyl-dodecanoate can be observed below in figure 7.9.

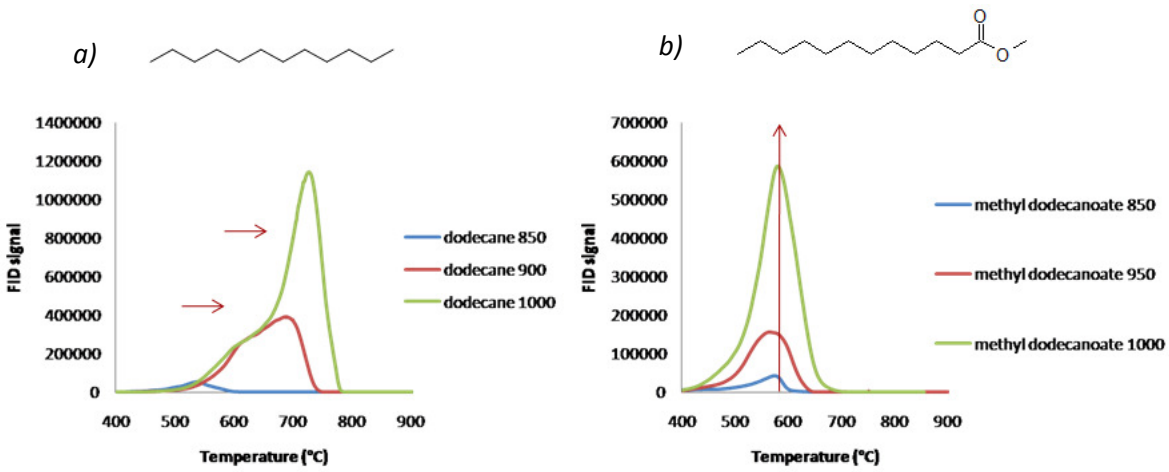


Figure 7. 9 TPO profiles for dodecane and methyl-dodecanoate deposited at 850, 950, and 1000°C. MPI measurements were conducted by Pilar Ruiz at OU.

In this case, the TPO profiles tell an excellent story. For dodecane, as the temperature is increased, the peaks appear to shift to higher temperatures, indicating an increase in particle size as was reported earlier for toluene. Note further the shape of the peaks. As the temperature is increased, the curves appear to be very asymmetrical, with a sharp drop at the end. This is an indication of a 0^{th} order burning, which indicates (as supported by the data with toluene) that this is a diffusion limited reaction. For methyl-dodecanoate, however the profiles are dramatically different. The maximum peak height in this case remains a relatively low temperatures, and even with more carbon deposited, the peaks remain somewhat more symmetrical. This is an indication that the burning in this case is not simply diffusion limited, as would be indicated by much smaller particles.

It should be noted that the amount of soot on methyl dodecanoate is much less than for dodecane. For this reason, one could argue that the symmetry of the peaks is

due to smaller amounts of carbon on the surface. This argument can be nullified, however, when one looks at the amount of carbon deposited in figure 7.8 for methyl dodecanoate at 1000°C when compared with dodecane at 950°C. The amount of carbon from methyl dodecanoate in this case is clearly greater, while the peak remains symmetrical. This supports the aforementioned hypothesis.

The reason for this is likely due to the fact that the radical scavenging ability of the oxygen groups tends to prevent the growth of large particles on the surface. For this reason, the particle size distribution should be much smaller for this case.

This result could help to explain why biodiesel is known to produce a smaller average diameter of particle sizes than regular diesel fuel. This is commonly assumed to be due only to the decreased nature of the biodiesel to form soot when compared with conventional diesel fuel. These results provide evidence that the particle size due to pyrolysis alone may be decreased as well. This is an interesting result which may not be deduced from traditional sooting methods, such as TSI[6] or YSI[7], which are unable to separate the pyrolysis from the combustion.

7.3.2.2. Aromatic oxygenates

Fast pyrolysis oil, or bio-oil, contains a large range of oxygenated compounds. Many of these are aromatic oxygenates. In order to understand better how these types of compounds will influence the pyrolytic sooting tendency of a fuel, a similar analysis as above was performed for toluene, benzaldehyde, and benzyl alcohol. This allows one to distinguish the differences which are inherent of the various oxygen containing

compounds in the presence of an aromatic ring. As a first approach, we compare this with the traditional sooting tendency measurement, smoke point,[8] which is utilized in order to obtain TSI. This measurement is conducted by measuring the maximum height of a smokeless diffusion flame for the various fuels. Smoke point values were measured through the utilization of an ASTM D-1322 compatible smoke point lamp purchased from Koehler Instrument Company, Inc. Results, along with standard deviations can be observed below in figure 7.10. From this, it can be concluded that there is no statistical influence of oxygen on the smoke point of the fuel. Smoke point is not a simple pyrolytic measurement, however, as it is a combination of the fuel to form soot as well as oxidize at atmospheric conditions, which is dependent on several parameters. For this reason, it may not behave as a fuel would under the conditions in a diesel engine. This provides a nice point for comparison with the pyrolytic sooting tendency alone, as any differences can be utilized to distinguish pyrolysis from oxidation.

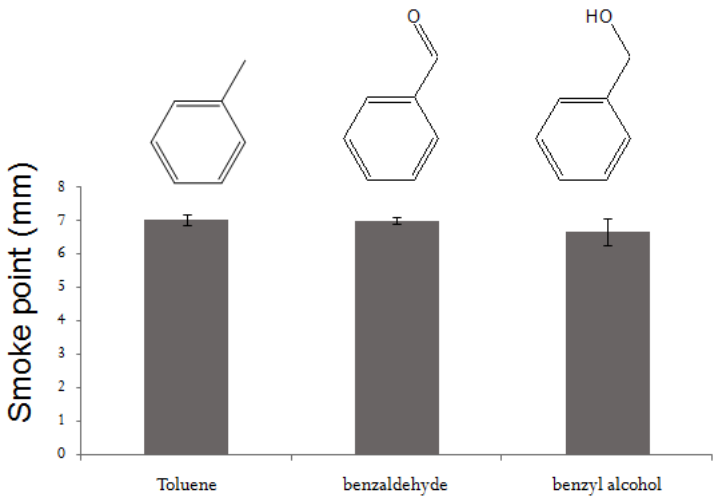


Figure 7. 10 Measured smoke point heights for toluene, benzaldehyde, and benzyl alcohol.

Results from MPI measurements for these three compounds are shown in figure 7.11. While the same conclusion can be made between smoke point and MPI for benzaldehyde and toluene, this cannot be said of benzyl alcohol. Benzaldehyde and toluene have very similar sooting tendencies as a function of temperature. While the proposed explanations for this are numerous, the most likely is that the conjugation of the aldehyde double bond with the ring provides increased stability, and thus limits its ability to act as a radical scavenger. Benzyl alcohol, however, appears to have a significant decrease in sooting tendency, providing an indication that the lack in conjugation brought about by the two extra hydrogen atoms allows this molecule to break apart and form radical scavenging groups.

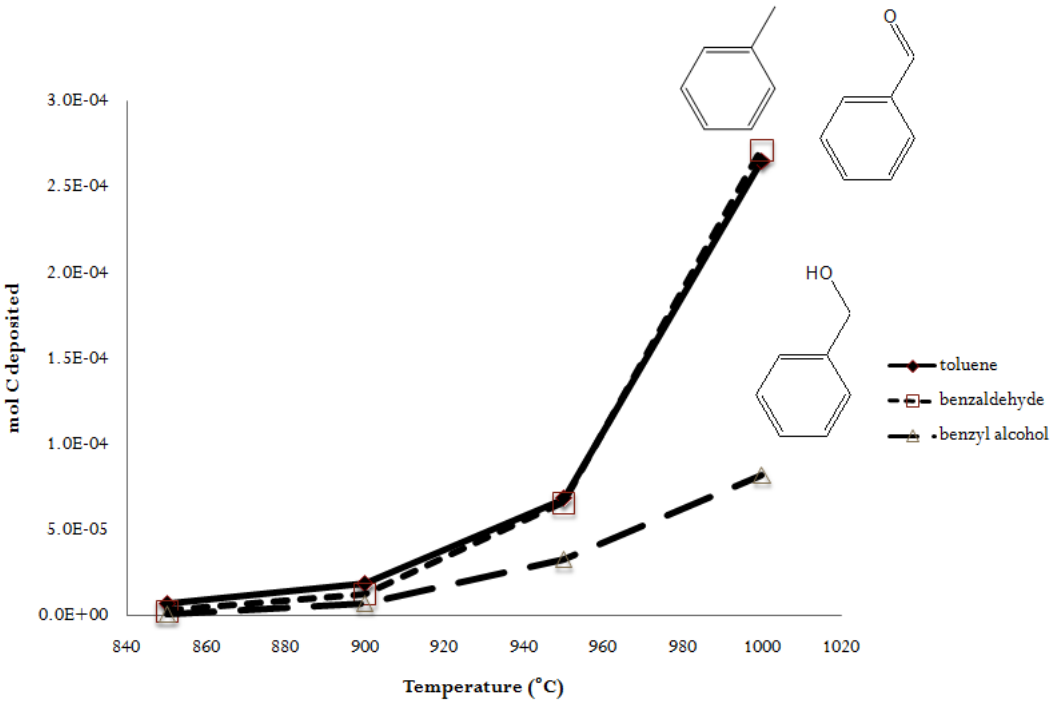


Figure 7. 11 Mol C deposited as a function of temperature for toluene, benzaldehyde, and benzyl alcohol. MPI measurements were conducted by Pilar Ruiz at OU.

Further evidence supporting this argument arises from the nature of TPO profiles of these molecules. It can clearly be observed in table 7.1 that the maximum peak temperature in the TPO appears very similar for both benzaldehyde and toluene, while the maximum peak height remains at lower temperatures for all cases for benzyl alcohol. This provides an indication, as discussed in section 7.3.2.1, that the average particle size is much smaller in the case of benzyl alcohol, and it therefore has a greater radical scavenging ability. This provides an interesting critical difference between pyrolytic and oxidative sooting tendency. For oxidative sooting tendency, both molecules will likely quickly oxidize to benzoic acid, thus having the identical impact on sooting tendency, while for the case of pyrolysis alone, the alcohol may be allowed to pyrolyze and lower soot particle size. This is an extremely important result, as actual

conditions inside a droplet of diesel fuel will be subject to a wide variety of oxygen concentrations. In the center of the droplet, for example, there may be no oxygen and thus pyrolysis will be the dominant reaction. Studies such as these can be used to help explain these phenomena.

Table 7.1 Maximum peak heights of TPO profiles as a function of temperature for toluene, benzaldehyde, and benzyl alcohol.

	Temp at peak maximum in TPO		
Temperature °C	*900*	*950*	*1000*
toluene	650	690	700
benzaldehyde	625	660	700
benzyl alcohol	**575**	**625**	**600**

7.4 Application to molecular engineering strategy

Important variances in sooting tendency were investigated in this case. This provides a first step towards understanding the influence that particular molecules will have on the fuel property MPI, and may provide some insight as to what will happen in an actual engine. While the ultimate goal will be to develop a database in order to predict the influence of oxygen on the sooting tendency of a fuel, this study provides a valuable first step.

References

1 S. Crossley, P. Ruiz, L. Zhang, D. Resasco (To be published)

2 S.P. Crossley, W.E. Alvarez, D. E. Resasco *Energy and Fuels* **2008**, *22(4),* 2455.

3 L. K. Huynh, A. Violi, *J. Org. Chem.* **2008**, *73(1)*, 94.

4 J. Song, M. Alam, A.L. Boehman, U. Kim, *Combust Flame* **2006**, *146*, 589.

5 F. Tao, V. I . Golovitchev, J. Chomiak, *Combust Flame* **2004**, *136*, 270.

6 H.F. Calcote, D.M. Manos, *Combust Flame* **1983**, *49*, 289.

7 C. S. McEnally, L. D. Pfefferle, *Combust Flame* **2007**, *148*, 210.

8 ASTM D1322, Annual Book of ASTM Standards,West Conshohocken, PA, 2000.

CHAPTER 8

8. Development of Strategies for Upgrading of Renewable Fuels

8.1 Introduction

As outlined in chapter 6, multiple opportunities are presented when one considers applications of the molecular engineering strategy towards the upgrading of fuels from renewable sources. In the case of biofuels refining, several renewable feedstocks may benefit from the molecular engineering strategy. The focus of this chapter has been narrowed to the use of heterogeneous catalysts for the upgrading of vegetable oils and fast-pyrolysis oils via model compound studies, although several other opportunities obviously exist. These strategies will be outlined below with examples. The end result is identical to those discussed earlier for conventional fuels. This is an approach guided by fuel property optimization in which model compound studies are utilized in order to understand the fundamental surface interactions which are responsible for improving the quality of a fuel.

8.2 Upgrading of triglycerides and methyl esters to fuels and specialty chemicals

8.2.1 Introduction

The most common process utilized today to upgrade triglycerides to fuels is based on the transesterification to methyl esters, or biodiesel. Both triglycerides and methyl esters still pose problems with stability and cold flow properties, making further upgrading attractive. Issues with triglycerides arise from four molecular aspects: long chain lengths, olefin content, ester groups, and free fatty acids. The former two aspects can be improved through conventional processing well established in refinery operations, though selective hydrogenation of the olefin groups has been the focus of recent publications.[1] The latter two, however, lead to problems with water solubility, storage, and corrosion. Selective reaction of acid and ester groups has been the focus of many recent studies.[2] Over Pd catalysts, C=C double bonds are first hydrogenated to form saturated acids, followed by selective decarbonylation and decarboxylation of the oxygen species. Through this approach, some carbon is lost as CO, but at the same time less hydrogen is necessary in the process. This can be a very practical approach due to the large hydrocarbons involved. The loss of CO still results in linear hydrocarbon products well in the diesel range, with improved heating value, and once hydrogenated, the resulting products are linear paraffins, with a high CN. The main disadvantage of these paraffinic hydrocarbons is their poor cold flow properties.[3] In order to further improve the cold flow properties of the fuel, such as viscosity, cloud point, and pour point, the resulting deoxygenated hydrocarbons may be isomerized to produce branched

isoparaffins. This process has been implemented commercially.[4] In this commercial process, the vegetable oils are first hydrogenated and deoxygenated over conventional hydrotreating catalysts. The resulting n-paraffins then undergo mild isomerization over an acidic catalyst to produce isoparaffins with improved cold flow properties. While this process is very practical and utilizes existing equipment present in most refineries, the catalytic procedures themselves could potentially be optimized further. Sulfur species are not inherently present in vegetable oil while conventional hydrotreating catalysts are highly optimized to react sulfur molecules and not oxygenates. Therefore, more active and selective metal catalysts, specific for oxygenates, such as those based on Pt, Pd, or Ru, could be better fits for this application. Furthermore, one may fine tune the operating conditions to shift from hydrodeoxygenation to decarbonylation and decarboxylation which may also produce paraffins, or olefins in the absence of hydrogen or a metal with hydrogenation capability.[5] Future improvements could potentially be made where isomerization and hydrogenation are included in one reactor. This could potentially take advantage of the ability to isomerize linear olefins to branched hydrocarbons while hydrogenating in the same reactor. Ideally, one could maximize isoparaffin yield while minimizing hydrogen consumption and the number of reactors.

If the decarboxylation and decarbonylation reactions are utilized to remove oxygen groups while minimizing hydrogen consumption, the primary product of these reactions is inherently an alpha olefin. This provides the added potential for producing specialty chemicals from renewable resources if one is able to maximize this intermediate, as alpha olefins can readily be functionalized in order to produce

surfactants and other valuable compounds. Because of this, for each of the model compounds employed, an effort is made to determine the olefin concentration, as well as position of the olefin on the resulting hydrocarbon as this could have enormous potential for the surfactant industry.

8.2.2 Influence of deoxygenation of on fuel properties

Upgraded triglycerides are typically used as diesel fuel blendstocks. For this reason, important fuel properties which should be considered are cloud point, viscosity, water solubility, stability, sooting tendency, and cetane number. While water solubility is not a typical fuel property which is considered for diesel fuel, the oxygen containing groups of triglycerides and methyl esters make this an inherent issue. The first question which should be asked is which triglyceride based fuel alternative is more beneficial; methyl esters via transesterification or non-oxygenated paraffins via decarboxylation or decarbonylation. The optimum fuel would contain no water solubility such that it is truly fungible with diesel fuel and the existing infrastructure. Besides this, stability is much improved by removing the ester group, although a great amount of instability attributed to biodiesel arises from the double bonds present in the molecule as well. The heating value of a deoxygenated hydrocarbon will be significantly higher due to the fact the oxygen atoms do not contribute to this property. To this point, the changes in fuel properties between the two routes have been trivial, with the deoxygenated version being the superior route in all cases. The only property which is known to be disadvantageous after deoxygenation is the sooting tendency, as discussed in chapter 7.

An interesting story arises for the case of CN. Oxygen containing groups typically lower cetane number, but in order to convert a methyl ester to its corresponding alkane via decarbonylation/decarboxylation, one must lose two carbon atoms. It is well known that CN increases with the number of carbon atoms in the molecule, so the net effect will not be clear. A graph of CN for methyl esters and linear paraffins can be observed in figure 8.1. It should be noted that the x axis is the total number of carbons excluding the end methyl group attributed to the methyl ester. In order to convert a methyl ester to a conventional hydrocarbon, one must lose one more carbon atom, as indicated by the black two-way arrows. For low molecular weight esters, the advantage of removing the oxygen is great, even at the expense of a carbon atom. This is indicated by the leftmost arrow when comparing the deoxygenation of methyl-dodecanoate to nonane, the resulting CN increase is roughly 30 CN values. For larger esters, however, this advantage is much less pronounced, as can be seen by the smaller arrow comparing the conversion of a methyl-eicosanoate to nonadecane. Even though this increase is marginal, when combined with the other properties which are improved, there is still a great need for investigation of this reaction to produce fuels and specialty chemicals.

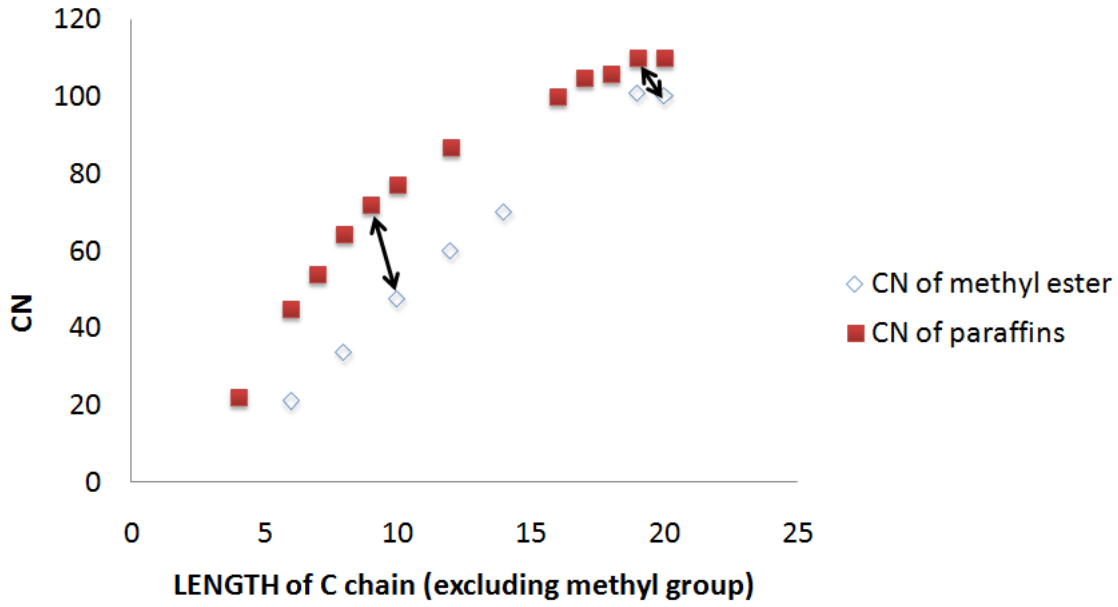


Figure 8. 1 Cetane numbers obtained from the literature[6] of methyl esters and n-paraffins as a function of the length of the continuous carbon chain.

8.2.3 Estimation of olefin content and alpha olefin selectivity

As triglycerides and methyl esters undergo decarbonylation and decarboxylation, the alpha olefins which are produced provide extremely high value for the surfactants industry. For this reason, the first step should be to determine the selectivity towards these olefins in order to better understand how the catalyst can be tailored to maximize the yield and selectivity of alpha olefins. While gas chromatographs may be able to separate olefin isomers of relatively small molecules, large olefin isomers resulting from triglycerides become extremely difficult to differentiate the hydrogenated paraffins and alpha olefins. Because of this, some other

technique must be employed. For overall olefin content, the iodine number is oftentimes utilized in order to obtain an overall balance of olefin content for a particular sample. This technique, while extremely valuable, unfortunately destroys the sample thus inhibiting further analysis while not having the ability to differentiate between alpha and internal olefins. For this reason, a new technique was developed through the use of H-NMR, which along with GC-FID results provides extremely valuable results.

This technique takes advantage of the hydrogen balance which is inherent for alpha, internal, and terminal hydrogens on any paraffinic molecule. H-NMR has the ability to distinguish these groups of hydrogen atoms with great clarity. As an example, Figure 8.2 shows a comparison of the H-NMR spectra which result from heptane, 1-heptene, 2-heptene, and 3-heptene. One can clearly see the inherent differences which result from alpha vs. internal olefins. α-Olefins have two distinct peaks which are responsible for three protons on the molecule. These appear at chemical shifts of 4.9 and 5.7 ppm. Internal olefins have a distinct peak at 5.3ppm that corresponds to two protons. By taking this into account, and observing the terminal hydrogen peak at ~1ppm which is present, along with the inherent terminal hydrogen peak at 1.6ppm which results from β-olefins, one can conduct a mol balance on the system assuming that all of the products are either paraffins or mono-unsaturated olefins. This proves to be an extremely valuable tool when utilized along with GC-FID, as one has the ability to estimate the percentage of total and alpha olefins which are present in the sample. These results can be corrected for the case of impure samples by measuring the percentage of acids, esters, aldehydes, and alcohols via GC-FID and accounting for the

additional influence that these will have on the terminal hydrogen peak and thus the overall mol balance.

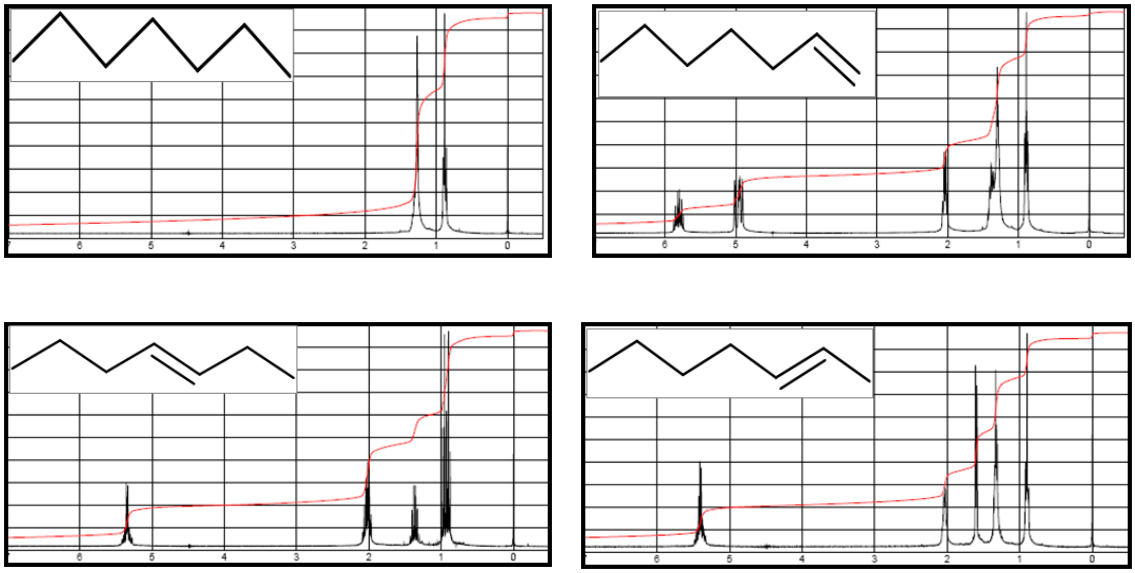


Figure 8. 2 H-NMR spectra of n-heptane, 1-heptene and its olefinic isomers

Through the use of this technique, one now has the ability to measure not only catalytic conversion, but also α-olefin selectivity and olefin isomerization which results. This will be the primary focus of the next catalytic strategy, with the applications towards generating fuels being the secondary objective. As will be observed later, these techniques have a very common goal, as the optimum catalyst which maximizes olefin selectivity turns out to be the best catalyst for deoxygenating methyl esters and triglycerides while minimizing hydrogen consumption as well.

8.2.4 Proof-of-concept reactive distillation semi-batch reactor for maximizing alpha olefin yields

As a first approach towards maximizing alpha olefin concentration, the methyl ester methyl-laurate will be considered as the feed probe molecule. This will provide insight towards the production of olefins for specialty chemicals, as well as hydrocarbons for fuels. Because alpha olefins have a rapid rate of isomerization associated with them, and olefins are often attributed to deactivation of catalysts via coke formation, some method for rapidly removing the intermediate alpha olefins must first be developed. Although the ideal approach would be either a reactive distillation or monolithic type reactor, as a first approach this can be accomplished by operating a semi-batch reactor under conditions with which alpha olefins will preferentially vaporize.

A schematic of the reactor system can be observed below in figure 8.3. The objective is to operate at a pressure such that C11 olefins will vaporize as soon as they are produced, thus inhibiting further isomerization while the feed and solvent will remain in the liquid phase.

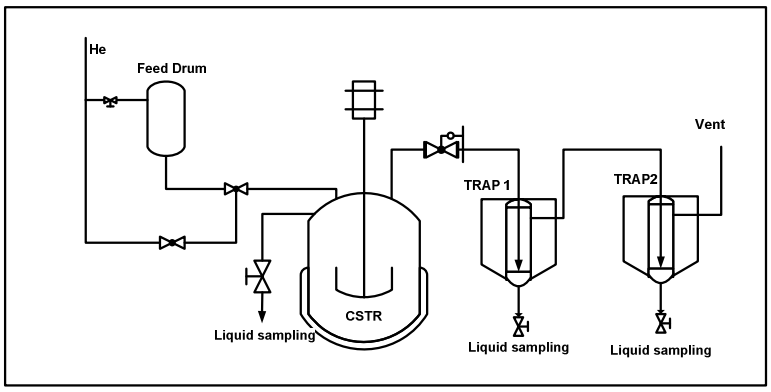


Figure 8. 3 Schematic of novel reactor for α-olefin conversion from methyl esters and triglycerides.

[Courtesy of Martina Chiappero at OU[7]]

By operating under these conditions, one can potentially react the feed molecules selectively, and continuously remove the high value olefins which are produced. Liquid phase reactions were conducted by Martina Chiappero at OU[7]. For methyl laurate, 1g of the catalyst of interest was first placed inside the reactor, which was then reduced under hydrogen at 350°C for two hours. The reactor was then purged with helium and the feed + solvent (hexadecane) was injected to the system under conditions at which the olefins would be in the vapor phase while the feed would remain liquid at equilibrium. For methyl laurate, these conditions were 320°C, 80psig. A helium flow rate was maintained at 100mL/min in order to purge the gaseous products into the liquid traps 1 and 2 downstream.

Catalysts investigated were 1wt%Pt/SiO_2 and 1wt%Pt-1.3wt%Sn-1.5wt%K/SiO_2. Pt was chosen as a first step as this catalyst is known to be very active for decarbonylation and decarboxylation. SiO_2 was utilized as the support in order to ensure that the results were not skewed by any acidity provided by the support. The

addition of Sn has multiple effects on Pt, including a lowering of Pt ensembles which are responsible for olefin isomerization, as well as the electronic effect which lowers the adsorption strength of olefins to the Pt surface, which also should result in a lower degree of isomerization. K was initially added in order to neutralize any residual acidity from the chloride precursors that were utilized to create the alloy. It was later found by Phuong Do and Min Shen by XPS that the chloride atoms are not strongly bound to the surface, and K actually increases the Cl concentration on the surface by stabilizing them, although they are neutralized. Other effects of the K, such as evidence that the K partially segregates the Pt-Sn alloy, are currently under investigation[8].

Results after 3 hours for each of these catalysts can be observed below in table 8.1. Through a combination of GC-FID with H-NMR, one is able to obtain the conversion of the feed, as well as the selectivity towards alpha and internal olefins. One can clearly observe the dramatic advantage of the PtSnK catalyst. Not only is the catalyst much more selective towards olefin conversion, but it also is more selective towards producing alpha olefins. As one may deduce, these resulting products are highly correlated. Because the Sn reduces the ensemble size of the Pt atoms, and decreases the adsorption strength of olefins on the surface, there is a lesser degree of coke formed, which subsequently deactivates the catalyst. Coke formation at the same time generates a source of hydrogen, such that the overall olefin selectivity is much lower. Because of this, PtSnK is the superior catalyst in terms of not only alpha olefin selectivity, but also catalyst lifetime.

Table 8. 1 Resulting product distributions from the conversion of methyl laurate at 320°C and 80psig.
[Courtesy of Martina Chiappero[7]]

Product Distribution of Methyl Laurate	1% Pt/SiO_2	1%Pt-1.3%Sn-1.5%K/SiO_2
	Trap	Trap
C_{11} Alpha	11.40	35.80
C_{11} Internal	45.60	51.20
C_{11} Paraffin	28.79	1.40
Light oxygenate	0.00	0.00
Lights < C_{11}	9.54	8.46
C_{12} range	4.66	3.14
Alpha/internal	0.25	0.70
Total olefin	57%	87%
conversion	15.00	29.50

As a second step, these catalysts can be utilized to measure the conversion of triglycerides directly without the need of a prior transesterification step. The results for an identical reaction where the feed is now trilaurin, or a triglyceride with three hydrogenated C12 chains, can be observed below in table 8.2.

Table 8. 2 Resulting product distributions from the conversion of trilaurin at 320°C and 80psig.

[Courtesy of Martina Chiappero[7]]

Product Distribution of Trilaurin	1%Pt/SiO_2	1%Pt-1.3%Sn-1.5%K/SiO_2
	Trap	Trap
C_{11} Alpha	20.00	27.60
C_{11} Internal	35.00	51.40
C_{11} Paraffin	20.00	11.40
Light oxygenate	0.00	0.70
Lights < C_{11}	16.00	3.00
C_{12} range	8.50	6.00
Alpha/internal	0.57	0.64
Total olefin	55%	79%
conversion	20%	90%

All of the advantages observed for PtSnK for methyl esters are still observed for the case of the triglyceride. In this case, the total conversion, total olefin selectivity, and alpha olefin selectivity are still all much higher for the case of the PtSnK catalyst than the Pt catalyst alone.

This provides an indication as to how a catalyst and reactor can be developed in order to obtain a selective product which resembles conventional fuels from a renewable resource. The molecular engineering strategy is very much a part of this

study, although, as with the hydrogenation of aromatics, the overall desired product is very well defined.

8.3 Influence of equilibrium and metal particle size on the hydrogenation/hydrogenolysis of diethylketone[9]

8.3.1 Introduction

As more emphasis is placed on renewable sources of energy, the value of knowledge of oxygenate conversion chemistry becomes increasingly important. Specifically, understanding conversion of C=O bonds to alcohols, and alcohols to olefins and saturated hydrocarbons. Increased knowledge in these areas can lead to not only improving the properties of fuels and making them more fungible, but also the development of several high-value specialty products. Symmetrical ketones are produced as the result of decarboxylative ketonization of light acids. This is a very promising reaction for converting the light acids in bio-oil to higher value products. Knowledge gained for their conversion is not only fundamentally important, but has a strong practical aspect as well.

One area which has not been studied as rigorously with oxygenates as with hydrocarbon fuels is the influence of temperature on reaction rates and product selectivity. Palladium is a well known catalyst for hydrogenation of ketones and aldehydes to their corresponding alcohols under mild conditions, as well as

hydrogenolysis to the corresponding alkene and alkane at higher temperatures. At temperatures greater than ~350°C, Pd has proven to be a good catalyst for cleavage of C-C bonds and decarbox/onylation reactions as well.[1,2] Very little work has been done, however, with regard to the effects of temperature on product selectivity and reaction rates. Furthermore, the effects of metal particle size and support have not been studied for most deoxygenation reactions. For these reasons, a study using the simple symmetrical ketone, 3-pentanone (diethylketone) was conducted in a flow reactor in the presence of hydrogen in order to determine these effects on product selectivities and reaction rates.

Diethylketone (DEK) was chosen as the model compound in this case for a variety of reasons, the main one being its practicality as a product of propanoic acid decarboxylative ketonization. Several ketones are also found in pyrolysis oil, although many are aromatic ketones, information learned from this simple model compound can be applied to guide the deoxygenation of more complicated molecules to form both specialty chemicals and fungible fuels. All of these place great value on a deeper understanding of the role of temperature and particle size on the conversion of oxygenates.

8.3.2 Experimental

8.3.2.1 Catalyst preparation

Each of the catalysts used in this case were Pd based, produced via wet impregnation at incipient wetness utilizing a $Pd(NO_3)_2$ precursor stabilized in an aqueous solution containing 10wt% nitric acid. Once the metal precursor was deposited, the catalyst was dried overnight at 120°C and then calcined at 400°C in air for 3 hours. A liquid/solid ratio of 0.9ml/g was used for the γ-Al_2O_3 (HP-140, Sasol), and 1.0ml/g for the SiO_2 (HiSil 210, Pittsburg Plate Glass Co.).

8.3.2.2 Catalyst characterization

CO chemisorption was conducted via the dynamic adsorption method in a flow cell. The catalyst was first reduced in H_2 for 2h at 200°C, and then cooled to room temperature in He. CO pulses were then sent through the catalyst bed and the resulting signal was monitored via an FID detector until the area of each pulse did not vary within ±1%. The gas exiting the reactor was passed through a methanator catalyst of 6wt% Ni/Al_2O_3 with a co-flow of hydrogen maintained at 400°C in order to convert the unreacted CO to methane. This final area was taken as the amount of CO in each pulse and the difference between this area and the area of the first injections was taken as the amount adsorbed on the sample. From this method, the ratio of moles of CO/moles of total Pd was found for each sample.

8.3.2.3 Catalytic Activity Measurements

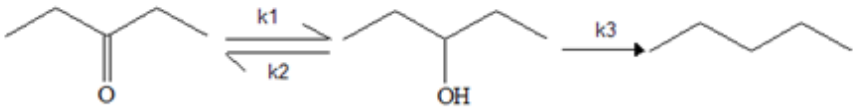
Each of these experiments was conducted in a tubular flow reactor at atmospheric pressure. The catalyst was reduced for 2hr in H_2 at 200°C prior to the introduction of the diethylketone (DEK) feed. A H_2/feed molar ratio of 30 was maintained throughout the course of the reaction. The feed was then introduced to the reactor via an IscoLC-5000 high-pressure syringe pump. Samples exiting the reactor were passed through a 100μL loop and samples were injected online via a 6-port valve to a Hewlett-Packard 5890 plus GC equipped with a FID detector for compositional analysis. After the 6-port valve, a glass trap in a dry ice and acetone bath maintained at -80°C was used to trap the reaction products for identification purposes. Product identification was achieved through the use of a Shimadzu GC-MS-QP5000. Pure component standards were also utilized in order to further verify each of the reaction products.

W/F was varied in each case by maintaining the same flow rate of diethylketone (0.7mL/h) and varying the amount of Pd catalyst for each case. Inert SiO_2 was mixed with the active catalyst in order to maintain a constant reactor bed size and eliminate bypass of reactants for small W/F values. All catalytic W/F comparisons were made with data taken at 1 hour TOS. No significant deactivation was observed for any of the cases of this study.

8.3.3 Results and Discussion

8.3.3.1 Product equilibrium as a function of temperature

In the presence of hydrogen and metals, ketones are readily hydrogenated to their corresponding alcohols, which can undergo subsequent CO hydrogenolysis to produce the resulting hydrocarbons. This is illustrated below for DEK, with saturated and unsaturated hydrocarbons grouped together as the focus of this study is on the hydrogenation/hydrogenolysis of the CO bond.



It is well known that the equilibrium between the conversion of ketones and aldehydes to their corresponding alcohols is highly temperature dependent, with equilibrium favoring the alcohol at lower temperatures. In order to illustrate this, the equilibrium between diethylketone and 3-pentanol was calculated as a function of temperature as can be seen in figure 8.4.

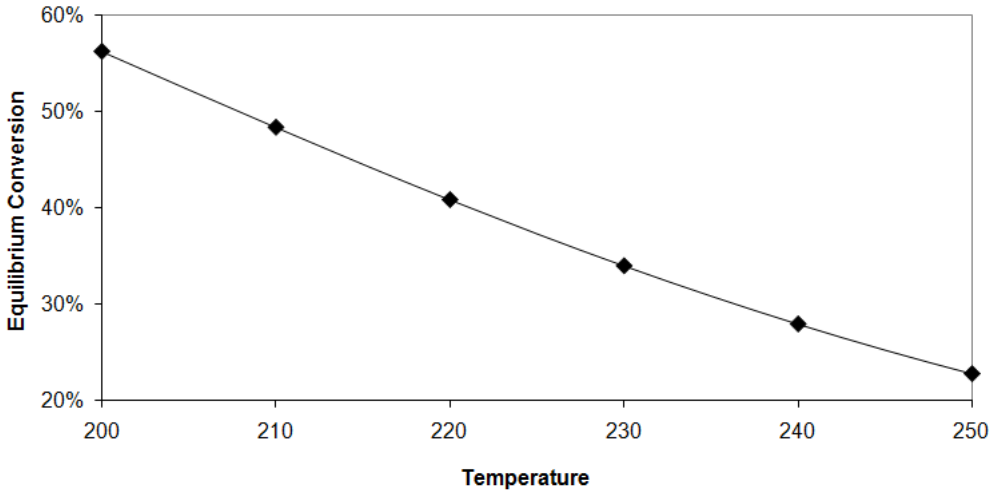


Figure 8. 4 Equilibrium conversion of diethylketone to 3-pentanol as a function of temperature.

These results were calculated through the use of SimSci Pro/II software while utilizing the Soave-Redlich-Kwong Panagiotopoulos-Reid equation of state. The results show that the equilibrium conversion of DEK to 3-pentanone becomes decreasingly favored as the temperature is increased. On the other hand, reaction rates increase with temperature, and 3-pentanol can be sequentially converted to the corresponding olefin and then saturated hydrocarbon. Hydrocarbons are favored by equilibrium under all temperatures considered, but C-O hydrogenolysis has a higher activation energy than ketone hydrogenation. For these reasons, it is not straightforward what the product distribution will be at various temperatures.

8.3.3.2 Reaction results as a function of temperature

Due to the equilibrium trend of decreasing concentration of alcohol at higher temperature, but faster rates of reaction, the influence of temperature on product selectivity is a very interesting phenomenon. In order to separate the kinetic and thermodynamic influence each will have on the product selectivity, reactions have been conducted as a function of increasing catalyst amount (1wt%Pd/γ-Al_2O_3 CO/Pd-0.25) at three different temperatures 200, 225, and 250°C. The reaction results at 200°C can be observed below in figure 8.5.

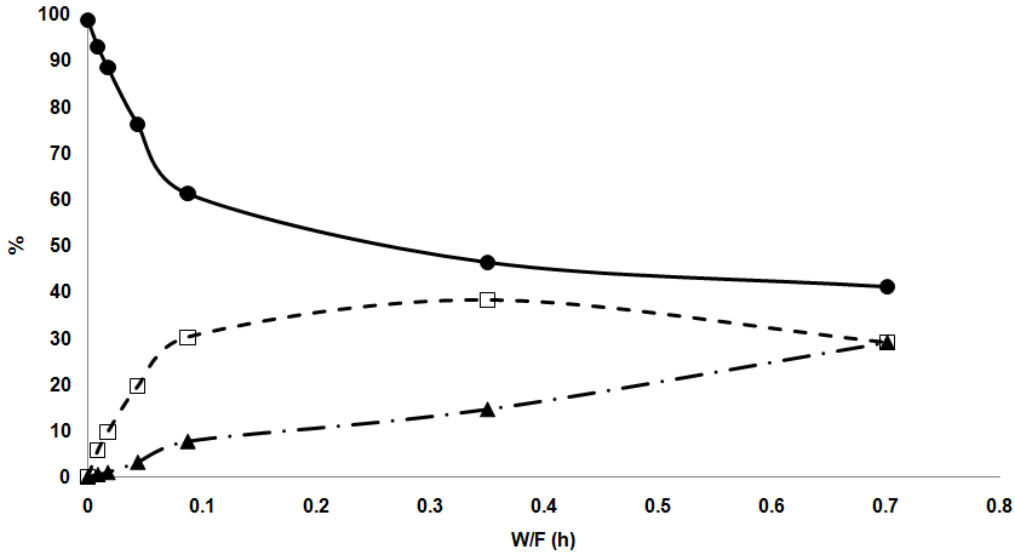


Figure 8. 5 Concentrations leaving the reactor as a function of W/F at 200°C. Solid circles represent the feed (diethylketone), hollow squares represent 3-pentanol, and solid triangles represent pentane and pentene. [9]

Note the rapid conversion of DEK to 3-pentanol at low conversions. This is to be expected as the alcohol is the primary product, but both the alcohol and the aldehyde curves experience a sharp change in slope at a W/F of just greater than 1h. It is

hypothesized that this is due to the alcohol and aldehyde approaching the equilibrium concentration. In order to verify this, the alcohol/aldehyde ratio was plotted against W/F, and compared with the calculated equilibrium concentration at this temperature according to figure 8.4. The results confirm this hypothesis, as can be observed in figure 8.6. Note the rapid approach to equilibrium at W/F values up to ~1hr. Shortly thereafter, the equilibrium ratio is approached and the highly selective rapid conversion to 3-pentanol is drastically reduced.

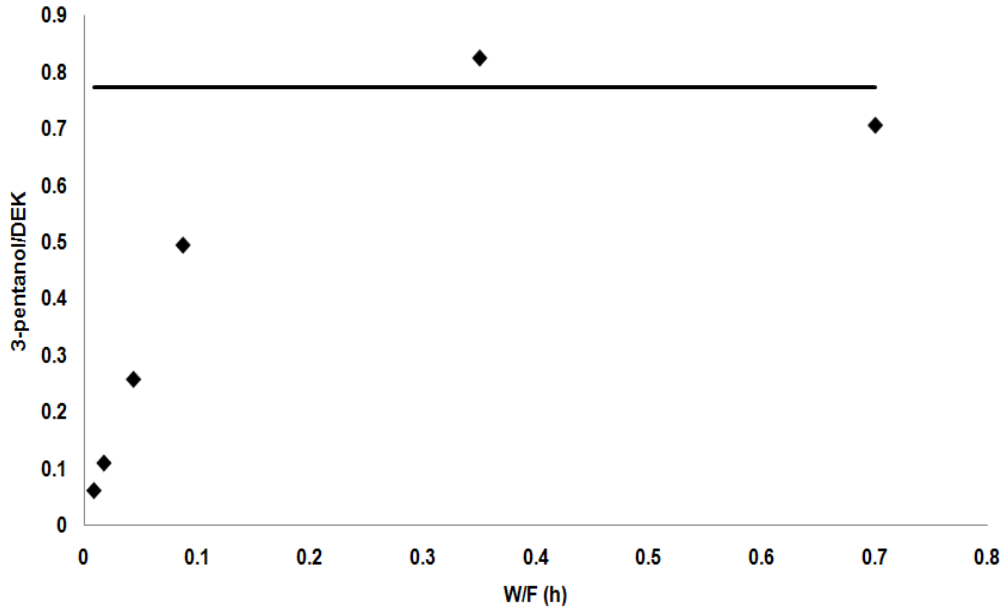


Figure 8. 6 Ratio of 3-pentanol/diethylketone as a function of W/F at 200°C. Symbols represent experimental ratios while the line represents the equilibrium ratio.[9]

While this is an interesting example, it is not unexpected, as this is a common phenomenon. The true interesting aspect is how this behavior changes as temperature is

increased. As a first step, the same analysis as a function of W/F was performed at the increased temperature of 225°C. Results can be observed below in figure 8.7.

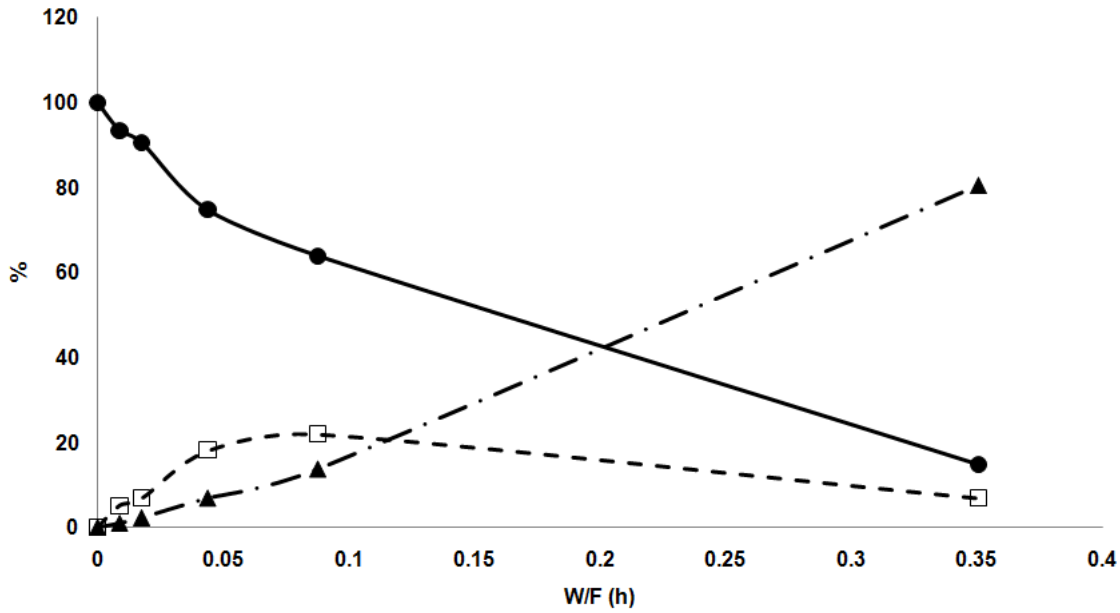


Figure 8. 7 Concentrations leaving the reactor as a function of W/F at 225°C. Solid circles represent the feed (diethylketone), hollow squares represent 3-pentanol, and solid triangles represent pentane and pentene.[9]

For this case, the change in slope is much less dramatic than was observed at 200°C. Furthermore, the alcohol reaches a maximum concentration at a much lower W/F and percent conversion than was observed at 200°C. This can be explained either by thermodynamics, kinetics, or a combination of the two. As temperature is increased, the thermodynamic equilibrium is shifted towards the ketone, thus making conversion to the alcohol less favorable. At the same time, the rate of C-O hydrogenolysis of the alcohol to the hydrocarbon will be much faster at higher temperatures, and the surface coverage of the more strongly adsorbed oxygenates will be lower. In order to

differentiate the two, one can again observe the approach to equilibrium, as indicated in figure 8.8.

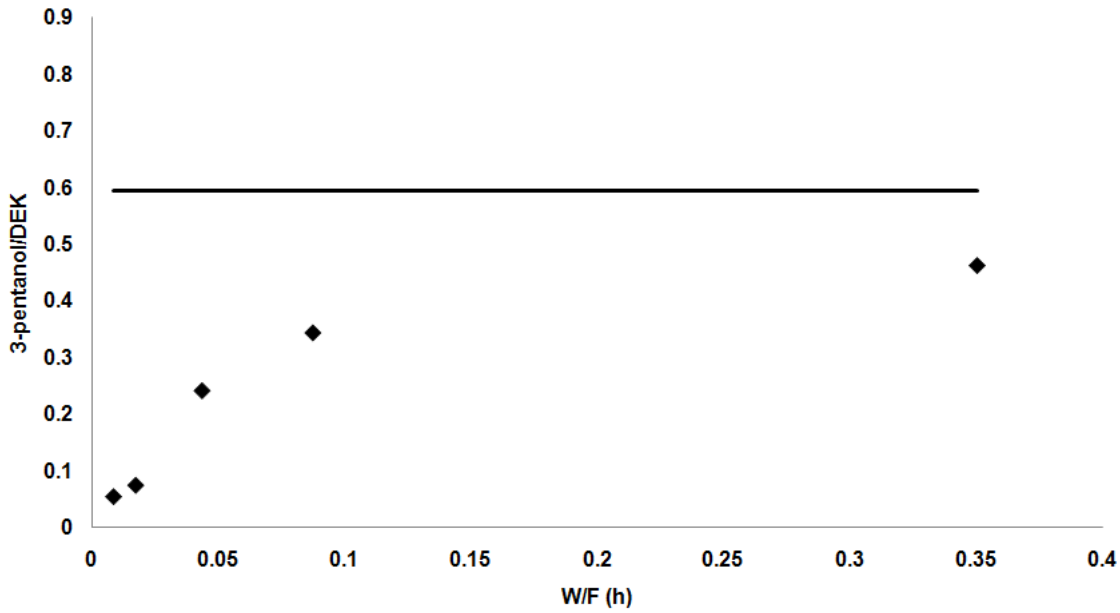


Figure. 8. 8 Ratio of 3-pentanol/diethylketone as a function of W/F at 225^{o}C. Symbols represent experimental ratios while the line represents the equilibrium ratio.

Note that in this case, the equilibrium is still approached, but never reached. This could be explained kinetically as the alcohol is converted to the corresponding hydrocarbon much more rapidly, indicating a higher temperature dependence, and thus higher activation energy of the C-O hydrogenolysis reaction. If this reaction now proceeds faster than the first hydrogenation step to the alcohol, this would keep the alcohol/aldehyde ratio below the equilibrium value. An alternative explanation could be made due to a lower surface coverage of the strongly adsorbed aldehydes on the surface at higher temperatures, allowing the alcohols to subsequently react to form hydrocarbons.

To further demonstrate this principle, the temperature was increased to 250°C. The results can be observed below in figure 8.9. In this case, it is very clear that the alcohol is quickly converted to the hydrocarbon, as a very minute concentration of alcohol is observed for each case. To further demonstrate that this is not due only to equilibrium limitations, figure 8.10 shows that the equilibrium ratio of alcohol/DEK is never approached for this case. This is an interesting concept, as the reaction appears to be thermodynamically driven at 200°C, while an increase to only 250°C completely shifts the dominant pathway towards conversion to the hydrocarbon.

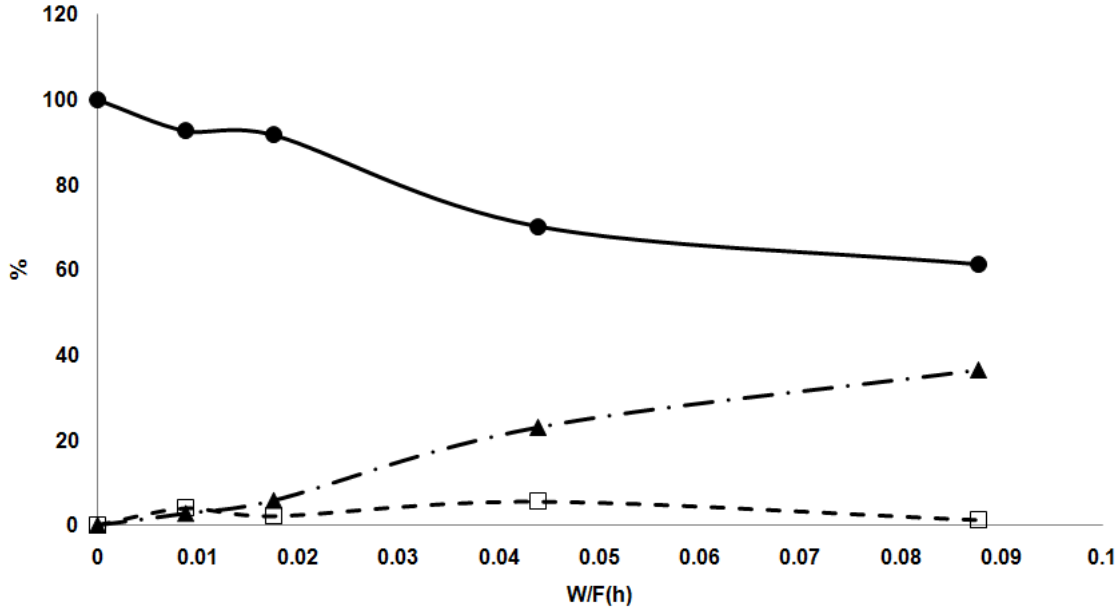


Figure 8. 9 Concentrations leaving the reactor as a function of W/F at 250°C. Solid circles represent the feed (diethylketone), hollow squares represent 3-pentanol, and solid triangles represent pentane and pentene.

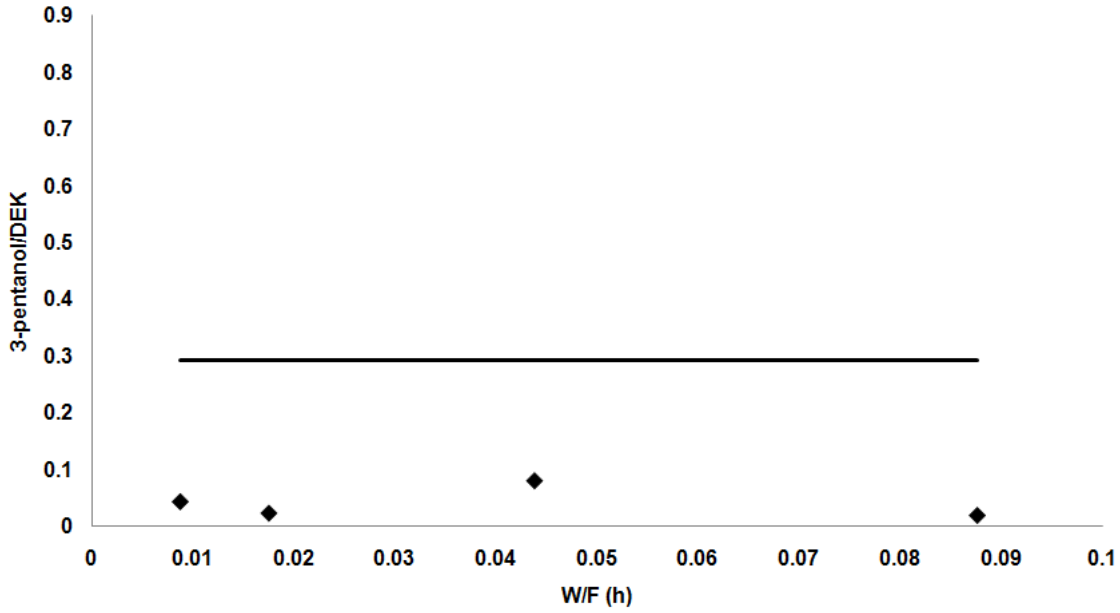


Figure 8. 10 Ratio of pentanol/diethylketone as a function of W/F at 250°C. Symbols represent experimental ratios while the line represents the equilibrium ratio.

8.3.3.3 Influence of metal particle size on product selectivity

Metal particle size is known to play an important role on selectivity and activity for many reactions involving conventional fuel upgrading. These effects have not been studied as extensively, however, for the case of hydrogenation and hydrogenolysis of CO bonds. For this reason, it is of high value to determine the influence of Pd metal particle size on CO hydrogenation and hydrogenolysis reactions.

Pd metal particle size was modified by changing the Pd loading, as well as support. Catalysts compared were 1wt%Pd/Al_2O_3, 1wt%Pd/SiO_2, and 0.5wt%Pd/SiO_2, each prepared as indicated in section 8.3.2.1. Dispersions, as measured by CO chemisorption, as well as catalytic activity and selectivity data are summarized in table 8.3.

Table 8. 3 Influence of metal particle size and support on catalytic activity and selectivity at 200°C. TOF were measured at 12% conversion of DEK, assuming 1 adsorbed CO molecule per active site as measured by CO chemisorption.

	catalyst		
	1wt% Pd/SiO_2	**0.5 wt% Pd/SiO_2**	**1wt% Pd/Al_2O_3**
Dispersion (CO/Pd)	**16.5%**	**23.4%**	**39.7%**
TOF (molecules DEK converted*site $^{-1}$*second^{-1})	**0.097**	**0.219**	**0.564**
Hydrocarbon/alcohol ratio	**0.478**	**0.157**	**0.107**

Several interesting conclusions can be made from this table. One is the influence of the support. Al_2O_3 is known to prevent Pd sintering, as indicated by the higher dispersion when prepared via identical methods as the 1wt% Pd/SiO_2. Furthermore, γ-Al_2O_3 is known to be an active catalyst for dehydration of alcohols to their corresponding olefins at higher temperatures. This is shown to not be a significant factor, as the hydrocarbon/alcohol ratio is lower for the alumina supported catalyst than for the two silica supported catalysts. While this does not rule out any dehydration, it does provide evidence that this is not the dominant reaction.

Comparing the influence of particle size on activity, as measured by the turnover frequency, one can observe a very clear and strong trend. Small deviations in CO/Pd result in large variations in turnover frequency, with better dispersions resulting in higher activity. As particle size decreases the fraction of the flat (111) plane decreases, while the fraction of low coordination corners and edges increases. It should be noted here that the CO/(exposed Pd atom) ratio changes as a function of dispersion. At relatively high dispersions, the CO/exposed Pd atom ratio is approximately 1, while this approaches 0.5 at very low dispersions due to the varying nature of adsorption sites on the various Pd faces. For this reason, under this range of dispersions, small differences in the measured CO/Pd may actually indicate a much more dramatic change in true dispersion. This could help explain the large shift in TOF with a relatively small change in CO/Pd.

The second interesting phenomenon which occurs as a result of varying particle size is the product selectivity. By comparing the ratio of hydrocarbon/alcohol at a fixed conversion of the feed of 12%, one can gain insight as to the preferential reactions which are occurring on the various facets of the catalyst surface. The obvious trend is that the hydrocarbon/alcohol ratio decreases with increasing dispersion. Keeping in mind that the TOF dramatically increases with increasing dispersion, one can draw conclusions about the nature of the molecules on the various sized particles. The most obvious explanation for this phenomenon is that the increasing steps and edges which result from increasing dispersion preferentially increase the rate of hydrogenation of the ketone to the alcohol, while the rate of C-O hydrogenolysis to the corresponding alkane

is not much improved. If the edge and defect sites significantly lower the activation energy barrier for the first hydrogenation step, this could explain this behavior.

These results can be explained by the surface intermediates which result from varying particle sizes. As the particle sizes are decreased (higher dispersion), the fraction of steps and edges on the surface increases. Steps and edges preferentially adsorb aldehydes and ketones via the η^1 mode consisting of a bond directly with the lone pair of electrons in the oxygen atom. The (111) planes, however, are known to adsorb aldehydes and ketones via the η^2 mode first through an overlap with the π orbital, and then back donation from the metal to the π^* orbitals of the O and carbonyl carbon.[10] This forms much stronger bonds with the surface when compared with the η^1, so the molecule has much more time to decompose on the surface to form hydrogenolysis products. For this reason, it is believed that the steps and edges may rapidly react the aldehydes to form alcohols that quickly desorb from the surface, while the η^2 species react much more slowly, but at the same time have a higher tendency to remain on the surface and undergo C-O hydrogenolysis to form the hydrocarbon. These preferential surface intermediates can explain both the shifts in TOF and product selectivity that occur by varying particle size.

These results can be utilized, in part, to explain the results obtained in section 8.3.3.1 over 1wt%Pd/Al_2O_3 as a function of temperature. As the temperature is increased from 200-250°C, the Pd particles may slightly sinter, resulting in a lower concentration of steps and edges. This effect is more pronounced on 1wt%Pd/SiO_2. After reduction for two hours at 200°C and 1hr reaction at 200°C, the conversion was found to be 6.7% with a hydrocarbon/alcohol ratio of 0.52. Afterwards, the catalyst was

subjected to sintering at 300°C for two hours in hydrogen. The reactor was then cooled back down to 200°C, and the feed again introduced. The conversion was observed to decrease to 4.3%, but the hydrocarbon/alcohol ratio increased to 0.95. Because the alcohol is the primary product, and hydrocarbon alcohol ratio was found to increase after sintering at a lower conversion, the effects of particle size are definitely playing a role in this case. Because the mobility of Pd on Al_2O_3 is much less than that on SiO_2, and results were obtained after only one hour TOS, this effect is likely minimal for the reactions described in section 8.3.3.1. Nonetheless, it still may play a role.

8.3.3.3. Influence of ketone hydrogenation on resulting fuel properties

While this fundamental study is useful for obtaining insight as to how temperature and metal particle size influence reaction activity and selectivity, it has not to this point provided any indication as to how these events will impact fuel properties. In order to achieve this, the fuel properties research octane number, vapor pressure, water solubility, and density were plotted as a function of conversion over 1wt%Pd/Al_2O_3 for the three temperatures of 200, 225, and 250°C. Fuel properties were calculated as described in chapter 6. Fuel properties exiting the reactor were taken as linear combinations of the properties of the compounds produced.

For each of the temperatures investigated, the trend is eventually the same, as the end product is pentane in all cases. Differences due to the selectivity and rate at which the alcohol is converted to pentane, however, may result in significantly different fuel properties as a function of conversion. This is most noticeable for each case at

200°C. At this temperature, the alcohol is the dominant product for a much wider range of conversion when compared with the other temperatures. For this reason, we have learned that an effective route for maximizing alcohol conversion over Pd catalysts is to utilize lower temperatures and higher dispersions.

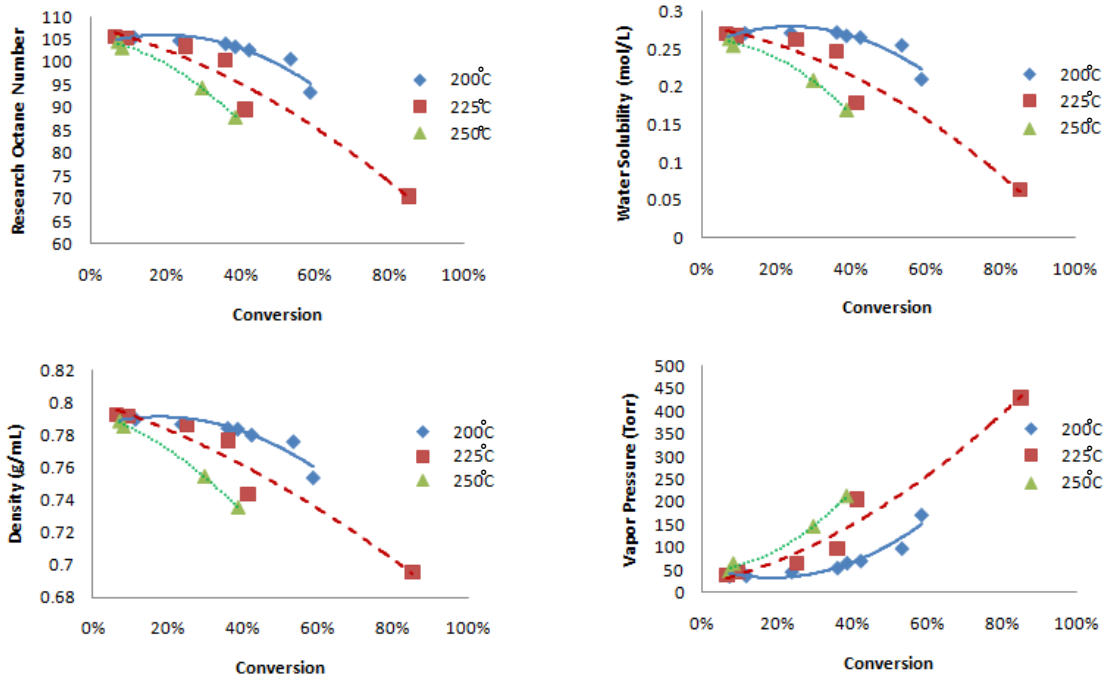


Figure 8. 11 Comparisons of research octane number, water solubility, density, and vapor pressure of products exiting the reactor as a function of conversion for 200, 225, and 250°C.

In this case, the fuel properties for the alcohol and the aldehydes are somewhat similar, with drastic differences, including the tradeoff between water solubility and vapor pressure being observed as the alcohol is converted to the hydrocarbon. This type of analysis should be conducted for many model compound studies, as it emphasizes the need to maximize not only one fuel property, but many. For this case, by converting the diethylketone, one is essentially trading beneficial octane number and high boiling

points for lower water solubility and increased volume of fuel. This is essential in order to gain practical insight from model compound studies, as even though nonlinear blending was not considered, this can still be utilized to provide important guidance for catalytic upgrading. Through this type of approach, one gains knowledge of how to link catalytic properties and conditions with the fuel properties which result.

8.3.4 Conclusions

The effects of temperature and particle size have been studied for the conversion of diethylketone over Pd. It was found that the increasing temperature prevents the alcohol/aldehyde ratio from reaching equilibrium, as CO hydrogenolysis becomes dominant at higher temperatures. Particle size was also found to play an important role, as smaller particle size was attributed to a much higher activity, but lower hydrocarbon/alcohol ratios at a given conversion.

8.4 Condensation of light compounds present in bio oil.

8.4.1 Introduction

Production of bio-oil by fast pyrolysis is a very interesting area for fuel upgrading. Bio-oil inherently contains several hundreds of different species which must be upgraded in order to produce a fungible fuel. The relatively low operating and capital costs of bio-oil compared to other biofuels make it attractive.[11] However, the poor inherent properties of this biofuel lower its potential for widespread application. The types of compounds present in bio-oil range from light to heavy oxygenates with a large variety of functional groups. Bio-oil cannot be separated via traditional distillation as many of its components polymerize upon heating, resulting in the formation of solids. On the light end, small acid compounds such as acetic and propanoic acid pose corrosion problems. Because of this, pretreatment steps to remove the most active functional groups are required before any traditional upgrading can be achieved.[12] While conversion studies have been conducted using bulk bio-oil over either traditional hydrotreating catalysts or acidic zeolites, this is likely not the best approach. Ideally, a process which condenses the light (<C5) acids, aldehydes, and ketones into higher molecular weight hydrocarbons would be desirable. Removing reactive groups of the larger aromatic oxygenates and thus inhibiting oligomerization to low-value solids and improving the fuel stability would be highly desirable. The conditions required to achieve these results are vastly different. Acid-catalyzed ketonization and aldol reactions would be required for the condensation of small

oxygenates. By contrast, metal catalyzed mild hydrodeoxygenation would be required for the heavier compounds.

Upon simple addition of water, bio-oil has been shown to separate into an aqueous phase containing carbohydrate derived compounds, while heavy lignin derived compounds settle to the bottom.[13] Through the use of this as well as known interactions between model compounds in the two phases, an optimized approach for creating fungible fuels from bio-oil could potentially be developed. Knowledge derived from the use of model compounds in fundamental studies will be essential. In fact, many model compound studies that might be almost directly applied in the bio-oil upgrading have actually been studied in the development of specialty chemicals, fine chemicals, and pharmaceutical products.[14] Small acids and aldehydes are present in bio-oil, and their selective condensation to form higher value products by producing larger hydrocarbons connected through C-C bonds could be very desirable. C-C linkages are preferred in fuels over C-O linkages such as those in ethers or esters, as C-C condensed products can undergo further hydrotreatment while maintaining their molecular backbone. Model compound studies for the production of pesticides, pharmaceuticals, or solvents have been conducted towards producing ketones by acid-acid, acid-aldehyde, aldehyde- aldehyde, or aldehyde-ketone condensation to form C-C linkages via aldol condensation over either solid acidic or solid basic catalysts.[15,16]

At the other end of the spectrum, heavy lignin-derived species present in bio-oil exhibit stability issues as they are prone to oligomerization and can result in heavy compounds that solidify easily and have low fuel value. For this reason, it is desirable to have an alternative strategy for the heavy oil-soluble compounds present in bio-oil.

A possible strategy to upgrade these compounds is mild hydrogenation and deoxygenation of the most unstable functional groups. These types of model studies have received moderate attention in recent years. For these types of reactions, it is desirable to selectively hydrogenate the oxygen functionalities, while avoiding wasting valuable hydrogen in saturating aromatic rings. Model aromatic compounds, such as guaiacols, present in bio-oil have been reacted over commercial hydrotreating catalysts with decarbonylation and decarboxylation functions that remove the oxygen groups.[17] Not much work has been done, however, using more novel metal catalysts with improved selectivities.

While both of these areas provide important areas for biofuel upgrading, the focus of this section will be on the condensation of small oxygenates to larger compounds. Novel techniques are needed in order to maximize the utilization of these low value hydrocarbons towards creating a fuel which is compatible with the current infrastructure.

8.4.2 Condensation of light aldehydes and acids

As a first step towards the upgrading of light acids and aldehydes towards high value fungible fuels, the most promising catalysts are acidic and basic. The first barrier to overcome is to create methods which can convert the reactive acids towards something which is not so problematic. Many catalysts which have shown excellent results for the conversion of aldehydes deactivate in the presence of carboxylic acids. An example in the literature was given by James Dumesic's group[18] for the upgrading

of sugars. They observed that metal+base $CuMg_{10}Al_7O_x$ catalyst was found to be excellent for conversion of light aldehydes to higher value products in the vapor phase, but the catalyst was quickly deactivated in the presence of acids. They proposed that these acids must be converted as a preliminary step, either via titration with a homogeneous base, or via decarboxylative ketonization.

Decarboxylation of acids to form ketones is a very valuable first step, as the benefits to further upgrading are more than enough to compensate for the loss of one carbon which is sacrificed. Ketonic decarboxylation occurs with high selectivity at elevated temperatures over reducible metal oxides, although it can be achieved over a range of acid and base catalysts as well[19]. Some of the most promising catalysts are the highly reducible Titania and Ceria Zirconia catalysts. This reaction produces ketones, either symmetrical or asymmetrical depending on the reactants, which can be upgraded via either hydrogenation as discussed in section 8.3, or further condensation. The optimal second approach should depend on the size of the ketone product. If it is in the diesel fuel range, it should be hydrogenated as discussed above, but if it is still a light product, further condensation should be achieved.

The optimum approach for further condensation, both of aldehydes and ketones, is through aldol condensation. This reaction is extremely valuable due to the fact that it produces condensation products with C-C linkages, such that the carbon backbone will be maintained after the excess oxygen is removed via hydrotreating. This reaction is known to occur for virtually any carbonyl containing compounds with an alpha hydrogen through the utilization of either an acid or base catalyst under a variety of conditions. Basic catalysts are much more active for aldol condensation at low

temperatures than acid catalysts. A schematic of the base-catalyzed aldol condensation reaction can be observed below in figure 8.12.

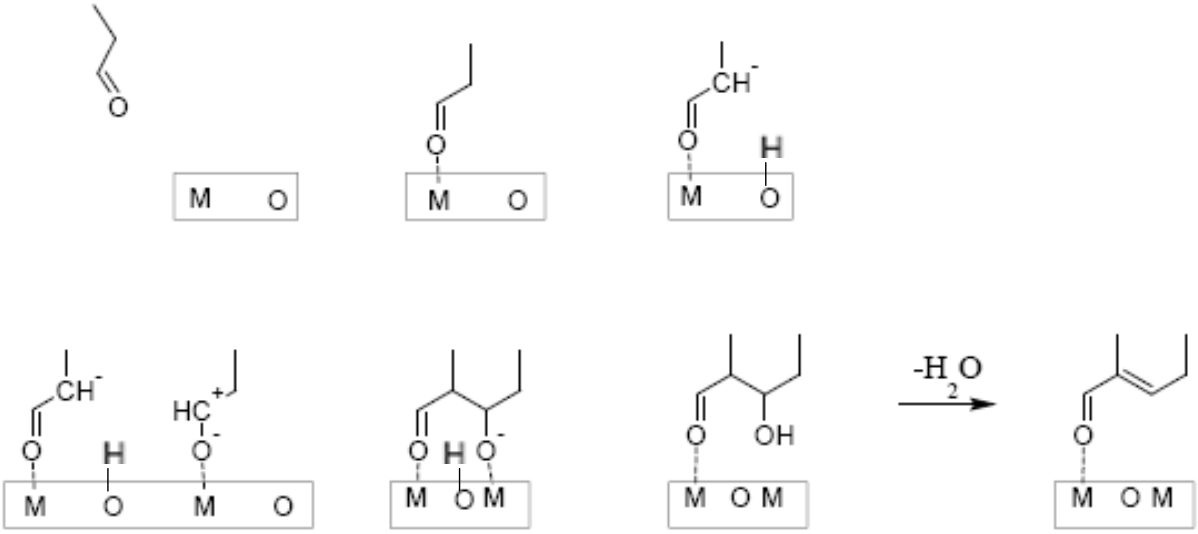


Figure 8. 12 Schematic base catalyzed of aldol condensation mechanism for propanal. (Courtesy of Quincy Amen at OU)[20]

Aldol condensation reactions are known to occur for both aldehydes and ketones, so long as an alpha hydrogen is present. Carbonyl containing compounds without alpha hydrogens can also undergo aldol condensation, but must be the subject of attack of the enolate ion. That is, there must be some carbonyl containing compound present with an alpha hydrogen in order for this reaction to occur. For this reason, not only dimers, but also trimers and tetramers may result from these reactions.

In the presence of a bifunctional catalyst, interesting results may be obtained. Quincy Amen at OU[20] has investigated aldol condensation in the vapor phase over basic and bifunctional catalysts. At 300°C under atmospheric pressure and a W/F of 0.745h, he observed an interesting trend over basic zeolites. NaX was the most active catalyst

initially, but also the most prone to deactivation. This was explained by the high amount of residual acidity due to the relatively hard Na ion. Furthermore, a cyclic trimer product was observed as the result of a Nazarov ring closure, which is an acid catalyzed reaction. For this reason, it was concluded that the acidity of the Na was playing an important role in the reaction. This was confirmed by moving to the larger cation, Potassium. KX showed a lower initial activity, but much improved catalyst stability. The ratio of cyclic trimer/dimer was also found to be much lower for this case. This shows that both acidity and basicity can play important roles in the condensation of light aldehydes.

Once all of the propanal is converted to dimer, no further aldol condensation may take place, as no compounds are left with an alpha hydrogen. In order to further this reaction, a metal can be added to the catalyst in order to selectively hydrogenate the olefin and allow aldol condensation to progress further. The metal employed will depend on the temperature at which the reaction is taking place. Under low temperature conditions (<100°C), a highly dispersed Pd catalyst would make a good choice, as it is extremely selective towards hydrogenating the olefin. As an example, the dimer from the aldol condensation of propanal, 2-methyl-2-pentenal, was hydrogenated in the liquid phase over 1wt%Pd/SiO_2 (same catalyst as utilized in section 8.3). 100mg of the catalyst was placed in a round bottom flask and reduced at 100°C for two hours while flowing hydrogen at atmospheric pressure. A mixture containing 5mL of 2-methyl-2-pentenal and 50mL n-heptane was then placed inside the reactor at room temperature. After 5.5 hours at 50°C, 15% of the feed had converted with 100% selectivity towards the saturated aldehyde. Further increases in temperature would result in faster rates, but

temperatures in excess of ~150°C result in significant amounts of decarbonylation. This result confirms that Pd can be utilized to selectively hydrogenate the double bond at lower temperatures, and potentially allow aldol condensation to continue. Under these conditions, the reaction would then not be limited by the amount of propanal in the system as the dimer could convert further. The reaction would now be controlled by the desorption of the heavy condensation products produced.

If higher temperatures are utilized for aldol condensation, as may be desirable if one wishes to work in the gas phase and increase reaction rates, the catalyst of choice should be chosen such that it inhibits decarbonylation and C-O hydrogenolysis. For this reason, Cu or PdCu alloys make good candidates, as both of these catalysts are known to rapidly hydrogenate olefins and CO bonds to alcohols, but hydrogenolysis and decarbonylation reactions are much inhibited. While Cu is not selective for C=C hydrogenation as is Pd, the equilibrium at higher temperatures favors the aldehyde or ketone, which further supports its use under these conditions.

While aldol condensation is an extremely useful route for increasing the size of the molecule while preserving the hydrocarbon backbone, large condensation products which are formed on the surface may serve to deactivate acid and base catalysts. Because of this, it may be of interest to work under conditions where only the dimer is maximized in order to avoid catalyst deactivation. Under these conditions, the aldol condensation products may not be large enough to fit into the conventional gasoline and diesel fuels, so further condensation of these dimers would be desirable. Furthermore, because these reactions produce either an aldehyde or ketone, these products require further hydrogenation as a second step in order to reduce water solubility and increase

oxidative stability. It would be extremely valuable if both of these could be accomplished in one step, as will be outlined in the next section.

8.4.3 Ether formation from aldehydes and alcohols via metal catalysts

As a second step for upgrading of aldol condensation dimers, metal catalysts may potentially be employed in order to produce large ethers. This reaction has a very narrow range of applicability, but a very high return. Etherification has been found to occur readily for light aldehydes, alcohols, and ketones over specific metals under relatively mild conditions (100-130°C).[21] Pd is especially active for forming ethers among the various groups, with the explanation due to the relatively weak adsorption of carbonyl groups on the Pd surface. It has been proposed that the formation of ethers results from a η^1, or atop adsorbed species, next to a η^2, or di-σ adsorbed species.[22] It has been proposed via theoretical calculations that the preferential adsorption state of aldehydes and ketones on Pd (111) is via the η^2 di-σ intermediate.[23] At the same time, it has been proposed that alcohols preferentially form alkoxide species by adsorbing via the η^1 intermediate.[21] Because of this, several cases have been reported where an alcohol preferentially reacts with either an aldehyde or alcohol to form an ether.[22,24-28] Ethers can be formed in very high selectivities, but only under a very mild range of conditions. If temperatures are too mild (<100°C), etherification will not take place, while at very high temperatures, side reactions of decarbonylation and C-O hydrogenolysis begin to occur.

Because of the high potential for this reaction to be applied towards condensing dimers and trimers of aldol condensation products to the diesel range, it is of high value to test the validity of etherification over Pd catalysts with feeds representative of aldol condensation products. As a first step, the hydrogenated product of propanal condensation, 2-methylpentanal, was utilized as a model feed. Trung Pham at the University of Oklahoma[29] has conducted reactions in a flow reactor at 125°C. Detailed experimental details may be found elsewhere.[29] Results can be observed below in table 8.4.

Table 8.4. Reaction results from the etherification of 2-methylpentanal over Pd/SiO_2 catalysts in a flow reactor maintained at 125°C in H_2. Courtesy of Trung Pham at OU.[30]

Reduction T(C)	150	150	150	200
2-methyl pentanal (feed)				
Catalyst Pd wt%	3%	10%	16%	16%
Dispersion (CO/Pd)	7.1%	5.3%	3.9%	-
T (C)	125	125	125	125
W/F (hr)	2	1	1	1
X	20.86	20.38	23.76	20.044
pentane	6.98	5.29	5.5	6.358
2-methyl-pentanol	6.67	7.43	6.37	0.599
ether	7.21	7.67	11.9	13.087

Selectivity

W/F (hr)	2	1	1	1
pentane	33.48	25.95	23.14	31.72
2-methyl pentanol	31.96	36.44	26.81	2.99
ether	34.56	37.61	50.06	65.29

A clear trend is observed as particle size is increased. It should be noted that larger particle sizes indicate a greater presence of Pd (111), and less steps and edges. Furthermore, as observed in the rightmost column, an increase in reduction temperature further increases the selectivity towards ether formation. This indicates that a high degree of sintering could produce a catalyst with high ether selectivity without the need to utilize such high Pd loadings. This supports the explanation that the aldehydes preferentially adsorb via the η^2 route over Pd (111), while alcohols may adsorb via η^1, thus producing ethers from larger compounds to create diesel range products. These products can have extremely promising fuel properties as well. As an example, if one

assumes that the oxygen in the molecule was a carbon, this molecule would be 4,6-demethylundecane, which has a CN of 58. Now, if one compares ethers with hydrocarbons, the properties become even more promising. n-Propane has a CN of -20, while n-pentane has a CN of 30, if one now replaces the middle carbon to produce dimethyl ether and diethyl ether, the resulting CNs are 67 and 150, respectively.[6] This provides strong evidence that ether products in this range will have extremely high diesel fuel qualities, while the influence of the oxygen on water solubility will be minimal due to the large C/O ratio.

Further support for this hypothesis of an alkoxide next to an n^2 aldehyde resulting in ether formation has also been observed by Trung Pham through the co-feeding of alcohols with 2-methylpentanal. Increased selectivities towards ether formation were observed when alcohols were utilized, while asymmetrical ethers were observed with high selectivity when an alcohol besides 2-methylpentanol was used. This is an excellent result for bio oil upgrading, as this etherification can provide a second step for upgrading of products resulting from aldol condensation reactions. Pd can serve the dual purpose of hydrogenating any unsaturated compounds at the same time.

8.4.4. Overview of strategy for condensation of light bio-oil compounds

These results indicate that an optimal path for converting oxygenates would be to first ketonize acids to form ketones, followed by an aqueous phase solid base catalyzed aldol condensation reaction between aldehydes and the newly formed

ketones, combined with a metal to hydrogenate the double bonds and further the condensation. This will yield a product mixture which contains a much lower degree of polarity, so it will likely form an organic layer which is insoluble in water. This phase can then undergo a hydrogenation/etherification step in order to selectively hydrogenate unwanted olefins, while forming ethers with aldehydes, alcohols, and potentially ketones over either a Pd catalyst with a low dispersion or a promoted Pt catalyst.[21] This route could produce a very high quality diesel fuel from a very low initial value feedstock. A schematic of this route is shown in figure 8.13.

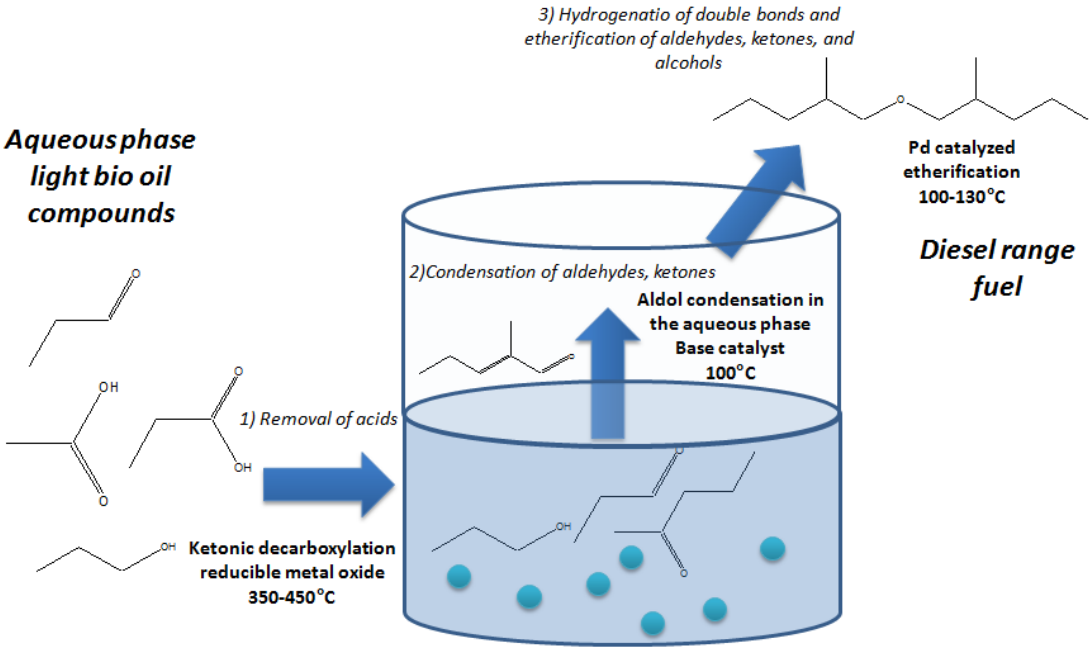


Figure 8. 13 Schematic of potential route for producing valuable diesel range products from low value bio oil streams.

8.5. Conclusions

We have considered several strategies for upgrading of biofuels while utilizing novel catalytic strategies. Each of these strategies was guided by a purpose which was ultimately driven by fuel properties. The end result in each case is a deeper understanding of reaction intermediates occurring on the surface, and their relationship to the catalyst. By knowing the fuel properties of the compounds which may be produced, and using this as guidance, the ability has been gained to tailor a catalyst in order maximize the desired fuel properties, and develop novel strategies to obtain optimized fuels from renewable sources.

References

1 I.L. Simakova, O.A. Simakova, A.V. Romanenko, D.Y. Murzin *Ind Eng Chem Res.* **2008**, *47*, 7219.

2 M. Snare, I. Kubickova, P. Maeki-Arvela, D. Chichova, K. Eraenen, D.Y. Murzin *Fuel* **2008**, *87,* 933.

3 R.J. Taylor, R.H. Petty *Appl Catal, A.* **1994**, *119*, 121.

4 P. Aalto, O. Piirainen, U. Kiiski Finnish patent FI 100,248 (1997).

5 T. Sooknoi, T. Danuthai, L. Lobban, R.G. Mallinson, D.E. Resasco *J Catal*. **2008,** *258,* 199.

6 J. D. Taylor, J. Michael in "Compendium of Experimental Cetane Number Data", **2004**. Golden, Colorado: National Renewable Energy Laboratory, 48.

7 Martina Chiappero Master's Thesis (In Progress)

8 Phuong Do PhD Dissertation (In Progress)

9 S. Crossley, A. Botero, D. E. Resasco (to be published)

10 R. Shekhar, M.A. Barteau, R.V. Plank, J.M. Vohs *J Phys Chem B.* **1997**, *101(40)*, 7939.

11 G.W. Huber, S. Iborra, A. Corma *Chem Rev*. **2006,** *106*, 4044.

12 D.C. Elliott, E.G. Baker, J. Piskorz, D.S. Scott, Y. Solantausta *Energy Fuels* **1988,** *2*, 234.

13 S. Czernik, A.V. Bridgwater *Energy Fuels* **2004**, *18*,590.

14 P.D. Vaidya, V.V. Mahajani *Ind Eng Chem Res* **2003,** *42*, 3881.

15 T.S. Hendren, K.M. Dooley *Catal Today* **2003,** *85,* 333.

16 M.J. Climent, A. Corma, V. Forne, R. Guil-Lopez, S. Iborra *Adv Synth Catal.* **2002,** *344*, 1090.

17 E. Laurent, B. Delmon *Appl Catal, A*. **1994,** *109*, 97.

18 E.L. Kunkes, D.A. Simonetti, R.M. West, J.C. Serrano-Ruiz, C.A. Gärtner, J.A. Dumesic *Science* **2008**, *322*, 417.

19 M. Renz *Eur. J. Org. Chem.* **2005**, 979.

20 Quincy Amen Master's Thesis (in progress)

21 G. M. R. van Druten, V. Ponec *Appl Catal A, Gen* **2000**, *191*, 163.

22 A. van der Burg, J. Doornbos, N.J. Kos, W.J. Ultee, V. Ponec *J. Catal.* **1978,** *54*, 243.

23 F. Delbecq, P. Sautet *Surf. Sci.* **1993**, *295*, 353.

24 T.P. Kobylinski, H. Pines *J. Catal* **1970,** *17*, 384.

25 H. Pines, J. Haensel, J. Simonik *J. Catal* **1972**, *24*, 220.

26 J.F. Hemidy, F.G. Gault *Bull. Soc. Chim. Fr.* **1965**, *17*, 10.

27 E. Licht, Y. Schächter, H. Pines *J. Catal* **1974,** *34*, 34.

28 V. Bethmont, F. Fache, M. Lemaire *Tetrahedon Lett* **1995,** *36,* 4235.

29 Trung Pham PhD Dissertation (in progress)

30 T. Pham, S. Crossley, L. Lobban, D. Resasco, R. Mallinson, (to be published)

CHAPTER 9

9. Novel Emulsion Catalysts for Upgrading of Bio-Oil

9.1 Introduction

The upgrading of bio-oil introduces several interesting challenges and opportunities for the molecular engineering strategy. As discussed in chapter 8 section 4, these compounds may be separated based on their boiling points and water solubilities into somewhat broad "cuts". While true distillation is impossible, as high temperatures cause a heavy degree of polymerization and loss of valuable products, treatments such as low temperature vacuum distillation and sequential quenching provide promise for breaking this oil into several treatable streams. In order to gain further separation, potentially the most advantageous method of separation is through each molecule's polarity. This can be accomplished through the addition of either water or oil to a particular fraction of bio-oil.[1]

Even within these fractions, there will likely be a broad distribution of products, some which should be condensed to larger products as discussed in chapter 8 section 4, and some which should be deoxygenated in order to improve stability. A schematic of this problem is shown below in figure 9.1.

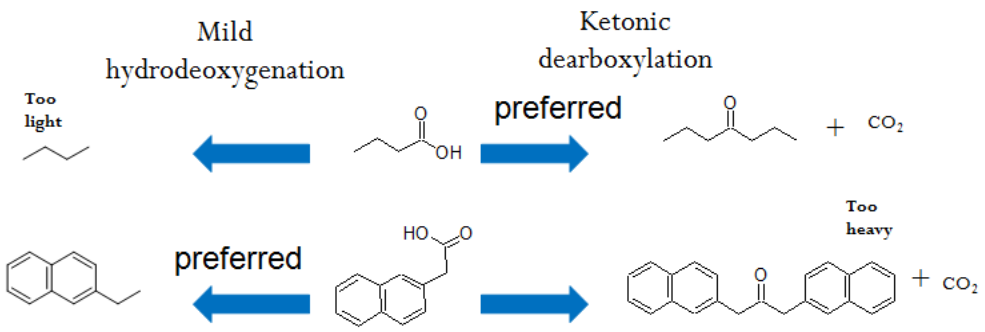


Figure 9. 1 Conceptual illustration emphasizing the need for selective strategies for upgrading of bio-oil.

One strategy cannot be utilized to improve the properties of bio-oil, but rather a unique strategy should be utilized for each phase. By taking advantage of the water solubility of each phase one could, for example, selectively condense the aqueous phase while selectively hydrogenating the aqueous phase. If one were able to do this in a single reactor, this would be of enormous benefit for bio-oil processing. This provides the basis for the idea, but the possibilities created from the system which results can be virtually endless.

The potential solution for this is an interfacial catalyst, one which is capable of selectively performing reactions in both phases. In order to accomplish this, as well as increase catalytic surface area for reaction, an ideal solution would be to create a multifunctional emulsion which is able to catalyze specific reactions in the two phases. This approach could become a reality through the creation of Pickering emulsions with multifunctional catalytic properties. While Pickering emulsions are not uncommon in the literature for stabilizing oil/water droplets with solid particles[2-6] no example has

been shown to this point where these can be utilized as multifunctional catalysts capable of reacting both phases independently.

Potential candidates have been proven to exist through the use of "black sand" nano-hybrids, which are single wall carbon nanotubes, as well as the silica support on which they were grown. Black sand is inherently amphiphilic, as it prefers to orient selectively at the water oil interface. An example is shown in the image below (figure 9.2) for a mixture of heptane (top layer) and water (bottom layer).



Figure 9. 2 Preferential orientation of black sand at the oil/water interface upon addition to an oil/water mixture. The top phase is 1-heptene, while the bottom is water.

The proposed idea is that, while black sand is amphiphilic, it contains nanotubes and silica which have very different wettabilities in the two phases. Nanotubes which are free of defects should preferentially orient themselves on the oil side of the interface, while silica should orient more on the polar side. If the slightly polar silica is playing the larger role, the nano-hybrids will preferentially stabilize oil in water emulsions, while if the non-polar nature of the nanotubes is playing the stronger role, the emulsions will be reversed. A schematic of these types of emulsions is shown in figure 9.3.

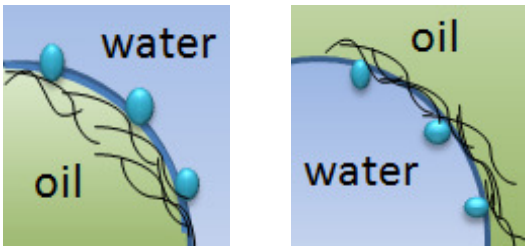


Figure 9. 3 Schematic of water in oil vs. oil in water emulsions as prepared via nano-hybrids. Blue spheres represent silica particles while black lines represent carbon nanotubes.

Black sand does not create thermodynamically stable emulsions, but it can stabilize oil in water or water in oil emulsions if kinetic energy is added to the system. These emulsions can be created simply by addition of oil to a dispersed solution of nanotubes in water, followed by stirring. Dr. Min Shen at OU has shown that the particle size can be dramatically influenced by the degree of sonication of the oil+water mixture, and the emulsion volume can vary dramatically depending on the oil/water ratio. As an example, Figure 9.4 shows various emulsions of 2wt% black sand with

varying decalin/water ratios produced via the CoMoCAT process, and provided by SouthWest Nanotechnologies Inc. (SWeNT).



Figure 9. 4 Influence of varying decalin/water ratio on emulsion volume. Emulsions are indicated by the black, non-transparent layer. Image courtesy of Dr. Min Shen at OU.

For catalytic purposes, it would be highly desirable to create some selective activity through either the deposition of metals selectively on the nanotubes or silica, or through the acid or base functionalization of either phase. As a first step, Pd metal deposition will be applied to study the reactivity and selectivity of dopant molecules in decalin water emulsion mixture. Octanal was chosen as the model compound soluble in the oil phase, and glutaraldehyde was chosen as the model compound which is most soluble in the water phase. These molecules are readily hydrogenated over Pd, and were chosen in order to give a proof-of-concept for this type of reaction to indicate its potential.

9.2 Experimental

This project is a collaboration with Jimmy Faria and Min Shen at OU.

9.2.1 Catalyst preparation

Black sand was obtained from SouthWest Nanotechnologies Inc. (SWeNT) via the patented CoMoCat process. As-synthesized particles were passed through a micro-fluidizer in order to achieve more uniform particle sizes. 5wt%Pd was deposited on the nanotubes via incipient wetness impregnation with a $Pd(NO_3)_2$ precursor stabilized in a 10wt% nitric acid solution. Samples were dried overnight at 110°C and subsequently heated in a flow of He to 300°C for two hours.

9.2.2 Reaction procedure

Reactions were conducted by placing 30mg of black sand in 15 mL of water. The black sand was then dispersed in the water via 15 minutes of sonication in a horn sonicator. To this mixture, 15mL of decalin (>98%, Fluka) was added. This mixture was then placed inside a Parr reactor and brought to 200psig in He while continually stirring the mixture in order to produce and maintain emulsions. The mixture was then heated to 100°C, where it was reduced in bubbling H_2 (100mL/min) for 2 hours before introducing the reactive model compounds. A 5mL mixture of equimolar octanal and glutaraldehyde was then introduced to the system via a connected bomb which was pressurized with He. The reactant mixture was then maintained at 100°C and 200psig for three hours while continuously bubbling hydrogen at 100mL/min.

After reaction, the mixture was cooled to room temperature in He while maintaining 200psig of pressure. The pressure was then slowly released, and the contents of the reactor were vacuum filtered in order to separate the liquid sample from the nano-hybrids. The volume of each phase was subsequently measured in order to ensure that the mass balance was closed, and a sample of each phase was injected into a HP-6890 GC-FID for product quantification.

For single phase reactions, an identical procedure was followed, with 30mg of nano-hybrids introduced to 30mL of either water or decalin, sonicated for 15 minutes, and then treated identically to the emulsion reactions. For each of these cases, double the amount of glutaraldehyde or octanal was introduced to the single phase water or oil reactions, respectively, in order to maintain identical concentrations in each case while maintaining similar volumes in the Parr reactor.

9.3 Results and Discussion

In both the emulsion and single phase reactions, glutaraldehyde yields as a primary product 5-hydroxypentanol. This product was not observed, however, as only the cyclic hemiacetal product was present after the reaction. This occurs via attack from the nucleophilic oxygen of the alcohol towards the carbonyl carbon, identical to the cyclization of glucose. The secondary product observed was 1,5-pentanediol. For the case of octanal, the only product observed was 1-octanol. The results from the glutaraldehyde/octanal emulsion mixture are very interesting, with the most important

result being the activity and selectivity of the emulsions when compared with the single phases. Results from these activity tests are shown in figure 9.5.

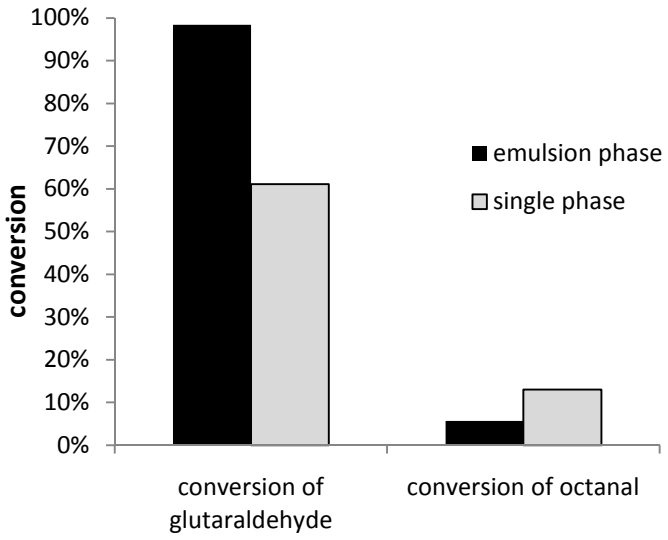


Figure 9. 5 Conversion of model compounds in the emulsion vs. oil or water phase alone.

There are two interesting conclusions which may be drawn from this graph. One is the increase in conversion of glutaraldehyde for the emulsion phase when compared with the water phase alone. This is to be expected, as the increase in surface area from the emulsions provides increased surface area for reaction and lowers diffusion limitations. This result presents a strong case for these emulsions, as it provides evidence that increases in activity may be achieved.

The second trend observed is the decrease in conversion of octanal in the emulsion phase when compared with the oil phase. This is suspected to be due to a higher percentage of Pd located on the polar silica than the non-polar nanotubes,

although further investigation is needed to confirm this hypothesis. If this is true, then the reaction in a single oil phase will have access to the Pd located on both the silica and the nanotubes, while the reaction in the emulsion phase will only have preferential access to the Pd on the nanotubes. This suggests that the nano-hybrids are modifying both the activity and selectivity towards reaction in both phases.

9.4 Conclusions and potential applications

These results provide promising proof-of-concept evidence for the use of these nano-hybrids for the selective reaction of a biphasic mixture at the interface. The potential applications which may arise from this type of approach are extremely numerous. For bio-oil upgrading, one could potentially introduce basic functionality on the polar end, either by depositing active components on the silica, or by growing the nanotubes on a basic support. If metal can then be placed selectively on the nanotubes, one could potentially do the aldol condensation as well as hydrogenation/etherification step as outlined in chapter 8 in one reactor. Other potential applications will likely soon result, including aqueous phase reforming, specialty chemical production, sugar upgrading to fuels, lignocellulosic bio-oil selective hydrotreating, triglyceride conversion, and many more. This serves as an extremely promising first step for what should be a very exciting area of research in the near future.

References

1 S. Czernik, A.V. Bridgwater *Energy Fuels* **2004**, *18*,590

2 P. Pieranski *Physical Review letters* **1980**,45(7).

3 G.M. Whitesides, B. Grzybowski, *Science*, **2002**, *295.*

4 A. D. Dinsmore, Ming F. Hsu, M. G. Nikolaides, M. Marquez, A. R. Bausch, D. A. Weitz *Science* **2002**, *298*,1006.

5 B.P. Binks, S.O. Lumsdon *Langmuir* **2000**, *16*, 8622.

6 B. P. Binks, *Current Opinion in Colloid and interface Science **2002***, *7,* 21.

CHAPTER 10

10. Outlook and Path Forward

The molecular engineering strategy as applied to fuels has proven to be an extremely valuable approach towards developing of novel catalytic strategies as potential solutions for a variety of areas. This work serves as a demonstration of the types of problems this approach can be utilized to solve. The transition from conventional fuels to renewable fuels should serve as an example that, while the reactions involved and conditions employed to improve the various fuels may be widely different, the underlying approach is the same.

While virtually every fundamental study has some degree of practical driving force, and most practical catalytic screening tests contain some degree of guided intuition, this approach serves as, in my opinion, the optimal blend of the two. By conducting practically driven fundamental catalytic studies, while continually linking them to the important resulting fuel properties, a synergistic effect is obtained. As viewed from a fundamental approach, fundamental researchers are less limited by practical studies in order to determine if a particular approach is practical. As viewed from a practical standpoint, practical researchers now are less limited by fundamental studies in order to determine what is guiding their results. The end result of this approach serves as a catalyst for facilitating communication between the two areas. Through this, strategies are obtained in a timely manner which were built on a sturdy fundamental foundation.

This approach is arguably the best for determining rapid solutions to important problems. This approach serves as an extremely valuable tool for approaching and obtaining optimal strategies for a variety of challenges in the energy industry. It is likely that this type of approach which will play a large role in solving not only our current challenge of utilizing renewable fuels, but the many unforeseen challenges which will be presented to the energy industry in the future.